HHS Public Access

Author manuscript

J Biol Inorg Chem. Author manuscript; available in PMC 2018 April 01.

Published in final edited form as:

J Biol Inorg Chem. 2017 April ; 22(2-3): 253–288. doi:10.1007/s00775-016-1415-2.

Activation of dioxygen by copper metalloproteins and insights from model complexes

David A. Quist[1], **Daniel E. Diaz**[1], **Jeffrey J. Liu**[1], and **Kenneth D. Karlin**[1]

[1]Department of Chemistry, Johns Hopkins University, Baltimore, MD 21218, USA

Abstract

Nature uses dioxygen as a key oxidant in the transformation of biomolecules. Among the enzymes that are utilized for these reactions are copper-containing met-alloenzymes, which are responsible for important biological functions such as the regulation of neurotransmitters, dioxygen transport, and cellular respiration. Enzymatic and model system studies work in tandem in order to gain an understanding of the fundamental reductive activation of dioxygen by copper complexes. This review covers the most recent advancements in the structures, spectroscopy, and reaction mechanisms for dioxygen-activating copper proteins and relevant synthetic models thereof. An emphasis has also been placed on cofactor biogenesis, a fundamentally important process whereby biomolecules are post-translationally modified by the pro-enzyme active site to generate cofactors which are essential for the catalytic enzymatic reaction. Significant questions remaining in copper-ion-mediated O_2-activation in copper proteins are addressed.

Keywords

Copper; Dioxygen activation; Copper enzymes; Enzymatic mechanisms; Cofactor biogenesis

Introduction

The reductive activation of dioxygen (O_2) is a central process in biological, synthetic, and industrial systems [1–3]. This process is well known in aqueous systems and proceeds through various intermediates including superoxide ($O_2^{\cdot-}$), hydrogen peroxide (H_2O_2), and hydroxyl radical ($^{\cdot}OH$); two equivalents of water are produced from this reaction (Scheme 1) [4–7]. However, it is also important to know how these processes occur in the presence of metal ions, as many important oxidative transformations have been attributed to various reactive metal–oxygen species [3, 8–11].

Copper-containing metalloproteins activate O_2 (or its reduced forms, i.e., $O_2^{\cdot-}$) for a variety of biological functions [12]. Monooxygenases oxidize substrates by incorporating one atom of O_2; the second atom of O_2 is converted to water, a combined four-electron process. Copper-containing monooxygenases have one or two (coupled or non-coupled) copper ions in their active sites. Dioxygenases, only one of which has been found to contain copper to date, oxidize substrates by incorporating both atoms of O_2 into the product. Oxidases are responsible for the reduction of O_2, occurring with proton transfer, by either two electrons (making H_2O_2) or four electrons (making two equivalents of H_2O). This is usually coupled to cofactor (organic or metal ion) oxidation or other biological functions (i.e., proton

pumping in cytochrome *c* oxidase (C*c*O), vide infra). Mononuclear, homo-multinuclear, and hetero-multinuclear copper active sites have been found in copper-containing oxidases. The timing and source of protons to these reduced O_2 species is still an ongoing area of research. One form of superoxide dismutase, which is responsible for the dismutation of $O_2^{\cdot-}$ to O_2 and H_2O_2, contains one copper ion and one zinc ion in its active site. In mollusks and arthropods, the binuclear copper enzyme hemocyanin is responsible for O_2 transport. Each of these copper metalloproteins must undergo redox reactions in order to activate O_2 for substrate or cofactor oxidation, transport, or to decrease the amount of harmful superoxide (Scheme 1).

This review will focus on O_2 activation by copper-containing metalloproteins. An overview of the enzymatic mechanisms involved in this crucial multi-faceted biological reaction will be presented. Emphasis will be given to recent information on the fundamental activation of O_2 by copper-containing enzymes gained from studies of both enzymatic and model systems, as well as computational studies on each. The interplay of electron and proton transfer, structural and spectroscopic data of reactive intermediates, and lingering questions will be discussed.

Structurally characterized copper-dioxygen species

Reduction of O_2 using copper complexes and the subsequent reactivity of the resultant intermediates have both been widely studied [13–17]. Many different Cu_nO_2 intermediates can be formed and have been extensively investigated in terms of spectroscopy and reactivity (Fig. 1). The first major breakthrough in this field came from Karlin and coworkers in 1988, when they were able to structurally characterize, for the first time, a copper-dioxygen adduct [18]. This complex has peroxide bound to two Cu^{II} centers in a *trans*-μ-1,2 fashion. Kitajima and coworkers followed soon after, in 1989, with a crystal structure of a dicopper species with peroxide bound side-on (μ-η^2:η^2) to the two Cu^{II} ions [19]. In 1996 and 1997, the groups of Tolman and Stack published on the spectroscopic and structural features of dicopper(III) bis-μ-oxide complexes, where dioxygen has been fully reduced by four electrons and the O-O bond has been cleaved [20–23]. Peroxodicopper(II) complexes supported by phenolate-bridging ligands have also been described [24–27]. Recently, Meyer and coworkers published the crystal structure of a peroxodicopper(II) complex ligated by a pyrazolate-based binucleating ligand [28]. This complex shows the peroxide bound in an intermediate geometry between *cis* and *trans*, and it was found to have an $S = 1$ electronic ground state; all other peroxo-bridged dicopper(II) complexes previously described (Fig. 1) show (where measured) antiferromagnetic coupling ($S = 0$ ground state) between the Cu^{II} ions [29, 30]. The first spectroscopic characterization of a mononuclear 1:1 copper-dioxygen intermediate was reported in 1991 by Karlin and coworkers [31]. Two crystal structures of cupric superoxide model complexes have since been reported, with superoxide binding either in an η^2 or η^1 fashion [32, 33]. The reactivity of cupric superoxide model complexes, as well as their importance in biology, has recently been reviewed [17]. Tolman and coworkers have published on other mononuclear high-valent copper-(di)oxygen intermediates, including side-on Cu^{III}-peroxide and Cu^{III}-hydroxide species [34, 35], the latter of which was found to be capable of performing oxidations of strong C–H bonds (BDE <99 kcal/mol) [36, 37].

Dioxygen binding studies

"Flash-and-trap" techniques have been a useful tool to study metal CO/O_2 binding dynamics in heme systems [42–47]. The Karlin group has applied and extended these methods to investigate the kinetic and thermodynamic properties of O_2 reduction by Cu^I model complexes [48, 49]. When a Cu^I(TMPA)-carbonyl complex is photolyzed in the presence of O_2, the kinetic parameters for O_2 binding can be obtained, a process too fast for typical bench-top experiments (Scheme 2a). From these studies, the rates of O_2 binding and release (extrapolated to room temperature, 298 K) were found to be nearly diffusion limited at 1.3×10^9 M^{-1} s^{-1} and 1.5×10^8 s^{-1}, respectively [48]. The extrapolated O_2 binding rates are 10–100 times faster than those of myoglobin and hemoglobin (Table 1) [50]. However, the rates of release of O_2 are up to 10^7 times faster in the case of this copper model complex, suggesting that O_2 is bound much tighter (with respect to thermodynamics) in myoglobin and hemoglobin [48, 50].

Experiments using transient absorption spectroscopy have also been conducted to determine the thermodynamic parameters of O_2 photorelease and rebinding from a cupric superoxide model complex bearing the TMG_3Tren ligand (Scheme 2b) [49]. Photoexcitation of $[Cu^{II}(TMG_3Tren)(O_2^{\cdot-})]^+$ leads to O_2 release, which then quickly rebinds to the Cu^I ion, resulting in the reformation of the starting cupric superoxide complex. The experimental set-up used allowed for the quantification of kinetic and thermodynamic parameters for O_2 binding [49]. Analysis of the kinetic and thermodynamic parameters found the rate of O_2 binding for the TMG_3Tren complex is orders of magnitude smaller than for the complex bearing TMPA (Table 1). This slower reactivity was explained by the sterically bulky tetramethylguanidine groups, which may deter O_2 rebinding.

Prior to these sophisticated experiments, the reversible binding of O_2 was most often demonstrated by purging a solution of a copper-dioxygen intermediate with an inert gas (i.e., nitrogen or argon) and/or applying a vacuum to regenerate the Cu^I complex [18, 55, 56]. Addition of O_2 to the resulting Cu^I solution leads to the reformation of the original copper-dioxygen intermediate. This process can be repeatedly cycled with minimal decomposition of the Cu complex.

Single copper active sites

Monooxygenases

PHM, DβM, TβM—Three copper-containing monooxygenases share remarkable similarities, both in amino acid sequence, active site coordination, and reactivity [57]. Peptidylglycine α-hydroxylating monooxygenase (PHM), dopamine β-monooxygenase (DβM), and tyramine β-monooxygenase (TβM) are responsible for the synthesis of important hormones and neurotransmitters in mammals (PHM and DβM) and insects (TβM). PHM hydroxylates a C-terminal glycine residue of a glycine extended prohormone as one domain of the bifunctional enzyme petidylglycine α-amidating monooxygenase (PAM). DβM is responsible for the oxidation of dopamine to norepinephrine, two important neu-rotransmitters found in humans, while TβM hydroxylates tyramine to octopamine in insects (Scheme 3).

Each of these three enzymes contains a non-coupled binuclear active site, where the two copper ions are ~11 Å apart (Fig. 2 shows a crystal structure of PHM) [38]. In the Cu_H site, the copper ion is coordinated by three His residues. In the Cu_M site, the copper ion is coordinated by one Met and two His residues. O_2 activation and substrate hydroxylation occur at the Cu_M site, while the Cu_H site is responsible for electron transfer [57]. A very recent paper by Blackburn and Kline reports that a conformational change at the Cu_M site occurs upon addition of substrate, postulated to promote O_2 binding and activation [58]. One major breakthrough was the structural characterization of dioxygen bound to Cu_M (Fig. 2) [38]. For many years, PHM was the only one of these three enzymes that had been crystallographically characterized. Recently, the first crystal structure of DβM was published [59]. Two different conformations of the enzyme were observed; one conformation, similar to PHM and called the open conformation, showed the two copper binding sites ~14 Å apart, while the other, called the closed conformation, showed the binding sites ~4 to 5 Å apart. The authors proposed two possible reasons for the existence of the closed conformational form. The first is that this is an artifact due to the way the enzyme was expressed. The second is that the closed conformation may be catalytically active, similar to binuclear enzymes such as tyrosinase and catechol oxidase possessing adjacent copper ions (vide infra). Thus far, supporting evidence for this possibility does not yet exist; further studies are required.

The mechanism of substrate hydroxylation for these enzymes has been well studied (Scheme 4). In the prevailing mechanism, it is thought that, following O_2 coordination and reduction at Cu_M, a cupric superoxide is responsible for hydrogen atom transfer (HAT) from the substrate, resulting in a cupric hydroperoxide complex (**Hp**) and substrate radical [17]. The next step of the mechanism can go through two different paths. In path 1, the O-O bond of the cupric hydroperoxide species is homolytically cleaved (induced by proton and electron transfer), resulting in a cupric oxyl (**Cp**) intermediate. The substrate radical then rebounds with **Cp**, giving product bound to the copper ion. In path 2, **Hp** reacts directly with the substrate radical, cleaving the O-O bond and hydroxylating the substrate. This gives product and a **Cp** species that can then be reduced and protonated to give a cupric hydroxide complex. Addition of an external proton and electron returns the enzyme to its reduced state in both paths.

Copper model systems have played a key role to help determine the mechanism of action in these enzymes. Multiple cupric superoxide complexes have been reported and characterized using a variety of spectroscopic techniques, including UV–Vis and resonance Raman (rR) spectroscopies [17, 62]. Substrate reactivity studies accompanied by mechanistic insights with model complexes have been reported by the groups of Karlin and Itoh. Using the TMPA-based ligands ^{PV}TMPA and ^{DMM}TMPA, Karlin and coworkers have shown that cupric superoxide complexes can react with exogenous substrates containing weak C–H and O–H bonds (Scheme 5a, b) [63, 64]. These studies found that kinetic isotope effects (KIEs) for substrate oxidation with the model complexes were similar to the reported KIEs for the enzymes PHM and DβM [57]. Itoh and coworkers have published the first series of superoxide complexes with neutral tridentate ligands bearing different *p*-substituents on the intramolecular phenyl ring [65]. Following their initial study, the authors thoroughly

investigated the O_2 binding of the Cu^I complexes, as well as the rates of superoxide decomposition, which led to ligand hydroxylation (Scheme 5d) [52]. The O_2 binding rates for a copper complex similar to this set were shown to be significantly slower than the previously reported results for TMPA and TMG_3Tren (Table 1, vide supra). Using the rates of ligand hydroxylation, a Hammett analysis was conducted and showed a ρ value similar to that reported for DβM, suggesting a mechanism involving hydrogen-atom abstraction chemistry [66].

The role of the methionine residue binding to Cu_M has been, and still is, an intriguing mystery, especially considering the propensity of thioether moieties to be oxidized to their respective sulfoxides or sulfones. Multiple studies on the structural effects of N_2S and N_3S ligands and the reactivity of the corresponding copper complexes with oxidants such as H_2O_2 and O_2 have been reported [68–76]. Recently, the first model cupric superoxide complex bearing thioether ligation was reported [67]. This complex was shown to be more reactive towards exogenous substrates than previously published complexes; reactivity with *N*-methyl-9,10-dihy-droacridine was achieved at –135 °C (Scheme 5c), while other superoxide complexes could only achieve such reactivity above –100 °C. Future investigations may help elucidate the exact function of the methionine residue bound to copper in these enzymes.

Lytic polysaccharide monooxygenases—Lytic polysaccharide monooxygenases (LPMOs), found in fungi and bacteria, are mononuclear copper enzymes responsible for the degradation of polysaccharides, in cellulose, chitin, and starch, by cleaving the glycosidic bond (Fig. 3b) [77]. Four different families of LPMOs have been reported, differentiated by substrate specificity or the organism in which they are found. The active site coordination is similar in all families, with the copper ion bound by two His residues, one of which acts as a bidentate ligand in a histidine brace motif (His brace, Fig. 3a), while other ligands can be bound in the cupric state [78]. Some subtle differences in the active sites between the four families are the presence of different amino acids in the secondary coordination sphere and, in some cases, the N-methylation of the His brace. A recent crystal structure with chloride bound to copper shows the substrate bound in the enzyme pocket (Fig. 3a) [78]. Crystal structures with reduced forms of O_2 have also been reported [39], but the Cu–O distance in these structures rules out formal bonds and it has been suggested that such species may be due to photoreduction by the X-ray beam [79].

While LPMOs have been studied less than other copper-containing monooxygenases, enzymatic and computational studies have led to the proposals of reaction mechanisms which may be similar to those suggested for PHM, DβM, and TβM; however, other possibilities exist [17, 77, 80–82]. Possible copper-(di)oxygen intermediates involved in HAT from substrate are shown in Fig. 4. In a computational study, Beckham and coworkers proposed that a Cu^{II}-$O^{\cdot}$ species (Fig. 4a, left) has a lower energy activation barrier than a $Cu^{II}-O_2^{\cdot-}$ intermediate (Fig. 4b) for HAT chemistry [81]. Tolman and coworkers have postulated that Cu^{III}-OH (Fig. 4a, right) may be a viable intermediate in the catalytic cycle of LPMOs [83]. Such a species could exist as a tautomer of the Cu^{II}-$O^{\cdot}$, with deprotonation of the His brace NH_2 group leading to an amide anion ($–NH^–$) donor for such a Cu^{III}-OH

species. The Cu^{III}-OH model complexes reported by Tolman and coworkers provide support for this hypothesis, due to the presence of negatively charged amide ligand donors used to support the high-valency and HAT reactivity of the Cu^{III}-OH species [36, 37, 83].

Oxidases

Amine oxidase—Copper-containing amine oxidases (CAOs) are a family of enzymes found in every domain of life with the exception of *Archaea* [12]. These enzymes carry out the reaction of converting primary amines to the corresponding aldehyde [85]. The active site of CAO is found to contain a type 2 (T2) copper site coordinated by three histidine residues and one water molecule in the oxidized (active) state, in addition to a unique 2,4,5-trihydroxylphenylalanine qui-none (TPQ) cofactor, formed through post-translational modification of a highly conserved active site tyrosine residue (Fig. 5) [86–88]. Copper plays an essential role in the cofactor biogenesis of TPQ. Crystal structures of the apo-enzyme from *A. globiformis* reveal the presence of an active site tyrosine which, following the addition of copper, converts to TPQ (see “Cofactor biogenesis” section) [87]. This six-electron oxidation of tyrosine is copper-dependent as evidenced by site-directed mutagenesis experiments where a histidine copper ligand is mutated to a glutamate. The resulting enzyme lacks detectable TPQ and is unable to exhibit amine oxidase activity [89].

The catalytic mechanism of CAO involves the oxidation of a primary amine to an aldehyde through a ping-pong mechanism facilitated by two half-reactions [85, 91]. In the reductive half-reaction, TPQ_{OX} oxidizes the substrate amine to give the two electron reduced TPQ aminoquinol (TPQ_{AMQ}) and the product aldehyde. The oxidative half-reaction uses O_2 and a water molecule to regenerate TPQ_{OX} and yield H_2O_2 and NH_4^+ (Scheme 6). Although there is general consensus on the overall catalytic enzymatic mechanism, uncertainty remains on the role Cu^{II} plays in the oxidative half-reaction, namely whether O_2 is reduced directly by TPQ_{AMQ} (outer-sphere mechanism) or if TPQ_{AMQ} reduces Cu^{II} to Cu^{I}, which then reacts with O_2 to form a cupric super-oxide intermediate (inner-sphere mechanism) [85]. Klinman and coworkers have performed studies that favor an outer-sphere mechanism (Scheme 6, bottom). They have shown that under O_2-saturating conditions, a Co^{II}-containing AO exhibits a similar k_{cat} value relative to the native copper containing analog, despite Co^{II} being significantly more difficult to reduce ($E_{1/2}$ is 800 mV more negative) relative to Cu^{II} [92, 93]. Other studies done by Dooley and coworkers have favored an inner-sphere mechanism on the basis of stopped flow experiments and global fitting models (Scheme 6, top). Data analyses are consistent with electron transfer (ET) from TPQ_{AMQ} to Cu^{II} and not direct ET from TPQ_{AMQ} to O_2 as required in the outer-sphere mechanism [94]. Both inner-sphere and outer-sphere pathways converge on the formation of a cupric superoxide and TPQ semiquinone (TPQ_{SQ}), which undergoes proton coupled electron transfer (PCET) to form TPQ iminoquinone (TPQ_{IMQ}) and a cupric hydroper-oxide [95]. TPQ_{IMQ} is then hydrolyzed to regenerate TPQ_{OX}, while the addition of a proton to the cupric hydroperoxide liberates H_2O_2, returning the enzyme to the active state.

Itoh and coworkers have developed a CAO model complex using a TPQ-derivatized ligand copper compound (see cofactor biogenesis section) [96]. The authors illustrated the

competence of this system in facilitating transamination of benzylamine to *N*-benzylidene benzylamine (Scheme 7). This reaction is known to occur in TPQ analogs [97].

Despite numerous results gained through enzymatic and model system studies of CAO, uncertainty remains regarding a critical step in the catalytic mechanism. Namely, does the reduction of O_2 to $O_2^{\cdot-}$ occur via an inner-sphere path-way or outer-sphere pathway during the catalytic cycle? There is compelling evidence against the outer-sphere pathway; however, an inner-sphere pathway has not been unambiguously established.

Galactose oxidase—Galactose oxidase (GO) is a copper-dependent enzyme featuring a stable enzyme radical in the protein active site [91, 98, 99]. The overall catalytic reaction of GO involves the stereospecific two-electron oxidation of primary alcohols to aldehydes and, at a reduced rate, aldehydes to carboxylic acids [100]. Crystal structure data of the oxidized GO active site from *D. dendroides* show an active site containing a cupric ion coordinated to two histidines, two tyrosines, and a labile site containing acetate or water in a square pyramidal geometry (Fig. 6) [101]. One of the coordinated tyrosine residues possesses a very unusual cysteine cross-link at the *ortho*-position. This crosslink serves to lower the reduction potential of the modified residue (free tyrosine $E_{1/2}$ ~1000 mV vs. NHE; Tyr-Cys $E_{1/2}$ = 400 mV vs. NHE) [102, 103]. This modification allows for the stabilization of a tyrosyl radical (Tyr-Cys$^{\cdot}$) in the resting state, which provides the essential second oxidizing equivalent enabling the mononuclear copper active site to perform two-electron substrate oxidation [104].

The catalytic mechanism of galactose oxidase involves a ping-pong mechanism consisting of separate oxidation and reduction steps [98, 104]. The catalytically active form of GO contains a Cu^{II} center coordinated by two histidines, water (or buffer anion), tyrosine, and a tyrosyl radical. In the reductive half reaction, coordination and deprotonation of the alcohol substrate to the copper center initiates net HAT from a C–H bond of the alkoxide to generate a ketyl radical and tyrosine (Scheme 8). Electron transfer from the ketyl radical to Cu^{II} yields the product aldehyde and Cu^{I}. In the oxidative half-reaction, O_2 reacts with the reduced active site to yield a second equivalent of H_2O_2, with concomitant regeneration of the catalytically active state containing Cu^{II} and Tyr-Cys$^{\cdot}$ (Scheme 8).

Synthetic copper complexes containing phenolate coordination have been extensively studied as structural, functional, and potential mechanistic models for galactose oxidase [105–109]. Ghosh and coworkers reported the synthesis of a Cu^{II} complex supported by a ligand framework consisting of two nitrogen donors, a phenol donor, and a phenolate donor, very similar to the coordination observed in the enzymatic active site [110]. More remarkably, this complex was able to catalytically, and selectively, oxidize primary alcohols to aldehydes in the presence of O_2 and NaOH. Mukherjee and coworkers recently reported the synthesis of a mononuclear Cu^{II} complex using an aminophenol-salen derivative [111]. Upon metallation of the ligand with Cu^{II}, formation of a monoradical on the aminophenol ring occurs, yielding an isolable iminosemiquinone complex. The Cu^{II} phenoxyl radical character of the compound was verified by X-ray crystallography and SQUID measurements pointing to a ferromagnetically coupled $S = 1$ ground state. Exposure of this compound to air led to intramolecular hydroxylation at the benzylic position, but the radical character of

the iminosemiquinone was maintained. This oxygenated intermediate was also verified by X-ray crystallography and SQUID. It was found to possess an antiferromagnetically coupled $S = 0$ ground state, similar to the oxidized form of GO.

Dioxygenase

Quercetinase—Quercetinase (quercetin 2,4-dioxygenase, 2,4-QD) is a copper-containing dioxygenase enzyme found in some fungi and prokaryotes [12]. The resting state of the enzyme has two different geometries, a four-coordinate structure (70%) and a five-coordinate structure (30%) [112]. In both structures, the copper ion is coordinated by three His residues and a water molecule, while an additional Glu residue binds copper in the five-coordinate structure. Interestingly, 2,4-QD is one of two copper proteins that has a carboxylate moiety bound to copper. While 2,4-QDs isolated from fungi all contain an active site containing one copper atom, prokaryote 2,4-QDs have been isolated with a variety of different first row transition metals, depending on the metal content of the culture media [113–115]. Some of these other metals show enzymatic activity, but Cu-loaded 2,4-QD has been shown to have the highest activity. These data, along with all fungi 2,4-QDs containing copper active sites, provide strong evidence that 2,4-QD should be considered a copper-dependent enzyme [12].

An X-ray crystal structure of the 2,4-QD enzyme-substrate (ES) complex is shown in Fig. 7 [116]. Quercetin binds to the copper ion in a monodentate fashion, through the C3-OH group, with Glu73 still bound to copper and hydrogen bonding (H-bonding) with the substrate. Amino acid mutation studies have shown that this glutamate residue is critical to enzymatic function [112]. Glu73 has been proposed to deprotonate the substrate quercetin prior to dioxygenation, and this amino acid residue may also modulate the reduction potential of the copper ion [117].

2,4-QD breaks down quercetin and other flavonols to depsides, releasing CO. While the overall mechanism of this transformation is widely accepted, there is controversy over a main reaction step (Scheme 9) [12, 116]. When the substrate binds to the Cu^{II} ion, it is thought that this complex is in equilibrium with a Cu^{I}-substrate radical species. The latter is postulated to be responsible for O_2 activation. It is not known whether O_2 reacts directly with the substrate radical or with the Cu^{I} ion (path 1 or 2 in Scheme 9). Once the C2-O bond has been formed (either through direct reaction with O_2 or coupling with the cupric superoxide), the C4-O bond is made, resulting in an endoperoxide intermediate that undergoes O-O bond cleavage and releases CO.

While the overall mechanism of 2,4-QD has been elucidated from enzymatic studies, no direct mechanistic insight into the activation of O_2 has been reported. Exploration of model complexes has provided experimental evidence to help understand this important step. Speier and coworkers have published multiple studies on model complexes of 2,4-QD [118]. Under basic conditions, or in the presence of non-redox active metals (such as zinc), flavonolate was shown to directly reduce O_2 through single electron transfer (SET), producing flavonoxyl radical and free $O_2^{\cdot-}$ [119]. Studies involving model complexes containing copper have been shown to have greatly reduced rate constants when compared to the enzyme; these differences have been attributed to the bidentate coordination of

quercetin in model complexes, as opposed to the monodentate binding in the enzyme (Scheme 10) [120–122]. Addition of exogenous substituted acetates results in an increase in rate, most likely due to the shift of the flavonol to monodentate coordination (Scheme 10a) [123]. The authors proposed that this coordination difference resulted in more electron density on the flavonol, which allowed for the flavonol to reduce O_2 to $O_2^{\cdot-}$, the latter of which was found to be present in the reaction. Two recent papers by Sun et al. report the detailed study of a variety of metal complexes coordinated by two different tetradentate ligands with an intramolecular carboxylate group (Scheme 10c) [124, 125]. It was proposed that, unlike in previous model studies, the substrate flavonolate binds in a monodentate fashion to copper, which is consistent with EPR data. This coordination change, as well as tuning the electron density of the bound flavonolate by ligand design, resulted in higher catalytic reactivity compared to previously published model systems.

Computational studies have also helped provide insight into the step in which O_2 is reduced [126, 127]. A recent QM/MM computational study on 2,4-QD has provided support for the reduction of O_2 by Cu^I, resulting in a cupric superoxide species [127]. Formation of the cupric superoxide is concomitant with dissociation of the substrate. It is proposed that the active site geometry keeps the substrate locked in the correct conformation for the superoxide to attack C2. Direct reaction of O_2 with the substrate radical was calculated to go through a transition state 12.7 kcal/mol higher in energy than the reaction of Cu^I with O_2.

While much has been learned, both through model complex and computational studies, it is still unclear how O_2 is activated in 2,4-QD. While O_2 must react with the Cu^I-substrate radical complex, whether it results in a cupric superoxide or an organic peroxide is unknown. Formation of product without the presence of a redox-active metal and detection of $O_2^{\cdot-}$ in solution in the presence of redox-active metals support reduction of O_2 by flavonolate (i.e., path 1 in Scheme 9). Computational studies, on the other hand, reach a consensus that reduction of O_2 by a Cu^I ion, resulting in a cupric superoxide, is more energetically favorable. Future studies, both on the enzyme and also on model complexes, are needed to help elucidate this important step in the enzymatic reaction mechanism.

Homo-multinuclear copper active sites

O_2 transportation

Hemocyanin—Hemocyanin (Hc) is an extracellular dioxygen carrier protein found in the blood of arthropods and mollusks [85]. Unlike the other two dioxygen transport proteins known in biology, which contain iron in their active site (Hemoglobin, a heme-containing protein [128] and Hemerythrin, a binuclear iron protein [129]), Hc contains a coupled type 3 (T3) dicopper active site, where each copper is ligated by three ε-N His moieties. There are two different families of Hc, one that is found in arthropods (e.g., crabs, insects, lobsters, scorpions, shrimps, and spiders), and the other found in mollusks (e.g., octopi, snails, squids, chitons, cuttlefishes, and nautiluses); however, the His ligation and the spectral features of the binuclear copper site are highly conserved in both classes of Hc [12]. Molluskan Hc contains a distinctive C2His/S-Cys crosslink in the so-called Cu_A site. This post-translational modification is not usually found in biological systems (Fig. 8b) [130]. Despite

this feature, the spatial arrangements of the copper sites remain nearly identical for arthropodic and molluskan Hc (His-Cys crosslink formation is discussed in the cofactor biogenesis section, vide infra).

Hc contains a pair of Cu^I atoms separated by ~4.6 Å in the EPR silent fully reduced colorless form (deoxy-Hc). This large, multi-subunit, and highly cooperative protein binds dioxygen in the deoxy form, yielding oxy-Hc as an intense purple species (Fig. 8). Before the exact structure of oxy-Hc was known, Karlin and coworkers were able to spectroscopically model the absorption spectra observed in oxy-Hc [55, 132, 133]. Kitajima and coworkers were able to crystallographically characterize a μ-η^2:η^2-peroxodicopper(II) species of a tris(pyrazolyl)borate complex (Fig. 1) [19], which was later confirmed to be the copper–oxygen motif in oxy-Hc (Fig. 8) [40, 130, 134]. O_2 binding requires the transfer of two electrons from the Cu^I centers to dioxygen to form the bridged peroxide. According to the Mulliken population analysis along the O_2-binding coordinate, this formally spin-forbidden process, where the triplet ground state of dioxygen is converted to the antiferromagnetically coupled singlet of oxy-Hc, is overcome through the simultaneous reduction of dioxygen in the bridged structure by the two electrons from the Cu^I centers [135]. Contrastingly, the reactivity described for recent synthetic model systems is different from the proposed mechanism of O_2 reduction that occurs in Hc (vide infra).

Oxy-Hc has an intense absorption band at ~350 nm (ε = ~20,000 M^{-1} cm^{-1}) with an associated resonance-enhanced Raman vibration at ~750 cm^{-1} (Δ ~ −40 cm^{-1} upon $^{18}O_2$ isotope labeling). The high energy and high intensity absorption band at ~350 nm is associated with the charge-transfer from the peroxide $\pi^*_\sigma \rightarrow Cu^{II}$ LUMO. Additionally, a weaker absorption band at ~570 nm (ε = ~1000 M^{-1} cm^{-1}) is observed, which is associated with the charge-transfer from the peroxide $\pi^*_\upsilon \rightarrow Cu^{II}$ LUMO [131, 136]. The Cu-Cu distance in the oxy form of Hc is ~3.6 Å [130, 137, 138], and, like its deoxy form, oxy-Hc is EPR silent [139].

Although the primary function of Hc is the transport of dioxygen, catecholase activity has been observed in a native molluskan Hc isolated from *O. vulgaris* [140]. A significant increase of catecholase activity, and even monooxygenase activity, has been achieved in both arthropod and mollusk Hc through the use of protein denaturants such as SDS or urea [141–146], which induce a conformational change in the enzyme, as well as through proteolytic cleavage and protein-protein interactions [147–150]. These different approaches help substrate access the binuclear active site of Hc, which is suggested as part of the functional difference between the two T3 dicopper enzymes Hc and tyrosinase (vide infra).

Recent photoexcitation experiments of three peroxodicopper(II) model complexes using femtosecond transient absorption spectroscopy have been reported (Scheme 11) [151]. Interestingly, one-photon two-electron oxidation occurred, leading to the formation of O_2 and two Cu^I ions. It was proposed that this reaction occurs via a stepwise mechanism, with the observation of a new intermediate, a mixed-valent dicopper superoxide species, $Cu^{II}(O_2^{\cdot-})Cu^I$. This type of intermediate had never been seen before and showed that reaction of LCu^I_2 with O_2 must go through a superoxide species, that is, $Cu^{II}(O_2^{\cdot-})Cu^I$, before forming the peroxodicopper(II) species. This reactivity is different from Hc, where

the formation of a mixed-valent dicopper ($Cu^{I}Cu^{II}$) superoxide intermediate was shown to be unfavorable. The difference between Hc and model complexes may be accounted for by the close proximity of the copper ions in Hc enforced by the enzyme environment instead of the flexibility of the synthetic models [151].

Monooxygenases

Tyrosinase and catechol oxidase—Tyrosinase (Ty) and catechol oxidase (CaOX) belong to a coupled binuclear copper protein family able to carry out oxidation of phenols and catechols. Both Ty and CaOX perform the two-electron oxidation of *o*-catechols to quinones, but only Ty is able to catalyze the oxygenation of phenols to *o*-catechols [12]. These oxidases are structurally related to Hc. High-resolution crystal structures show that plant CaOX, bacterial Ty, and fungal Ty structures are similar to mollusk Hc [152–157], while insect Ty is structurally similar to arthropod Hc [157–159]. Both plant CaOX and bacterial Ty active sites have a highly conserved His-X(*n*)-His-X(8)-His sequence coordinated to Cu_A, and a His-X(3)-His-X(*n*)-His sequence coordinated to Cu_B (Fig. 9). Additionally, plant CaOX, fungal Ty, and mollusk Hc show a conserved Cys residue, which is crosslinked to one of the His ligands bound to Cu_A (see “Cofactor biogenesis” section) [130, 152, 156]. On the other hand, in insect Ty the active site has a His-X(3)-His-X(*n*)-His sequence for both Cu atoms.

Four different forms of active sites have been observed by X-ray crystallography for these binuclear copper enzymes: apo, deoxy, met and oxy (Fig. 9) [154]. Apo-Ty and deoxy-Ty show a similar organization of the His residues in the binuclear active site, which indicates that those His moieties are pre-aligned for Cu binding (Fig. 9a, b). Meanwhile, the oxy form of CaOX and Ty possesses structural and spectroscopic properties similar to those that have been found in oxy-Hc. Dioxygen binds the deoxy site as peroxide with a μ-η^2:η^2 coordination mode and a Cu-Cu distance of ~3.6 Å (Fig. 9d) [152, 154]. Oxy-Ty has an intense absorption band at ~345 nm (ε = ~18 000 M^{-1} cm^{-1}), with an associated rR vibration at ~755 cm^{-1} (Δ ~ −40 cm^{-1} upon $^{18}O_2$ isotope labeling), and another weak band at ~580 nm (ε = ~1000 M^{-1} cm^{-1}) [160]. The met form of CaOX and Ty can be found in a variety of different structures, where the binuclear Cu^{II} active site is bridged by zero, one, or two solvent ligands (Fig. 9c). The Cu-Cu distances in these structures have been found to be between 4.9 and 2.9 Å [152, 154, 158]. This flexibility suggests that other copper-dioxygen intermediates could be formed in the enzyme environment, such as a bis-μ-oxo species, which has been observed in model complexes (Cu-Cu distance: ~2.8 Å) [13]. The oxy and deoxy states, as well as the met-form, of these coupled binuclear copper enzymes are EPR silent.

Ty and CaOX can both perform catechol oxidase activity, a two-electron oxidation reaction, where an *o*-catechol substrate is converted to *o*-quinone (like 3,4-dihydroxy-L-phenylanaline (L-dopa) to L-dopaquinone) [12]. This reaction (Scheme 12, outer cycle) has two main phases (reductive and oxidative), and requires two equivalents of substrate for each equivalent of O_2 for every cycle. Kinetic studies of this catalytic cycle suggest that the rate-limiting step includes proton transfer [161, 162]. On the other hand, only Ty is able to carry out monooxygenase activity, a two-electron reaction converting a phenol substrate to an *o*-

catechol. Ty can then oxidize the *o*-catechol to *o*-quinone, making the oxidation of the original phenol an overall four-electron oxidation reaction (Scheme 12, inner cycle) [12]. One example of this reaction is the conversion of tyrosine to L-dopaquinone, a precursor in melanin biosynthesis. This catalytic cycle (Scheme 12, inner cycle) requires one equivalent of substrate and one equivalent of O_2 per turnover. Moreover, kinetics and mechanistic studies of mushroom Ty have shown that the rate-determining step of this reaction is the *o*-hydroxylation of the phenol in an electrophilic aromatic substitution (EAS) mechanism, which is supported by Hammett values of $\rho = -2.4$ and -1.7 obtained in different studies [163, 164].

Mutated variants of Ty have been used in order to analyze the effect of residues in the secondary coordination sphere on substrate binding. These studies have shown differential effects on the oxidase and oxygenase reactivity of Ty, which suggests that phenols and *o*-catechols interact with the enzyme pocket and bind the dicopper center in different ways [165–167]. Mechanisms have been proposed where phenols bind to Cu_A, while *o*-catechols bind at Cu_B. However, recently determined Ty crystal structures from *B. megaterium* with tyrosine and L-dopa in the active site have suggested otherwise. It was shown that both substrates were similarly oriented toward Cu_A [168]. Additionally, it has been speculated that a highly conserved glutamate (in both Ty and CaOX) and an asparagine (conserved mainly in Ty) bind and activate a conserved water molecule towards deprotonation of phenols. Based on this observation, it has been proposed that an active-site asparagine is responsible for differentiating between monooxygenase and catechol oxidase activity [168–170].

There is an overall consensus that the mechanism of hydroxylation of phenols by Ty proceeds via EAS. However, due to observations in model systems, the nature of the Cu_2O_2 reactive intermediate in the catalytic cycle remains under discussion. Tolman and coworkers demonstrated that the reaction of certain Cu^I model complexes with dioxygen generates a rapid equilibrium between the μ-η^2:η^2-peroxodicopper(II) and bis(μ-oxo)dicopper(III) cores (Scheme 13a) [20]. This equilibrium is controlled by many factors such as ligand donor ability, steric effect, solvent, and anion influences [13]. Stack and coworkers have provided evidence that phenolate can coordinate a μ-η^2:η^2-peroxodicopper(II) core, forming a phenolate-bound bis(μ-oxo)dicopper(III) complex, which can undergo internal hydroxylation of the phenolate through an EAS mechanism, giving the respective *o*-catechol (Scheme 13c) [171]. Karlin and coworkers have demonstrated that a μ-η^2:η^2-peroxodicopper(II) complex with a *m*-xylyl-linked binucleating XYL ligand, was also able to perform an intramolecular hydroxylation through an EAS mechanism (Scheme 13b). This conclusion was supported by Hammett analysis of *para*-substituted arenes, giving a ρ value of -2.1 [172–174]. Thus, model systems have demonstrated that both μ-η^2:η^2-peroxo and bis(μ-oxo) cores are able to perform hydroxylation through EAS. The remaining question is related with the nature of the actual active oxidant in the enzyme, and which factors govern this selection.

A final noteworthy observation from model system studies is that hydroxylation of phenols occurs when phenolate, in place of phenol, reacts with the μ-η^2:η^2-peroxo or bis(μ-oxo) cores [171, 175–177]. This is consistent with the idea of an activated water molecule, along

with conserved amino acid residues (glutamate and asparagine), playing a key role in the deprotonation of phenols during the catalytic cycle of Ty [168, 170].

NspF—In addition to the coupled binuclear copper enzymes that have been mentioned (Hc, CaOX, and Ty), a fourth subclass of this family has been discovered recently. NspF, a tyrosinase-like copper-containing monooxygenase, was found to perform the terminal step of 4-hydroxy-3-nitrosobenzamide biosynthesis in *S. murayamaensis,* converting *o*-aminophenols to nitrosophenols (hydroxyanilinase activity) [178].

Like other members of this family of enzymes, NspF reacts with dioxygen forming a μ-η^2:η^2-peroxodicopper(II) core, with absorption bands at 348 nm (ε = ~13 000 M^{-1} cm^{-1}, at 4 °C) and 635 nm. The first absorption has an associated rR vibration at 749 cm^{-1} (Δ = −38 cm^{-1} upon $^{18}O_2$ isotope labeling) [179]. NspF has shown catechol oxidase activity [178], as well as monooxygenase activity [179]. However, reactivity with *o*-aminophenols differs between NspF and Ty. While NspF achieves hydroxyanilinase activity, forming the nitroso product, Ty only performs the two-electron oxidation reaction, forming the corresponding *o*-iminoquinone. Thus, oxy-NspF is able to carry out all of Ty functions, along with the unique ability of oxygenating *o*-aminophenols to form *o*-nitrosophenols (Scheme 14) [178, 180]. A catalytic mechanism analogous to the monooxygenation of phenols by Ty, has been proposed for the hydroxyaniline activity of NspF with *o*-aminophenols (Scheme 15) [179]. It is interesting to note that recent biochemical studies have revealed non-heme di-iron enzymes, which carry out somewhat similar functions [181, 182].

Particulate methane monooxygenase—The oxidation of the strong C–H bond of methane is a challenging obstacle, both in nature and in industry. Utilizing methane as a source of carbon-derived energy may be an important step in the energy sector in the future [183–185]. In nature, methane is oxidized to methanol by methane monooxygenases (MMOs), found as soluble (sMMO; non-heme di-iron) and particulate (pMMO; multi-copper) membrane-bound forms [12]. The crystal structure of pMMO from *M. capsulatus* (Bath) shows three metal-binding sites consisting of a mononuclear copper site, a binuclear copper site, and a second mononuclear metal site containing zinc [186]. However, the crystal structure from *M. trichosporium* OB3b shows only two metal-binding sites; the binuclear copper site is conserved and there is a copper ion binding in the zinc site [187]. In the binuclear site, where it is proposed that methane oxidation occurs [188], one copper is bound in a bidentate fashion by the amine and imidazole groups of a protein terminal His residue (His brace motif, similar to that found in LPMOs), while the second copper ion is bound by two different His residues (Fig. 10). Stack and coworkers have reported model studies using histamine ligands to structurally mimic the His brace at the active site of pMMO, revealing special characteristics of the bonding to the copper center and the resulting O_2-adduct, a bis(μ-oxo)dicopper(III) moiety [189–192]. [Note: See also the articles in this special issue by Stack and separately Rosenzweig, and their coworkers].

Oxidases

Multicopper oxidases—Multicopper oxidases (MCOs) are enzymes containing at least four copper ions that couple the reduction of O_2 with the oxidation of various substrates,

either organic molecules (organic oxidases) or metal ions (metalloxidases) [12]. The four copper ions found in these enzymes are located in two distinct sites, including a mononuclear site and a trinuclear site (Fig. 11) [193]. A type 1 (T1; “blue” copper, with characteristic His2Cys(Met) ligation) copper ion, found in the mononuclear site, is responsible for substrate oxidation and electron transfer for O-O bond cleavage. The trinuclear site (TNC), where O_2 is reduced to water, consists of a T2 copper ion and a binuclear T3 site. In organic oxidases, the substrate binds in a hydrophobic pocket near the T1 site, while in metalloxidases, there are amino acid carboxylate residues nearby the T1 site that bind to the metal ion.

In order to investigate the reactivity of the TNC with O_2, the copper ion in the T1 site was removed, either through amino acid mutation or binding of an Hg^{II} ion instead of copper [194–198]. Reduction of O_2 by this mutated enzyme results in a Peroxy Intermediate (**PI**) that is not seen when the T1 copper site is intact. Through detailed DFT studies, with optimization coming from experimental observations, it was determined that **PI** has a peroxide ligand bridged between the three copper ions in the TNC site in a μ_3-1,1,2 fashion (Scheme 16), binding η^2 to one of the T3 copper ions [199, 200]. It is important to note that one of the T3 copper ions is not oxidized in this reaction and remains in the Cu^I oxidation state in **PI**, determined from no observable MCD signal and a silent EPR spectrum [194, 201].

With the T1 copper ion in the enzyme, a different intermediate is formed, instead of **PI**, from reduction of O_2. This intermediate has been termed the Native Intermediate (**NI**). From a variety of spectroscopic methods, including absorption, LT MCD, XAS, VTVH MCD, and EPR spectroscopies, it was determined that **NI** had to have a structure with all three of the copper ions in the TNC site bridged [202]. Two different possibilities for this structure are bridging of two hydroxide ions and a water molecule (TrisOH) or a μ_3-oxo structure. Model complexes demonstrating each of these bonding motifs have been spectroscopically characterized and analysis of EPR spectroscopy showed that either structure could be in the enzyme [203–206]. However, detailed analysis of LT MCD data of both model complexes and **NI** supports the assignment of **NI** having a μ_3-oxo structure (Scheme 16) [207]. From EXAFS spectroscopy, with the help of DFT calculations, it was determined that there is also a μ_2-OH ligand bridging the two T3 copper ions of the TNC [199, 208].

The mechanism of O_2 reduction at the TNC occurs through two steps, each involving the transfer of two electrons (Scheme 16) [12]. In the first step of O_2 reduction at the TNC, two electrons are transferred from the T2 Cu and one of the T3 Cu ions. The initial two-electron reduction of O_2 to form peroxide results in formation of **PI**. In the second step, two electrons are transferred from the second T3 Cu ion and the T1 Cu ion. This results in cleavage of the O-O bond, leading to formation of **NI**, with the two bridging oxygen atoms being derived from O_2. Proton and electron transfers lead to the loss of water, and reduction to form the fully reduced enzyme.

While analysis of the absorption spectrum of **PI** indicates that this species is different from the oxy form of hemocyanin and tyrosinase (vide supra), the proposed structure has only been supported by DFT calculations. Further elucidation of this binding motif of peroxide to

three copper ions is needed and (potentially) could be provided by model complex studies. The detailed spectroscopic interrogation of model complexes was invaluable in the determination of the structure of **NI**, and similar studies should be able to provide support for the proposed structure of **PI**. Previous reports of O_2 reactivity with model complexes bearing a trinuclear copper core leads to a $Cu_2^{II}Cu^{III}(\mu_3-O)_2$ complex, characterized by a variety of spectroscopies [192, 210–212]. Recently, novel ligand scaffolds, synthesized to create model complexes bearing tri-nuclear copper cores, have been reported [213, 214]. New scaffolds and future model studies may provide support for the proposed structure of **PI**.

Hetero-multinuclear copper active sites

Cytochrome *c* oxidase

Cytochrome *c* oxidase (C*c*O), and more generally heme-copper oxidases (HCO), play an essential role in aerobic life by coupling the exergonic four-electron reduction of O_2 to H_2O (−75 kcal/mol at pH 7 [215]) with the electrogenic transport of protons across the mitochondrial membrane. The electrochemical gradient thus generated is required for ATP synthase to convert ADP and inorganic phosphate to ATP [85, 216, 217]. C*c*O reduces O_2 without significant leakage of reactive oxygen species through the use of four redox active metal sites (Fig. 12, top left): heme *a* (Fe_a), coordinated by two axial histidines (Fig. 12, bottom left); heme a_3 (Fe_{a3}), coordinated by a single axial histidine (Fig. 12, bottom right); Cu_A, a binuclear T1 copper center bridged by two cysteines (Fig. 12, top right); and Cu_B, a mononuclear copper center coordinated by three histidines, one of which is covalently crosslinked with a tyrosine residue (Fig. 12, bottom right) [218, 219]. Heme *a* and Cu_A serve as electron transfer sites, with each center capable donating one electron in the reduced state (for this section, the reduced and oxidized states of Cu_A will be referred to as Cu_A^I and Cu_A^{II}, respectively). Heme a_3 and Cu_B compose the O_2 reduction site with the copper and iron centers located 5.1 Å apart in a very recent high resolution structure of the fully reduced bovine enzyme (Fig. 12) [217, 219].

The catalytic mechanism of C*c*O requires eight protons and four electrons to reduce O_2, yielding two equivalents of water and the movement of four protons across the mitochondrial membrane [216, 217]. Knowledge of the mechanistic details and relevant intermediates of O_2 reduction by C*c*O is essential to understanding the fundamental chemistry of how nature is able to deliver electrons and protons in a controlled and specific manner. These insights are important for designing new C*c*O inspired materials, electrocatalysts, and fuel cells [220, 221], and there are clear connections to many other chemical or enzymatic systems (utilizing copper, but also iron and manganese). Mechanistic studies of C*c*O have extensively used time resolved rR spectroscopy in combination with isotopic O_2 labeling to elucidate short-lived reduced dioxygen species. Upon addition of O_2 to fully reduced C*c*O an initial species known as the "**A**" or **Oxy** intermediate, containing an Fe–O stretch at 571 cm^{-1}, is formed (Scheme 17) [222–224]. This intermediate was assigned as an $Fe_{a3}^{III}-O_2^{\cdot-}$ species and is consistent with similar oxy-heme species [222]. The decay of intermediate **A** leads to the generation of two new bands attributed to intermediates

"**P**" and "**F**" at 804 cm^{-1} and 785 cm^{-1}, respectively. Early on a surprise, intermediate **P** was found to already be an O-O cleaved species, an $Fe^{IV}_{a3}=O$ entity, indicating that a four electron reduction of O_2 had occurred, despite only three electrons available in the O_2 reduction site (two electrons from heme a_3 and one electron from Cu_B) [225]. No intermediate at the peroxide oxidation level, formed by the reduction of intermediate **A** by the Cu^I center, has been detected, even though by chemical intuition one must go through a (hydro)peroxide species (Scheme 17). The exact source of the fourth electron is still under debate; however, Tyr244 has been proposed as a very likely candidate to provide the final reducing equivalent, plus a proton, necessary to convert O_2 to water [226, 227].

The 785 cm^{-1} band observed in the rR spectrum is attributed to intermediate **F** and has been also assigned as an $Fe^{IV}_{a3}=O$ [229, 230]. Time resolved optical spectroscopy suggests intermediate **F** exists in three states differentiated by the degree of oxidation of sites heme *a* and Cu_A and the oxidation and protonation state of Tyr244, a highly conserved active-site residue believed to be critical to the O_2 reduction reaction (Scheme 17) [228]. In $\mathbf{F_0}$, Fe_a is in the oxidized state following the reduction of the putative tyrosyl radical in **P**. In $\mathbf{F_I}$, the newly generated tyrosinate is protonated to form tyrosine. In $\mathbf{F_{II}}$, Fe_a is reduced by Cu^I_A to give Fe^{II}_a and Cu^{II}_A. Following the disappearance of the 785 cm^{-1} band, a new peak at 450 cm^{-1} appears and is attributed to a hydroxy species (Scheme 17). This assignment was partly made based on the sensitivity of the 450 cm^{-1} stretch with D_2O exchange [229], and partly on the similarities with other ferric heme hydroxides after accounting for H-bonding and assuming a high spin structure [217, 229].

As mentioned, critical to the O_2 reduction reaction is the highly conserved active site residue, Tyr244. In experiments where this tyrosine is mutated to a phenylalanine, the mutant enzyme is unable to perform oxidase chemistry [231]. The isolated modified enzyme contains 0.7 less coppers than the wild type, and rR spectroscopy suggests that heme a_3 exists as a six-coordinate low spin ferric species, where the would-be crosslinked His240 is coordinated to the iron center. Lu and coworkers have studied the effects of the active site tyrosine on O_2 reduction, engineering a Cu_B binding site into myoglobin models (Cu_BMb, Fig. 13, left) [232, 233]. In models where an active site tyrosine is not present, addition of O_2 to the reduced enzyme results in the formation of verdoheme, indicative of heme oxygenase chemistry where self-oxidation of the porphyrin ring occurs [234]. When a tyrosine is engineered into Cu_BMb (F33Y-Cu_BMb or G65Y-Cu_BMb, Fig. 13, middle-left), the mutant enzyme exhibits much greater turnovers (over one thousand for G65Y-Cu_BMb) of O_2 reduction [235]. The difference in reactivity was attributed to G65Y-Cu_BMb containing an H-bonding network which can facilitate delivery of protons to the peroxide intermediate. Hydrogen bonding to, or protonation of, the peroxide may favor heterolytic, rather than homolytic, O-O bond cleavage. Recently, evidence for the H-bonding network in iron-only F33Y-Cu_BMb was shown using EPR and ^{1}H-ENDOR spectroscopies, and X-ray crystallography, illustrating the interaction of discrete water molecules with the oxy-F33Y-Cu_BMb [236]. Further modification of the active site through incorporation of unnatural amino acid imiTyr, a tyrosine derivative containing an imidazole in the *ortho* position on the phenol ring, yielded imiTyrCu_BMb, which contains an active site Tyr-His cross-link (Fig. 13,

middle-right) [237]. The crosslinked mutant demonstrated eight-fold greater selectivity in reducing O_2 to water, and three-fold greater turnovers than the non-crosslinked derivative.

Most recently, Bhagi-Damodaran et al. reported on a study which reflects on why nature may have chosen copper as the non-heme metal in the O_2 reduction site of heme-copper oxidases [238]. In constructs related to those mentioned above, an Mb was engineered to contain a non-heme 3-His-1-Glu binding pocket for Zn, Fe or Cu (Fig. 13, right). Then, they compared the O_2 reactivity of (1) a fully reduced protein termed "Fe^{II}-Fe_BMb", containing an Fe^{II} atom in the non-heme site, with (2) a copper ion analog, "Cu^{I}-Fe_B-Mb". Both the non-heme (plus heme) Fe and Cu engineered proteins exhibit oxidase activity; however, the Cu derivative performed at a rate 3 times faster than that for Fe. The authors attributed this rate enhancement to the Cu ion center in Cu^{II}-Fe_B-Mb possessing a higher reduction potential relative to the non-heme Fe coordination moiety in Fe^{III}-Fe_B-Mb. This results in faster ET from an external reductant to the Cu ion within the hetero-binuclear center, corresponding to the overall rate-limiting step [238].

Various synthetic models have been made to gain additional insight into the catalytic cycle of C*c*O, with a particular emphasis on characterizing intermediates not observed in the native enzyme (such as a peroxide intermediate, which should form in between the **A** and **P** intermediates), and to understand the fundamental chemistry involved in transferring electrons and protons to O_2.

Collman and coworkers designed a binucleating C*c*O model (**1**) featuring a heme macrocycle with an axial imidazole connected via covalent tether and three covalently tethered imidazoles, which serve as ligands for a copper ion located directly above the porphyrin plane, opposite the axial imidazole ligand (Fig. 14, left) [239]. Reaction of **1** with O_2 yielded a species with a rR signal at 570 cm^{-1}, consistent with the **A**/**Oxy** intermediate ($\mathbf{1-O_2^{\cdot-}}$) observed in C*c*O (vide supra). Surprisingly, this complex does not react further to form a peroxide or terminal oxo intermediate due to the copper center remaining in the cuprous state. Addition of two equivalents of a phenol derivative to $\mathbf{1-O_2^{\cdot-}}$ are said to result in the generation of two equivalents of phenoxyl radical, which the authors suggest is consistent with the four electron reduction of O_2 to water [240]. The full reduction of O_2 to water was also complementarily achieved using **1** as an electrocatalyst in buffered aqueous media under physiologically relevant conditions of pH [241].

Naruta and coworkers have synthesized a binucleating C*c*O model featuring a tetradentate copper ligand covalently linked to the heme center (**2**, Fig. 14, middle) [242]. Oxygenation of **2** in MeCN at −30 °C led to the formation of a bridging peroxide species ($\mathbf{2-O_2^{2-}}$), displaying an isotope sensitive peak at 790 cm^{-1} in the rR spectrum. Remarkably, the crystal structure of this peroxide intermediate was obtained revealing a μ-η^2:η^1 bridging heme-copper peroxide, wherein the peroxide ligand is bound side-on with both O-atoms coordinated to the iron atom and end-on, i.e., with one of the peroxide O-atoms, ligated to the copper ion. Magnetic susceptibility and Mössbauer experiments concluded $\mathbf{2-O_2^{2-}}$ contains a high spin $S = 5/2$ iron center antiferromagnetically coupled to an $S = 1/2$ copper center, giving an overall $S = 2$ adduct.

Naruta and coworkers also synthesized a derivative of **2** with a phenol crosslinked imidazole and an axial imidazole base, closely mimicking the coordination of Cu_B and Fe_{a3} (**3**, Fig. 14, right) [243]. Upon oxygenation of **3** at −70 °C a new species ($\mathbf{3}-\mathbf{O_2^{2-}}$) with isotope sensitive rR signals at 787 and 803 cm^{-1} appears, consistent with the formation of a heme-copper peroxide adduct (the two rR signals are attributed to coupled vibrations between the bound O_2^{2-} molecule and the porphyrin molecule; a single peak at 751 cm^{-1} is observed when $^{18}O_2$ is used as the oxygen source). $\mathbf{3}-\mathbf{O_2^{2-}}$ is unstable and decays within 30 min to an intermediate with an isotope sensitive band at 574 cm^{-1}, consistent with a ferric heme superoxide ($\mathbf{3}-\mathbf{O_2^{\cdot-}}$). The conversion from $\mathbf{3}-\mathbf{O_2^{2-}}$ to $\mathbf{3}-\mathbf{O_2^{\cdot-}}$ is enhanced with the addition of water, which led the authors to suggest that water participates in a H-bonding network between the crosslinked phenol and the O_2 moiety, preferentially stabilizing the ferric superoxide state. When the phenol is protected with a methyl ether group (MOM), the generated peroxide complex no longer decays to a super-oxide species.

Karlin and coworkers have extensively studied the chemistry of O_2 reduction by heme-copper centers through variations in the copper and iron coordination environments. Addition of O_2 to a 1:1 mixture of $[Cu^I(TMPA)]^+$ and heme derivative $[(F_8)Fe^{II}]$ led to formation of a bridging peroxide complex $[(F_8)Fe^{III}\text{-}(O_2^{2-})\text{-}Cu^{II}(TMPA)]$ at −40 °C (Fig. 15, left). The identity of this compound was verified by rR spectroscopy, based on the presence of an isotope sensitive band at 808 cm^{-1} [244]. NMR and Möss-bauer spectroscopies revealed the peroxide adduct as a high spin $S = 5/2$ iron complex antiferromagnetically coupled to an $S = 1/2$ copper center, yielding an overall $S = 2$ ground state. Warm up of the peroxide adduct led to the formation of a μ-oxo complex along with 0.5 equivalents of O_2. A covalently tethered derivative of $[Cu^I(TMPA)]^+$ and $[(F_8)\ Fe^{II}]$, called $[(L^6)Fe^{II}Cu^I]$ (Fig. 15, middle), was shown to be a competent electrocatalyst for the selective four-electron reduction of O_2 to water [245]; in fact k_{cat} for the complex is ~10^5 $M^{-1}\ s^{-1}$, about 10-times greater than the best Collman electrocatalyst [241, 246]. Surface-enhanced Raman spectroscopy was concurrently measured during the catalytic reaction, revealing the emergence of an isotope sensitive peak at 819 cm^{-1}, consistent with the presence of a heme-copper bridging peroxide intermediate involved during the O_2 reduction process, the first such insight for electrocatalysis of this type.

Heme-copper peroxide adducts have also been explored using exogenous tridentate copper ligand sources. When $[Cu^I(AN)]^+$ and $[(F_8)Fe^{II}]$ were combined in a 1:1 ratio, addition of O_2 at −80 °C, in THF, led to the formation of peroxide complex $[(F_8)Fe^{III}\text{-}(O_2^{2-})\text{-}Cu^{II}(AN)]$, as supported by the finding of a rR stretch at 756 cm^{-1} [247]. The deviation in the O–O stretch between the two heme-copper peroxide adducts was examined using computational methods, and ultimately attributed to the coordination mode of the peroxide moiety to the copper center. $[(F_8)Fe^{III}\text{-}(O_2^{2-})Cu^{II}(TMPA)]$ was predicted to contain peroxide coordinating η^2 (side-on) to the heme center and η^1 to the copper center, consistent with Naruta's crystal of $\mathbf{2}-\mathbf{O_2^{2-}}$. $[(F_8)Fe^{III}\ O_2^{2-})\text{-}Cu^{II}(AN)]$ was predicted to contain peroxide coordinating η^2 to both heme and copper centers. When one equivalent of 1,5-dicyclohexylimidazole (DCHIm) was added to $[(F_8)\ Fe^{III}\text{-}(O_2^{2-})\text{-}Cu^{II}(AN)]$, a new species formulated as $[(F_8)(DCHIm)Fe^{III}\text{-}(O_2^{2-})\text{-}Cu^{II}(AN)]$ formed (Fig. 15, right). ^{2}H-NMR spectroscopy of the peroxide compound revealed an $S = 0$ ground state where the heme center is an $S = 1/2$ low spin state

antiferromagnetically coupled to the $S = 1/2$ copper center. The low spin compound was shown to be able to react with phenol derivatives to form the O–O cleaved products $[(F_8)Fe^{III}\text{-}OH]$ and $[(AN)Cu^{II}\text{-}OH]^+$ following warm-up, consistent with the two electron reduction of peroxide and the overall four electron reduction of O_2. Experiments using the same phenol derivatives with the corresponding high spin peroxide adduct yielded no such reactivity.

Recently, a new method for generating heme-copper peroxide adducts was reported via addition of 1 equiv. of $[Cu^{I}(MeCN)_4]^+$ to $[(F_8)Fe^{II}(O_2^{\cdot-})]$ at −125 °C (Scheme 18) [248]. The resulting oxygenated adduct, $[(F_8)Fe^{III}\text{-}(O_2^{2-})\text{-}Cu^{II}(solv)]^+$, was assigned as a high spin antiferromagnetically coupled $\eta^2{:}\eta^2$ peroxide-heme-copper complex based on rR spectroscopy ($\upsilon_{O-O} = 737\ cm^{-1}$) and a paramagnetically shifted pyrrolic peak {^{2}H-NMR spectroscopy; $\delta_{pyrrole} = 105$ ppm in THF}. The copper center in this naked synthon is susceptible to exchange the coordinated solvent molecules with exogenously added ligands, opening a new synthetic pathway for $Fe^{III}\text{-}(O_2^{2-})Cu^{II}$(ligand) generation. For example, when TMPA or AN is added to $[(F_8)Fe^{III}\text{-}(O_2^{2-})\text{-}Cu^{II}(solv)]^+$, the corresponding high spin peroxide adducts are reproduced, consistent with previous reports [244, 247]. Furthermore, both low spin analogs of the TMPA and AN heme-copper adducts can be generated through the “naked” method, with the addition of DCHIm.

Even though significant progress has been achieved in understanding the O_2 reduction process in C*c*O and related model systems, key mechanistic aspects still remain enigmatic. There is nearly no information on how post-translational modification of histidine and tyrosine occurs, and the role, if any, heme a_3 or Cu_B plays in the formation of the crosslink (vide infra). The transition from the **A**/**Oxy** intermediate to **P** remains unclear. Chemical intuition and model studies dictate that the reduction of O_2 to water must go through a peroxide intermediate, yet a peroxide has never been detected in the enzymatic system. The order and timing of electron and proton delivery to reach intermediate **P** is uncertain. One may cleave the O–O bond through direct reduction followed by protonation, protonation followed by reduction, or a concerted proton electron transfer process. The details of reductive O–O scission require further exploration and clarification. The nature of the fourth electron donor has yet to be definitively established. Mechanistic studies have shown that O_2 has been reduced by four electrons following the conversion from **A** to **P**, and evidence points to the Tyr244 playing a role as a redox active residue. These details are not only fundamental towards understanding the mechanism of C*c*O, but also how nature delivers protons and electrons in a specific and efficient manner.

Copper-zinc superoxide dismutase

Copper-zinc superoxide dismutase (CuZnSOD) is found as both an intra- and extracellular enzyme in almost all eukaryotic organisms [249]. The active site contains one copper ion ligated by three His residues (in the reduced form) and one zinc ion coordinated by one Asp and three His residues in a distorted tetrahedral geometry (Fig. 16a) [250]. In the oxidized structure, the copper ion is also bound by one water molecule and one of the His residues bound to zinc bridges the two metal ions (Fig. 16b) [251].

CuZnSOD is an antioxidant enzyme responsible for lowering the concentration of superoxide [252] (formed from electron leakage from the mitochondrial electron transport chain or released as a byproduct from some peroxidases [253]) in order to minimize the deleterious reactions of this reactive oxygen species [254–257]. An enzymatic mechanism for CuZnSOD superoxide dismutation has been proposed mainly on the basis of X-ray crystal structures and competitive oxygen kinetic isotope effects (KIEs), see Scheme 19, top and middle [258, 259]. This function proceeds through two near diffusion-limited reactions. In the first step, superoxide is oxidized by the Cu^{II} ion after first binding to the metal ion and inner-sphere ET results in the release of O_2 and generation of a Cu^{I} ion. A second equivalent of superoxide undergoes an outer-sphere reduction to give hydrogen peroxide, giving back the Cu^{II} ion. Neither step is pH dependent if both metal ions (Cu and Zn) are present. However, the absence of zinc (or another divalent metal in that site) leads to drop in function under basic conditions (pH >6) [249].

Early model studies by Lippard and coworkers into the mechanism of CuZnSOD focused on dicopper complexes with imidazolate-containing binucleating ligands [261–263]. Model complexes containing mononuclear copper and zinc complexes bridged by exogenous imidazolate were later studied in an attempt to understand the role of zinc [264–266]. However, reactivity was limited due to the lack of an open site for superoxide to bind. Fukuzumi and coworkers, taking inspiration from Lippard, improved on this aspect, synthesizing heterobinuclear Cu,Zn complexes also utilizing imidazolate-containing binucleating ligands [267, 268]. These Zn^{II}-(imidazolate)-Cu^{II} compounds exhibited the highest SOD activity among previously published models due to the large positive shift of the reduction potential when compared to the mononu-clear copper complex constituents. This observation, which seems counter-intuitive, implies that the Zn^{II} ion plays an important role in regulating the reduction potential, accelerating electron transfer from superoxide to copper [267]. A hydroperoxide complex bearing the same ligand was also reported as a possible intermediate in the SOD mechanism [268], although the reported enzymatic mechanism undergoes outer-sphere electron transfer to produce H_2O_2, precluding the formation of a hydroperoxide intermediate in the enzyme [258].

A recent model study contrasts this proposed enzymatic mechanism (Scheme 19, bottom) [260]. At room temperature, addition of $O_2^{\cdot-}$ to a Cu^{II} model complex resulted in 97% formation of O_2, as confirmed via electrochemical studies. However, at lower temperatures (−40 °C, in CH_3CN), the authors were able to identify a new species, proposed to be a cupric superoxide complex, characterized by UV–Vis spectroscopy, mass spectrometry, and cyclic voltammetry. It was shown that this new low-temperature intermediate does not release O_2, even upon warming. These results imply that the oxidation of $O_2^{\cdot-}$ to O_2 via the Cu^{II} model complex must occur via outer-sphere ET. The authors also showed that this new cupric superoxide species converts to a cupric hydroperoxide upon isolation, presumably gaining a hydrogen atom from solvent. Acidification results in release of hydrogen peroxide, completing the cycle. This synthetic model case exemplifies the fact that, while model systems can be instrumental in elucidating the mechanisms occurring in enzymes, they may proceed differently than in the biological systems.

Cofactor biogenesis

A number of copper-containing enzymes possess special active-site cofactors that are required for function [269–273]. These include the Tyr-Cys, His-Cys, and Tyr-His crosslinks observed in galactose oxidase, hemocyanin/tyrosinase, and C*c*O, respectively, as well as the TPQ cofactor in amine oxidases. They are all thought or known to proceed via formation of an inactive pro-enzyme, which undergoes cofactor biogenesis, all involving oxidation chemistries of nearby active-site amino acid residues. The reactivity and mechanisms of formation of these cofactors are, in fact, of considerable interest themselves with respect to the furthering of our understanding of copper mediated O_2-activation. Fundamental insights have been or can be obtained through elucidation of cofactor biogenesis reactivity.

Amine oxidase

The mechanism of TPQ biogenesis has been explored extensively through spectroscopy and crystallography by the groups of Klinman, Dooley, and Tanizawa (Fig. 17) [87, 273–275]. The consensus mechanism starts with binding of O_2 to a pocket in the protein, which induces a conformational change leading to deprotonation and coordination of the "preprocessed" active site tyrosine (the preprocessed- or pro-enzyme refers to CAO before oxidation of tyrosine to TPQ) and formation of a Cu^{II} tyrosinate complex (Fig. 17a). This Cu^{II} tyrosinate then reacts with O_2 in the binding pocket to form a bridging peroxide with the tyrosine moiety, which, with the addition of a proton, undergoes heterolysis yielding water and a cupric dihydroxyphenylalanine quinone (Cu^{II}-DPQ) intermediate (Fig. 17b).

The activation of O_2 by the Cu^{II} tyrosinate complex has been proposed to go through a Cu^{I}-tyrosyl radical (Scheme 20). However, Solomon and co-workers recently pointed out the lack of experimental evidence for this form of the copper complex [276, 277]. Calculations led them to suggest an alternative view, wherein a concerted two electron transfer from the tyrosinate moiety to dioxygen forms a bridged cupric-substrate peroxide (Scheme 20). In this mechanism, Cu^{II} plays the role of a "spin buffer" and reduces the forbiddenness of the two electron reduction of triplet O_2 by singlet tyrosinate [12].

Following peroxide formation, O-O bond cleavage is facilitated by a second highly conserved active-site tyrosine, postulated to hydrogen-bond to the distal oxygen (relative to copper), which is important in facilitating the direction of cleavage. Replacing this tyrosine with phenylalanine results in the formation of a highly peroxidized TPQ derivative as well as hydroxylation of a nearby methionine residue [278]. Copper-mediated hydrolysis of the DPQ intermediate yields TPQ_{red} (Fig. 17c), which can react with Cu^{I} and O_2 to give TPQ_{ox} and H_2O_2 (Fig. 17d, vide supra). DPQ generated from tyrosine oxygenation is also a key intermediate in the biosynthesis of lysine tyrosyl-quinone (LTQ), an essential cofactor in the lysyl oxidase subgroup of CAOs [273, 279].

Itoh and coworkers were able to model the TPQ biogenesis reaction using a phenol-containing bis-(6-phenylpyridylmethyl)-benzylamine (L^{OH}) Cu^{II} complex (Scheme 21) [96]. Starting with $[(L^{OH})Cu^{II}(CH_3CN)]^+$ in methanol at −60 °C, addition of two equivalents of tri-ethylamine yields $[(L^{O^-})Cu^{II}(CH_3O^-)]$, which reacts with O_2 to ultimately generate a *para*-quinone intermediate through cleavage of a proposed bridging peroxide, similar to the

generation of DPQ in CAO (Scheme 21). Subsequent attack by the copper-bound methoxide on the *para*-quinone gives the final TPQ-like product.

Galactose oxidase

GO can be expressed and isolated prior to formation of its required Tyr-Cys crosslink cofactor (Fig. 18) [280]. The pro-enzyme is able to undergo both aerobic and anaerobic conversion to yield the mature active enzyme. For the aerobic biogenesis reaction, it has been found that both Cu^{I} and Cu^{II} are capable of forming the Tyr-Cys crosslink, where the Cu^{I} reaction occurs 10^4 times faster [99].

Dooley and coworkers have proposed a mechanism for the aerobic and anaerobic biogenesis reaction involving a cupric ion in the pro-enzyme active site (Scheme 22a) [91, 281]. Initial deprotonation and coordination of cysteine to copper allows for ET, yielding a Cu^{I}-cysteinyl radical. This then attacks the nearby tyrosine, generating a one-electron reduced Tyr-Cys moiety. Under aerobic conditions, this moiety and Cu^{I} react with O_2 and a proton to give H_2O_2 and Cu^{II}, following re-aromatization of the Tyr-Cys residue. Under anaerobic conditions, the reduced Tyr-Cys moiety is oxidized by one electron and re-aromatization occurs, concurrent with the loss of a proton giving Cu^{I} and Tyr-Cys as final products.

Whittaker has reported on the crosslink reaction starting from a fully reduced Cu^{I} active site (Scheme 22b) [99]. Kinetics studies reveal the process as O_2 and pH dependent where maximal cofactor biogenesis and minimal solvent isotope effects occur at higher pHs. A mechanism was proposed based on these observations. First, O_2 reacts with the cuprous center to give a $Cu^{II}-(O_2^{\cdot-})$. Near pH 7, the cupric superoxide abstracts a hydrogen atom from the cysteine residue to generate a cysteinyl radical, which attacks a coordinated tyrosinate to give Tyr-Cys and Cu^{I}, following deprotonation and re-aromatization. An additional equivalent of O_2 completes the biogenesis reaction and forms Cu^{II}-(Tyr-Cys$^{\cdot}$). Under higher pH conditions, i.e., above pH 8, the cysteine residue is predominately in the deprotonated form, which would participate in an ET reaction rather than HAT with the cupric superoxide. At lower pH conditions, the release of hydroperoxyl radical from the protonation of the cupric superoxide competes with HAT from cysteine to form the crosslink. Very recently, Solomon and coworkers re-explored this biogenesis reaction using computational methods [282]. It was determined that the pH dependence of biogenesis was due to a rate-limiting deprotonation of the *ortho*-tyrosine proton, following cysteine radical coupling, to give the re-aromatized residue and Cu^{I}.

Many questions need to be addressed to fully understand the Tyr-Cys crosslink formation reaction during biogenesis in galactose oxidase. The oxidation state of copper in vivo prior to crosslink formation is unknown, as both Cu^{I} and Cu^{II} have been shown in vitro to perform the tyrosine-cysteine coupling. Furthermore, few intermediates in the biogenesis reaction cycle have been spectroscopically characterized, and more information must be gathered in order to support the published mechanistic proposals.

Hemocyanin, catechol oxidase, and tyrosinase

A crosslink between histidine and cysteine residues (His-Cys) has been discovered in crystal structures reported for Hc, CaOX, and Ty found in some organisms [130, 152, 156, 283]. The importance and function of this covalent C–S bond is still unknown, but it may simply be a structural requirement. Itoh and coworkers have studied the mechanism of the formation of this interesting crosslink in Ty [283–285]. By crystallographically characterizing both the apo- and holoforms of pro-tyrosinase, the authors were able to show that the crosslink is only formed upon addition of copper ions to the protein (Fig. 19) [284]. Through mutagenesis experiments, the authors also proposed that the Cys92 residue (along with two other Cys residues) may be responsible for chaperoning the copper ions into the active site.

The reactive intermediate in the initial step leading to the crosslink formation may be a μ-η^2:η^2-peroxodicopper(II) complex and multiple lines of evidence support this supposition [283]. This O_2-derived complex abstracts a hydrogen atom from Cys92 to form a cysteinyl radical. The latter then couples to the ε-C of His94 to form the C-S bond. The copper-oxygen species resulting from the initial HAT reaction could then abstract a second hydrogen atom, to give a bis-(μ-hydroxo)dicopper(II) complex and the fully formed His-Cys crosslink (Scheme 23) [285].

While μ-η^2:η^2-peroxodicopper(II) complexes are known to usually perform hydroxylation reactions (via EAS, vide supra) and not HAT reactions, there are a few examples of such chemistry in model systems. In 2005, Feiters and coworkers appended tri- and tetradentate ligands to diphenylglycoluril basket receptors in order to synthesize supramolecular catalysts [286]. In this study, it was shown that the $[\mathrm{Cu_2^{II}}(\mu-\eta^2:\eta^2-{O_2}^{2-})]^{2+}$ complex formed exhibited oxidative polymerization of phenols instead of hydroxylation. A more recent study by Franc Meyer and coworkers showed that μ-η^2:η^2-peroxodicopper(II) complexes formed with bis(oxazoline) ligands performed C–C bond coupling when using 2,4-di-*tert*-butylphenol as a substrate [287]. These model systems show that, while HAT is not common for μ-η^2:η^2-peroxodicopper(II) complexes, it can still be achieved.

Heme-copper oxidases

As discussed above, a post-translationally modified tyros-ine-histidine crosslink has been shown to be essential to C*c*O, and more broadly HCO function, yet virtually nothing is known about how this crosslink forms [233, 288]. Some studies with cytochrome *bo*, an HCO which contains the same Tyr-Cys crosslink as in C*c*O, give some evidence on possible intermediates in the cofactor biogenesis reaction. When cytochrome *bo* was grown using the fully ring-deuterated tyrosine derivative, d^4-Tyr, a 19% reduction in oxidase activity was observed vs. the native enzyme [289]. The authors postulated the decreased activity was due to a lower yield of mature enzyme containing the Tyr-Cys crosslink. The reduction in crosslink formation was attributed to a higher barrier in generating a radical on the *ortho*-carbon on tyrosine caused by deuteration at that position, and thereby deterring crosslink formation.

Obviously, significant experimental progress needs to be made to even begin to rationalize how the cofactor biogenesis reaction occurs in HCOs. Part of the problem in studying the

Tyr-His crosslink formation reaction can be attributed to the inability to isolate a pro-enzyme prior to crosslink formation. This may be an inherently difficult challenge due to the potential structural support the Tyr-His crosslink provides [231].

In spite of the lack of mechanistic studies reported for crosslink formation in HCOs, one may propose mechanisms based on information gained from the catalytic cycle or similar cofactor biogenesis reactions in copper-dependent enzymes (Scheme 24). In an O_2-dependent pathway inspired by the catalytic cycle (Scheme 24a) [217], an intermediate similar to **P** may be generated in the pro-enzyme active site from HAT-induced O-O bond cleavage by the active-site Tyr. A copper-coordinated imidazole could then attack the tyrosyl radical (possibly after initial deprotonation), forming the C–N bond and simultaneously reducing (and protonating) the high-valent Fe^{IV}=O moiety to give an Fe^{III}-OH species. Following re-aromatization of the Tyr residue, proton transfer gives the Hydroxy intermediate of the enzyme. Inspired by a mechanism put forth by Kitagawa and coworkers [289], an O_2-independent pathway is also proposed (Scheme 24b). Starting with the Hydroxy intermediate, deprotonation of the active-site Tyr residue and ET to Cu^{II} yields a Cu^{I} tyrosyl radical species. Attack of the imidazole coordinated to copper on the tyrosyl radical, with concomitant ET to heme a_3 and loss of proton, gives the crosslinked residue. Re-aromatization yields the fully reduced active site with the Tyr-His crosslink. An effective way to test the validity of the above proposed mechanisms may be through the use of small molecule synthetic complexes or engineered biomolecules.

Conclusions

Copper enzymes have been illustrated to process dioxygen in an efficient and purposeful manner. Working together, enzymologists and synthetic model chemists have, through careful and clever experimental design, pulled back the veil of mystery surrounding how nature is able to utilize the second most abundant gas in the atmosphere to accomplish the necessary transformations critical to sustaining aerobic life. Yet, the more we learn about these processes, we arrive at the realization of how much more there is left to understand. Issues at hand include the following: (1) What is the exact role of methionine ligation in non-coupled binuclear copper monooxygneases? (2) What is the reactive copper-oxygen species responsible for polysaccharide oxidation in LPMOs? (3) What is the identity of the species which reduces O_2 in mononuclear copper oxidases (CAO, GO)? (4) What role does the quercetin radical play in the activation of O_2 in 2,4-QD? (5) Does the two-electron reduction of O_2 occur via a stepwise or concerted process in Hc? (6) What is the active copper-oxygen species responsible for methane oxidation in pMMO and by what mechanism does this occur? (7) What is the coordination of O_2^{2-} in the MCO peroxy intermediate? (8) How are protons and electrons delivered (and in what order?) to the **A**/**Oxy** intermediate to give the **P** intermediate in CcO? Is it proton transfer or H-bonding that is key? (9) What are the relevant intermediates in the Tyr-Cys crosslink formation in GO cofactor biogenesis, and what is the in vivo oxidation state of copper responsible for biogenesis? (10) What is the importance of the His-Cys crosslink in coupled binuclear copper enzymes (Hc, CaOX, Ty)? (11) How is the Tyr-His crosslink formed in HCOs, and what are the relevant intermediates in crosslink formation?

Synthetic or engineered models serve as facile launching pads to systematically test and evaluate a plethora of ideas and hypotheses. However, models cannot, by definition, duplicate the exact conditions found in native biological systems, nor should they necessarily try. Only through continued collaboration between enzymologists and model chemists can we make further progress towards understanding the intertwinement between copper and oxygen in biological systems.

Acknowledgments

This work was supported by research Grants from National Institutes of Health (R01 GM 028962 and R01 GM 060353 to K.D.K).

References

1. Kroneck, PMH., Torres, MES., editors. Sustaining life on planet earth: metalloenzymes mastering dioxygen and other chewy gases. Springer International Publishing; Switzerland: 2015.
2. Campbell AN, Stahl SS. Acc Chem Res. 2012; 45:851–863. [PubMed: 22263575]
3. Mccann SD, Stahl SS. Acc Chem Res. 2015; 48:1756–1766. [PubMed: 26020118]
4. Gubelmann, MH., Williams, AF. Struct Bonding. Vol. 55. Berlin: 1983. p. 1-65.
5. Sawyer, DT. Oxygen chemistry. Oxford University Press; New York: 1991.
6. Bakac A. Inorg Chem. 2010; 49:3584–3593. [PubMed: 20380460]
7. Armstrong DA, Huie RE, Koppenol WH, Lymar SV, Merenyi G, Neta P, Ruscic B, Stanbury DM, Steenken S, Wardman P. Pure Appl Chem. 2015; 87:1139–1150.
8. Sheldon, RA., Kochi, JK. Metal-catalyzed oxidations of organic compounds. Academic Press, Inc; New York: 1981.
9. Ray K, Pfaff FF, Wang B, Nam W. J Am Chem Soc. 2014; 136:13942–13958. [PubMed: 25215462]
10. Engelmann X, Monte-Pérez I, Ray K. Angew Chem Int Ed. 2016; 55:7632–7649.
11. Sahu S, Goldberg DP. J Am Chem Soc. 2016; 138:11410–11428. [PubMed: 27576170]
12. Solomon EI, Heppner DE, Johnston EM, Ginsbach JW, Cirera J, Qayyum M, Kieber-Emmons MT, Kjaergaard CH, Hadt RG, Tian L. Chem Rev. 2014; 114:3659–3853. [PubMed: 24588098]
13. Mirica LM, Ottenwaelder X, Stack TDP. Chem Rev. 2004; 104:1013–1045. [PubMed: 14871148]
14. Lewis EA, Tolman WB. Chem Rev. 2004; 104:1047–1076. [PubMed: 14871149]
15. Hatcher LQ, Karlin KD. J Biol Inorg Chem. 2004; 9:669–683. [PubMed: 15311336]
16. Itoh, S. Copper-oxygen chemistry. Karlin, KD., Itoh, S., editors. Wiley; Hoboken: 2011. p. 225-282.
17. Liu JJ, Diaz DE, Quist DA, Karlin KD. Isr J Chem. 2016; 56:738–755.
18. Jacobson RR, Tyeklar Z, Farooq A, Karlin KD, Liu S, Zubieta J. J Am Chem Soc. 1988; 110:3690–3692.
19. Kitajima N, Fujisawa K, Morooka Y, Toriumi K. J Am Chem Soc. 1989; 111:8975–8976.
20. Halfen JA, Mahapatra S, Wilkinson EC, Kaderli S, Young VG, Que L, Zuberbühler AD, Tolman WB. Science. 1996; 271:1397–1400. [PubMed: 8596910]
21. Mahapatra S, Halfen JA, Wilkinson EC, Pan G, Wang X, Young VG, Cramer CJ, Que L, Tolman WB. J Am Chem Soc. 1996; 118:11555–11574.
22. Dubois JL, Mukherjee P, Collier AM, Mayer JM, Solomon EI, Hedman B, Stack TDP, Hodgson KO. J Am Chem Soc. 1997; 119:8578–8579.
23. Mahadevan V, Hou Z, Cole AP, Root DE, Lal TK, Solomon EI, Stack TDP. J Am Chem Soc. 1997; 119:11996–11997.
24. Karlin KD, Cruse RW, Gultneh Y, Hayes JC, Zubieta J. J Am Chem Soc. 1984; 106:3372–3374.
25. Pate JE, Cruse RW, Karlin KD, Solomon EI. J Am Chem Soc. 1987; 109:2624–2630.
26. Mahroof-Tahir M, Murthy NN, Karlin KD, Blackburn NJ, Shaikh SN, Zubieta J. Inorg Chem. 1992; 31:3001–3003.

27. Cao R, Saracini C, Ginsbach JW, Kieber-Emmons MT, Siegler MA, Solomon EI, Fukuzumi S, Karlin KD. J Am Chem Soc. 2016; 138:7055–7066. [PubMed: 27228314]
28. Kindermann N, Bill E, Dechert S, Demeshko S, Reijerse EJ, Meyer F. Angew Chem Int Ed. 2015; 54:1738–1743.
29. Baldwin MJ, Root DE, Pate JE, Fujisawa K, Kitajima N, Solomon EI. J Am Chem Soc. 1992; 114:10421–10431.
30. Tyeklar Z, Jacobson RR, Wei N, Murthy NN, Zubieta J, Karlin KD. J Am Chem Soc. 1993; 115:2677–2689.
31. Karlin KD, Wei N, Jung B, Kaderli S, Zuberbühler AD. J Am Chem Soc. 1991; 113:5868–5870.
32. Fujisawa K, Tanaka M, Morooka Y, Kitajima N. J Am Chem Soc. 1994; 116:12079–12080.
33. Würtele C, Gaoutchenova E, Harms K, Holthausen MC, Sundermeyer J, Schindler S. Angew Chem Int Ed. 2006; 45:3867–3869.
34. Aboelella NW, Lewis EA, Reynolds AM, Brennessel WW, Cramer CJ, Tolman WB. J Am Chem Soc. 2002; 124:10660–10661. [PubMed: 12207513]
35. Donoghue PJ, Tehranchi J, Cramer CJ, Sarangi R, Solomon EI, Tolman WB. J Am Chem Soc. 2011; 133:17602–17605. [PubMed: 22004091]
36. Gagnon N, Tolman WB. Acc Chem Res. 2015; 48:2126–2131. [PubMed: 26075312]
37. Dhar D, Yee GM, Spaeth AD, Boyce DW, Zhang H, Dereli B, Cramer CJ, Tolman WB. J Am Chem Soc. 2016; 138:356–368. [PubMed: 26693733]
38. Prigge ST, Eipper BA, Mains RE, Amzel LM. Science. 2004; 304:864–867. [PubMed: 15131304]
39. Li X, Beeson WT IV, Phillips CM, Marletta MA, Cate JHD. Structure. 2012; 20:1051–1061. [PubMed: 22578542]
40. Magnus KA, Hazes B, Ton-That H, Bonaventura C, Bonaventura J, Hol WGJ. Proteins Struct Funct Genet. 1994; 19:302–309. [PubMed: 7984626]
41. Wilmot CM, Hajdu J, McPherson MJ, Knowles PF, Phillips SEV. Science. 1999; 286:1724–1728. [PubMed: 10576737]
42. Atherton NM, Gibson QH, Greenwood C. Biochem J. 1963; 86:541–555. [PubMed: 13947736]
43. Brunori M, Noble RW, Antonini E, Wyman J. J Biol Chem. 1966; 241:5238–5243. [PubMed: 5928000]
44. Noble RW, Gibson QH, Brunori M, Antonini E, Wyman J. J Biol Chem. 1969; 244:3905–3908. [PubMed: 5805403]
45. Greenwood C, Gibson QH. J Biol Chem. 1967; 242:1782–1787. [PubMed: 4290651]
46. Ferguson-Miller S, Babcock GT. Chem Rev. 1996; 96:2889–2907. [PubMed: 11848844]
47. Szundi I, Liao GL, Einarsdóttir O. Biochemistry. 2001; 40:2332–2339. [PubMed: 11327853]
48. Fry HC, Scaltrito DV, Karlin KD, Meyer GJ. J Am Chem Soc. 2003; 125:11866–11871. [PubMed: 14505408]
49. Saracini C, Liakos DG, Zapata Rivera JE, Neese F, Meyer GJ, Karlin KD. J Am Chem Soc. 2014; 136:1260–1263. [PubMed: 24428309]
50. Momenteau M, Reed CA. Chem Rev. 1994; 94:659–698.
51. Zhang CX, Kaderli S, Costas M, Kim E-I, Neuhold Y-M, Karlin KD, Zuberbühler AD. Inorg Chem. 2003; 42:1807–1824. [PubMed: 12639113]
52. Kunishita A, Ertem MZ, Okubo Y, Tano T, Sugimoto H, Ohkubo K, Fujieda N, Fukuzumi S, Cramer CJ, Itoh S. Inorg Chem. 2012; 51:9465–9480. [PubMed: 22908844]
53. Andrew CR, McKillop KP, Sykes AG. Biochim Biophys Acta. 1993; 1162:105–114. [PubMed: 8448173]
54. Rodriguez-Lopez JN, Fenoll LG, Garcia-Ruiz PA, Varon R, Tudela J, Thorneley RNF, Garcia-Canovas F. Biochemistry. 2000; 39:10497–10506. [PubMed: 10956040]
55. Karlin KD, Haka MS, Cruse RW, Gultneh Y. J Am Chem Soc. 1985; 107:5828–5829.
56. Park GY, Qayyum MF, Woertink J, Hodgson KO, Hedman B, Sarjeant AAN, Solomon EI, Karlin KD. J Am Chem Soc. 2012; 134:8513–8524. [PubMed: 22571744]
57. Osborne, RL., Klinman, JP. Copper-oxygen chemistry. Karlin, KD., Itoh, S., editors. Wiley; Hoboken: 2011. p. 1-22.

58. Kline CD, Blackburn NJ. Biochemistry. 2016; doi: 10.1021/acs.biochem.6b00845
59. Vendelboe TV, Harris P, Zhao Y, Walter TS, Harlos K, El Omari K, Christensen HEM. Sci Adv. 2016; 2:e1500980. [PubMed: 27152332]
60. Evans JP, Ahn K, Klinman JP. J Biol Chem. 2003; 278:49691–49698. [PubMed: 12966104]
61. Chen P, Solomon EI. J Am Chem Soc. 2004; 126:4991–5000. [PubMed: 15080705]
62. Itoh S. Acc Chem Res. 2015; 48:2066–2074. [PubMed: 26086527]
63. Peterson RL, Himes RA, Kotani H, Suenobu T, Tian L, Siegler MA, Solomon EI, Fukuzumi S, Karlin KD. J Am Chem Soc. 2011; 133:1702–1705. [PubMed: 21265534]
64. Lee JY, Peterson RL, Ohkubo K, Garcia-Bosch I, Himes RA, Woertink J, Moore CD, Solomon EI, Fukuzumi S, Karlin KD. J Am Chem Soc. 2014; 136:9925–9937. [PubMed: 24953129]
65. Kunishita A, Kubo M, Sugimoto H, Ogura T, Sato K, Takui T, Itoh S. J Am Chem Soc. 2009; 131:2788–2789. [PubMed: 19209864]
66. May SW, Phillips RS, Mueller PW, Herman HH. J Biol Chem. 1981; 256:8470–8475. [PubMed: 7263663]
67. Kim S, Lee JY, Cowley RE, Ginsbach JW, Siegler MA, Solomon EI, Karlin KD. J Am Chem Soc. 2015; 137:2796–2799. [PubMed: 25697226]
68. Kodera M, Kita T, Miura I, Nakayama N, Kawata T, Kano K, Hirota S. J Am Chem Soc. 2001; 123:7715–7716. [PubMed: 11481001]
69. Tubbs KJ, Fuller AL, Bennett B, Arif Atta M, Makowska-Grzyska MM, Berreau LM. Dalton Trans. 2003:3111–3116.
70. Aboelella NW, Gherman BF, Cramer CJ, Tolman WB. J Am Chem Soc. 2006; 128:3445–3458. [PubMed: 16522125]
71. Zhou L, Powell D, Nicholas KM. Inorg Chem. 2006; 45:3840–3842. [PubMed: 16676937]
72. Zhou L, Powell D, Nicholas KM. Inorg Chem. 2007; 46:7789–7799. [PubMed: 17713902]
73. Zhou L, Nicholas KM. Inorg Chem. 2008; 47:4356–4367. [PubMed: 18399624]
74. Park GY, Lee Y, Lee D-H, Woertink JS, Narducci Sarjeant AA, Solomon EI, Karlin KD. Chem Commun. 2010; 46:91–93.
75. Tano T, Mieda K, Sugimoto H, Ogura T, Itoh S. Dalton Trans. 2014; 43:4871–4877. [PubMed: 24492382]
76. Maji RC, Bhandari A, Singh R, Roy S, Chatterjee SK, Bowles FL, Ghiassi KB, Maji M, Olmstead MM, Patra AK. Dalton Trans. 2015; 44:17587–17599. [PubMed: 26390838]
77. Beeson WT, Vu VV, Span EA, Phillips CM, Marletta MA. Annu Rev Biochem. 2015; 84:923–946. [PubMed: 25784051]
78. Frandsen KEH, Simmons TJ, Dupree P, Poulsen JN, Hemsworth GR, Ciano L, Johnston EM, Tovborg M, Johansen KS, von Freiesleben P, Marmuse L, Fort S, Cottaz S, Driguez H, Henrissat B, Lenfant N, Tuna F, Baldansuren A, Davies GJ, Lo Leggio L, Walton PH. Nat Chem Biol. 2016; 12:298–303. [PubMed: 26928935]
79. Span EA, Marletta MA. Curr Opin Struct Biol. 2015; 35:93–99. [PubMed: 26615470]
80. Hemsworth GR, Johnston EM, Davies GJ, Walton PH. Trends Biotechnol. 2015; 33:747–761. [PubMed: 26472212]
81. Kim S, Ståhlberg J, Sandgren M, Paton RS, Beckham GT. Proc Natl Acad Sci USA. 2014; 111:149–154. [PubMed: 24344312]
82. Walton PH, Davies GJ. Curr Opin Chem Biol. 2016; 31:195–207. [PubMed: 27094791]
83. Dhar D, Tolman WB. J Am Chem Soc. 2015; 137:1322–1329. [PubMed: 25581555]
84. Phillips CM, Beeson WT, Cate JH, Marletta MA. ACS Chem Biol. 2011; 6:1399–1406. [PubMed: 22004347]
85. Peterson, RL., Kim, S., Karlin, KD. Comprehensive inorganic chemistry II. 2. Reedijk, J., Poeppelmeier, K., editors. Elsevier; Oxford: 2013. p. 149-177.
86. Parsons MR, Convery MA, Wilmot CM, Yadav KDS, Blakeley V, Corner AS, Phillips S, McPherson MJ, Knowles PF. Structure. 1995; 3:1171–1184. [PubMed: 8591028]
87. Wilce MCJ, Dooley DM, Freeman HC, Guss JM, Matsunami H, McIntire WS, Ruggiero CE, Tanizawa K, Yamaguchi H. Biochemistry. 1997; 36:16116–16133. [PubMed: 9405045]

88. Li R, Klinman JP, Mathews FS. Structure. 1998; 6:293–307. [PubMed: 9551552]
89. Cai D, Klinman JP. J Biol Chem. 1994; 269:32039–32042. [PubMed: 7798196]
90. Kim M, Okajima T, Kishishita S, Yoshimura M, Kawamori A, Tanizawa K, Yamaguchi H. Nat Struct Biol. 2002; 9:591–596. [PubMed: 12134140]
91. Rokhsana, D., Shepard, EM., Brown, DE., Dooley, DM. Copper-oxygen chemistry. Karlin, KD., Itoh, S., editors. Wiley; Hoboken: 2011. p. 53-106.
92. Mills SA, Klinman JP. J Am Chem Soc. 2000; 122:9897–9904.
93. Mure M, Mills SA, Klinman JP. Biochemistry. 2002; 41:9269–9278. [PubMed: 12135347]
94. Shepard EM, Okonski KM, Dooley DM. Biochemistry. 2008; 47:13907–13920. [PubMed: 19053231]
95. Liu Y, Mukherjee A, Nahumi N, Ozbil M, Brown D, Angeles-Boza AM, Dooley DM, Prabhakar R, Roth JP. J Phys Chem B. 2013; 117:218–229. [PubMed: 23240607]
96. Tabuchi K, Ertem MZ, Sugimoto H, Kunishita A, Tano T, Fujieda N, Cramer CJ, Itoh S. Inorg Chem. 2011; 50:1633–1647. [PubMed: 21284380]
97. Mure M, Klinman JP. J Am Chem Soc. 1995; 117:8698–8706.
98. Whittaker MM, Whittaker JW. J Biol Chem. 1988; 263:6074–6080. [PubMed: 2834363]
99. Whittaker MM, Whittaker JW. J Biol Chem. 2003; 278:22090–22101. [PubMed: 12672814]
100. Kelleher FM, Bhavanandan VP. J Biol Chem. 1986; 261:11045–11048. [PubMed: 3733747]
101. Ito N, Phillips SEV, Stevens C, Ogel ZB, McPherson MJ, Keen JN, Yadav KDS, Knowles PF. Nature. 1991; 350:87–90. [PubMed: 2002850]
102. Johnson JM, Halsall HB, Heineman WR. Biochemistry. 1985; 24:1579–1585. [PubMed: 4005217]
103. Stubbe J, van der Donk WA. Chem Rev. 1998; 98:705–762. [PubMed: 11848913]
104. Whittaker JW. Chem Rev. 2003; 103:2347–2363. [PubMed: 12797833]
105. Thomas F, Gellon G, Gautier-Luneau I, Saint-Aman E, Pierre J-L. Angew Chem Int Ed. 2002; 41:3047–3050.
106. Thomas F. Eur J Inorg Chem. 2007; 2007:2379–2404.
107. Jazdzewski BA, Reynolds AM, Holland PL, Young VG, Kaderli S, Zuberbühler AD, Tolman WB. J Biol Inorg Chem. 2003; 8:381–393. [PubMed: 12761659]
108. Lyons CT, Stack TDP. Coord Chem Rev. 2013; 257:528–540. [PubMed: 23264696]
109. Itoh S, Taki M, Fukuzumi S. Coord Chem Rev. 2000; 198:3–20.
110. John A, Shaikh MM, Ghosh P. Dalton Trans. 2008:2815–2824. [PubMed: 18478142]
111. Ghorai S, Sarmah A, Roy RK, Tiwari A, Mukherjee C. Inorg Chem. 2016; 55:1370–1380. [PubMed: 26812584]
112. Fusetti F, Schröter KH, Steiner RA, Van Noort PI, Pijning T, Rozeboom HJ, Kalk KH, Egmond MR, Dijkstra BW. Structure. 2002; 10:259–268. [PubMed: 11839311]
113. Gopal B, Madan LL, Betz SF, Kossiakoff AA. Biochemistry. 2005; 44:193–201. [PubMed: 15628860]
114. Schaab M, Barney B, Francisco W. Biochemistry. 2006; 45:1009–1016. [PubMed: 16411777]
115. Merkens H, Kappl R, Jakob RP, Schmid FX, Fetzner S. Biochemistry. 2008; 47:12185–12196. [PubMed: 18950192]
116. Steiner RA, Kalk KH, Dijkstra BW. Proc Natl Acad Sci USA. 2002; 99:16625–16630. [PubMed: 12486225]
117. Steiner RA, Kooter IM, Dijkstra BW. Biochemistry. 2002; 41:7955–7962. [PubMed: 12069585]
118. Kaizer, J., Pap, JS., Speier, G. Copper-oxygen chemistry. Karlin, KD., Itoh, S., editors. Wiley; Hoboken: 2011. p. 23-52.
119. Balogh-Hergovich E, Speier G. J Org Chem. 2001; 66:7974–7978. [PubMed: 11722193]
120. Balogh-Hergovich E, Kaizer J, Speier G, Fulop V, Parkanyi L. Inorg Chem. 1999; 38:3787–3795.
121. Barhács L, Kaizer J, Pap J, Speier G. Inorg Chim Acta. 2001; 320:83–91.
122. Matuz A, Giorgi M, Speier G, Kaizer J. Polyhedron. 2013; 63:41–49.
123. Balogh-Hergovich E, Kaizer J, Speier G. J Mol Catal A Chem. 2003; 206:83–87.

124. Sun Y-J, Huang Q-Q, Tano T, Itoh S. Inorg Chem. 2013; 52:10936–10948. [PubMed: 24044415]
125. Sun Y-J, Huang Q-Q, Li P, Zhang J-J. Dalton Trans. 2015; 73:13926–13938.
126. Siegbahn PEM. Biochemistry. 2004; 43:16625–16630.
127. Saito T, Kawakami T, Yamanaka S, Okumura M. J Phys Chem B. 2015; 119:6952–6962. [PubMed: 25990020]
128. Liddington R, Derewenda Z, Dodson E, Hubbard R, Dodson G. J Mol Biol. 1992; 228:551–579. [PubMed: 1453464]
129. Holmes MA, Le Trong I, Turley S, Sieker LC, Stenkamp RE. J Mol Biol. 1991; 218:583–593. [PubMed: 2016748]
130. Cuff ME, Miller KI, van Holde KE, Hendrickson WA. J Mol Biol. 1998; 278:855–870. [PubMed: 9614947]
131. Eickman NC, Himmelwright RS, Solomon EI. Proc Natl Acad Sci USA. 1979; 76:2094–2098. [PubMed: 287049]
132. Karlin KD, Haka MS, Cruse RW, Meyer GJ, Farooq A, Gultneh Y, Hayes JC, Zubieta J. J Am Chem Soc. 1988; 110:1196–1207.
133. Karlin KD, Tyeklár Z, Farooq A, Haka MS, Ghosh P, Cruse RW, Gultneh Y, Hayes JC, Toscano PJ, Zubieta J. Inorg Chem. 1992; 31:1436–1451.
134. Magnus KA, Ton-That H, Carpenter JE. Chem Rev. 1994; 94:727–735.
135. Metz M, Solomon EI. J Am Chem Soc. 2001; 123:4938–4950. [PubMed: 11457321]
136. Loehr JS, Freedman TB, Loehr TM. Biochem Biophys Res Commun. 1974; 56:510–515. [PubMed: 4823878]
137. Brown JM, Powers L, Kincaid B, Larrabee JA, Spiro TG. J Am Chem Soc. 1980; 102:4210–4216.
138. Eccles TK. J Am Chem Soc. 1981; 103:984–986.
139. Dooley DM, Scott RA, Ellinghaus J, Solomon EI, Gray B, Dooley DM, Scott RA, Ellinghaust JOE, Solomon EI, Gray HB. Proc Natl Acad Sci USA. 1978; 75:3019–3022. [PubMed: 98765]
140. Salvato B, Santamaria M, Beltramini M, Alzuet G, Casella L. Biochemistry. 1998; 37:14065–14077. [PubMed: 9760242]
141. Zlateva T, Di Muro P, Salvato B, Beltramini M. FEBS Lett. 1996; 384:251–254. [PubMed: 8617365]
142. Nillius D, Jaenicke E, Decker H. FEBS Lett. 2008; 582:749–754. [PubMed: 18258201]
143. Decker H, Ryan M, Jaenicke E, Terwilliger N. J Biol Chem. 2001; 276:17796–17799. [PubMed: 11278677]
144. Baird S, Kelly SM, Price NC, Jaenicke E, Meesters C, Nillius D, Decker H, Nairn J. Biochim Biophys Acta Proteins Proteomics. 2007; 1774:1380–1394.
145. Morioka C, Tachi Y, Suzuki S, Itoh S. J Am Chem Soc. 2006; 128:6788–6789. [PubMed: 16719449]
146. Suzuki K, Shimokawa C, Morioka C, Itoh S. Biochemistry. 2008; 47:7108–7115. [PubMed: 18553939]
147. Decker H, Rimke T. J Biol Chem. 1998; 273:25889–25892. [PubMed: 9748264]
148. Lee SY, Lee BL, Söderhäll K. Biochem Biophys Res Commun. 2004; 322:490–496. [PubMed: 15325257]
149. Nagai T, Kawabata SI. J Biol Chem. 2000; 275:29264–29267. [PubMed: 10880508]
150. Nagai T, Osaki T, Kawabata SI. J Biol Chem. 2001; 276:27166–27170. [PubMed: 11375396]
151. Saracini C, Ohkubo K, Suenobu T, Meyer GJ, Karlin KD, Fukuzumi S. J Am Chem Soc. 2015; 137:15865–15874. [PubMed: 26651492]
152. Klabunde T, Eicken C, Sacchettini JC, Krebs B. Nat Struct Biol. 1998; 5:1084–1090. [PubMed: 9846879]
153. Virador VM, Grajeda JPR, Blanco-Labra A, Mendiola-Olaya E, Smith GM, Moreno A, Whitaker JR. J Agric Food Chem. 2010; 58:1189–1201. [PubMed: 20039636]
154. Matoba Y, Kumagai T, Yamamoto A, Yoshitsu H, Sugiyama M. J Biol Chem. 2006; 281:8981–8990. [PubMed: 16436386]

155. Sendovski M, Kanteev M, Ben-Yosef VS, Adir N, Fishman A. J Mol Biol. 2011; 405:227–237. [PubMed: 21040728]
156. Ismaya WT, Rozeboom J, Weijn A, Mes JJ, Fusetti F. Biochemistry. 2011; 50:5477–5486. [PubMed: 21598903]
157. Fujimoto K, Okino N, Kawabata S, Iwanaga S, Ohnishi E. Proc Natl Acad Sci USA. 1995; 92:7769–7773. [PubMed: 7644493]
158. Li Y, Wang Y, Jiang H, Deng J. Proc Natl Acad Sci USA. 2009; 106:17002–17006. [PubMed: 19805072]
159. Morrison R, Mason K, Frostmason S. Pigment Cell Res. 1994; 7:388–393. [PubMed: 7761346]
160. Eickman NC, Solomon EI, Larrabee JA, Spiro TG, Lerch K. J Am Chem Soc. 1978; 100:6529–6531.
161. Peñalver MJ, Rodríguez-López JN, García-Ruiz PA, García-Cánovas F, Tudela J. Biochim Biophys Acta Proteins Proteomics. 2003; 1650:128–135.
162. Fenoll LG, Peñalver MJ, Rodríguez-López JN, García-Ruiz PA, García-Cánovas F, Tudela J. Biochem J. 2004; 380:643–650. [PubMed: 15025557]
163. Yamazaki SI, Itoh S. J Am Chem Soc. 2003; 125:13034–13035. [PubMed: 14570470]
164. Fujieda N, Murata M, Yabuta S, Ikeda T, Shimokawa C, Nakamura Y, Hata Y, Itoh S. J Biol Inorg Chem. 2013; 18:19–26. [PubMed: 23053534]
165. Tripathi RK, Hearing VJ, Urabe K, Aroca P, Spritz RA. J Biol Chem. 1992; 267:23707–23712. [PubMed: 1429711]
166. Olivares C, García-Borrón JC, Solano F. Biochemistry. 2002; 41:679–686. [PubMed: 11781109]
167. Ben-Yosef VS, Sendovski M, Fishman A. Enzyme Microb Technol. 2010; 47:372–376.
168. Goldfeder M, Kanteev M, Isaschar-Ovdat S, Adir N, Fishman A. Nat Commun. 2014; 5:4505. [PubMed: 25074014]
169. Kanteev M, Goldfeder M, Fishman A. Protein Sci. 2015; 24:1360–1369. [PubMed: 26104241]
170. Solem E, Tuczek F, Decker H. Angew Chem Int Ed. 2016; 55:2884–2888.
171. Mirica LM, Vance M, Rudd DJ, Hedman B, Hodgson KO, Solomon EI, Stack TDP. Science. 2005; 308:1890–1892. [PubMed: 15976297]
172. Curse RW, Kaderli S, Karlin KD, Zuberbühler AD. J Am Chem. 1988; 110:6882–6883.
173. Nasir MS, Cohen BI, Karlin KD. J Am Chem Soc. 1992; 114:2482–2494.
174. Karlin KD, Nasir MS, Cohen BI, Cruse RW, Kaderli S, Zuber-bühler AD. J Am Chem Soc. 1994; 116:1324–1336.
175. Itoh S, Kumei H, Taki M, Nagatomo S, Kitagawa T, Fukuzumi S. J Am Chem Soc. 2001; 123:6708–6709. [PubMed: 11439064]
176. Osako T, Ohkubo K, Taki M, Tachi Y, Fukuzumi S, Itoh S. J Am Chem Soc. 2003; 125:11027–11033. [PubMed: 12952484]
177. Mirica LM, Rudd DJ, Vance MA, Solomon EI, Hodgson KO, Hedman B, Stack TDP. J Am Chem Soc. 2006; 128:2654–2665. [PubMed: 16492052]
178. Noguchi A, Kitamura T, Onaka H, Horinouchi S, Ohnishi Y. Nat Chem Biol. 2010; 6:641–643. [PubMed: 20676084]
179. Ginsbach JW, Kieber-Emmons MT, Nomoto R, Noguchi A, Ohnishi Y, Solomon EI. Proc Natl Acad Sci USA. 2012; 109:10793–10797. [PubMed: 22711806]
180. Toussaint O, Lerch K. Biochemistry. 1987; 26:8567–8571. [PubMed: 2964867]
181. Makris TM, Vu VV, Meier KK, Komor AJ, Rivard BS, Münck E, Que L, Lipscomb JD. J Am Chem Soc. 2015; 137:1608–1617. [PubMed: 25564306]
182. Komor AJ, Rivard BS, Fan R, Guo Y, Que L, Lipscomb JD. J Am Chem Soc. 2016; 138:7411–7421. [PubMed: 27203126]
183. Olah GA, Goeppert A, Prakash GKS. Angew Chem Int Ed. 2005; 44:2636–2639.
184. Sirajuddin S, Rosenzweig AC. Biochemistry. 2015; 54:2283–2294. [PubMed: 25806595]
185. Lawton TJ, Rosenzweig AC. J Am Chem Soc. 2016; 138:9327–9340. [PubMed: 27366961]
186. Lieberman RL, Rosenzweig AC. Nature. 2005; 434:177–182. [PubMed: 15674245]

187. Hakemian AS, Kondapalli KC, Telser J, Hoffman BM, Stemmler TL, Rosenzweig AC. Biochemistry. 2008; 47:6793–6801. [PubMed: 18540635]
188. Balasubramanian R, Smith SM, Rawat S, Yatsunyk LA, Stemmler TL, Rosenzweig AC. Nature. 2010; 465:115–119. [PubMed: 20410881]
189. Citek C, Lin B, Phelps TE, Wasinger EC, Stack TDP. J Am Chem Soc. 2014; 136:14405–14408. [PubMed: 25268334]
190. Citek C, Gary JB, Wasinger EC, Stack TDP. J Am Chem Soc. 2015; 137:6991–6994. [PubMed: 26020834]
191. Citek C, Herres-Pawlis S, Stack TDP. Acc Chem Res. 2015; 48:2424–2433. [PubMed: 26230113]
192. Gary JB, Citek C, Brown TA, Zare RN, Wasinger EC, Stack TDP. J Am Chem Soc. 2016; 138:9986–9995. [PubMed: 27467215]
193. Roberts SA, Weichsel A, Grass G, Thakali K, Hazzard JT, Tollin G, Rensing C, Montfort WR. Proc Natl Acad Sci USA. 2002; 99:2766–2771. [PubMed: 11867755]
194. Cole J, Ballou D, Solomon E. J Am Chem Soc. 1991; 113:8544–8546.
195. Palmer AE, Quintanar L, Severance S, Wang TP, Kosman DJ, Solomon EI. Biochemistry. 2002; 41:6438–6448. [PubMed: 12009907]
196. Kataoka K, Kitagawa R, Inoue M, Naruse D, Sakurai T, Huang HW. Biochemistry. 2005; 44:7004–7012. [PubMed: 15865445]
197. Ueki Y, Inoue M, Kurose S, Kataoka K, Sakurai T. FEBS Lett. 2006; 580:4069–4072. [PubMed: 16828082]
198. Silva CS, Damas JM, Chen ZJ, Brissos V, Marcins LO, Soares CM, Lindley PF, Bento I. Acta Crystallogr Sect D Biol Crystallogr. 2012; 68:186–193. [PubMed: 22281748]
199. Yoon J, Solomon EI. J Am Chem Soc. 2007; 129:13127–13136. [PubMed: 17918839]
200. Augustine AJ, Kjaergaard C, Qayyum M, Ziegler L, Kosman DJ, Hodgson KO, Hedman B, Solomon EI. J Am Chem Soc. 2010; 132:6057–6067. [PubMed: 20377263]
201. Shin W, Sundaram UM, Cole JL, Zhang HH, Hedman B, Hodgson KO, Solomon EI. J Am Chem Soc. 1996; 118:3202–3215.
202. Solomon EI, Ginsbach JW, Heppner DE, Kieber-Emmons MT, Kjaergaard CH, Smeets PJ, Tian L, Woertink JS. Faraday Discuss. 2011; 148:11–39. [PubMed: 21322475]
203. Suh MP, Han MY, Lee JH, Min KS, Hyeon C. J Am Chem Soc. 1998; 120:3819–3820.
204. Yoon J, Mirica LM, Stack TDP, Solomon EI. J Am Chem Soc. 2004; 126:12586–12595. [PubMed: 15453791]
205. Mirica LM, Stack TDP. Inorg Chem. 2005; 44:2131–2133. [PubMed: 15792444]
206. Yoon J, Solomon EI. Inorg Chem. 2005; 44:8076–8086. [PubMed: 16241158]
207. Yoon J, Mirica LM, Stack TDP, Solomon EI. J Am Chem Soc. 2005; 127:13680–13693. [PubMed: 16190734]
208. Yoon J, Liboiron BD, Sarangi R, Hodgson KO, Hedman B, Solomon EI. Proc Natl Acad Sci USA. 2007; 104:13609–13614. [PubMed: 17702865]
209. Solomon EI, Augustine AJ, Yoon J. Dalton Trans. 2008; 9226:3921–3932.
210. Taki M, Teramae S, Nagatomo S, Tachi Y, Kitagawa T, Itoh S, Fukuzumi S. J Am Chem Soc. 2002; 124:6367–6377. [PubMed: 12033867]
211. Gupta AK, Tolman WB. Inorg Chem. 2012; 51:1881–1888. [PubMed: 22268598]
212. Lionetti D, Day MW, Agapie T. Chem Sci. 2013; 4:785–790. [PubMed: 23539341]
213. Di Francesco GN, Gaillard A, Ghiviriga I, Abboud KA, Murray LJ. Inorg Chem. 2014; 53:4647–4654. [PubMed: 24745804]
214. Murray LJ, Weare WW, Shearer J, Mitchell AD, Abboud KA. J Am Chem Soc. 2014; 136:13502–13505. [PubMed: 25238198]
215. Feig A, Lippard S. Chem Rev. 1994; 94:759–805.
216. Kim E, Chufa EE, Kamaraj K, Karlin KD. Chem Rev. 2004; 104:1077–1133. [PubMed: 14871150]
217. Yoshikawa S, Shimada A. Chem Rev. 2015; 115:1936–1989. [PubMed: 25603498]

218. Tsukihara T, Aoyama H, Yamashita E, Tomizaki T, Shinzawa-Itoh K, Nakashima R, Yaono R, Yoshikawa S. Science. 1995; 269:1069–1074. [PubMed: 7652554]
219. Yano N, Muramoto K, Shimada A, Takemura S, Baba J, Fujisawa H, Mochizuki M, Shinzawa-Itoh K, Yamashita E, Tsukihara T, Yoshikawa S. J Biol Chem. 2016; 291:23882–23894. [PubMed: 27605664]
220. Nath I, Chakraborty J, Verpoort F. Chem Soc Rev. 2016; 45:4127–4170. [PubMed: 27251115]
221. Cracknell JA, Vincent KA, Armstrong FA. Chem Rev. 2008; 108:2439–2461. [PubMed: 18620369]
222. Varotsis C, Woodruff WH. J Am Chem Soc. 1989; 111:6439–6440.
223. Han SW, Ching YC, Rousseau DL. Proc Natl Acad Sci USA. 1990; 87:2491–2495. [PubMed: 2157201]
224. Ogura T, Takahashi S, Shinzawa-Itoh K, Yoshikawa S, Kitagawa T. J Biol Chem. 1990; 265:14721–14723. [PubMed: 2168389]
225. Proshlyakov DA, Ogura T, Shinzawa-Itoh K, Yoshikawa S, Appelman EH, Kitagawa T. J Biol Chem. 1994; 269:29385–29388. [PubMed: 7961916]
226. Proshlyakov DA, Pressler MA, Babcock GT. Proc Natl Acad Sci USA. 1998; 95:8020–8025. [PubMed: 9653133]
227. Proshlyakov DA, Pressler MA, DeMaso C, Leykam JF, DeWitt DL, Babcock GT. Science. 2000; 290:1588–1591. [PubMed: 11090359]
228. Sucheta A, Szundi I, Einarsdottir O. Biochemistry. 1998; 37:17905–17914. [PubMed: 9922158]
229. Ogura T, Takahashi S, Hirota S, Shinzawa-Itoh K, Yoshikawa S, Appelman EH, Kitagawa T. J Am Chem Soc. 1993; 115:8527–8536.
230. Ogura T, Hirota S, Proshlyakov DA, Shinzawa-Itoh K, Yoshikawa S, Kitagawa T. J Am Chem Soc. 1996; 118:5443–5449.
231. Das TK, Pecoraro C, Tomson FL, Gennis RB, Rousseau DL. Biochemistry. 1998; 37:14471–14476. [PubMed: 9772174]
232. Sigman JA, Kwok BC, Lu Y, Sigman JA, Kwok BC, Lu Y. J Am Chem Soc. 2000; 122:8192–8196.
233. Bhagi-Damodaran A, Petrik I, Lu Y. Isr J Chem. 2016; 56:773–790. [PubMed: 27994254]
234. Sigman JA, Kim HK, Zhao X, Carey JR, Lu Y. Proc Natl Acad Sci USA. 2003; 100:3629–3634. [PubMed: 12655052]
235. Miner KD, Mukherjee A, Gao YG, Null EL, Petrik ID, Zhao X, Yeung N, Robinson H, Lu Y. Angew Chem Int Ed. 2012; 51:5589–5592.
236. Petrik ID, Davydov R, Ross M, Zhao X, Hoffman B, Lu Y. J Am Chem Soc. 2016; 138:1134–1137. [PubMed: 26716352]
237. Liu X, Yu Y, Hu C, Zhang W, Lu Y, Wang J. Angew Chem Int Ed. 2012; 51:4312–4316.
238. Bhagi-Damodaran A, Michael MA, Zhu Q, Reed J, Sandoval BA, Mirts EN, Chakraborty S, Moënne-Loccoz P, Zhang Y, Lu Y. Nat Chem. 2016; doi: 10.1038/nchem.2643
239. Collman JP, Sunderland CJ, Berg KE, Vance MA, Solomon EI. J Am Chem Soc. 2003; 125:6648–6649. [PubMed: 12769571]
240. Collman JP, Decréau RA, Sunderland CJ. Chem Commun. 2006:3894–3896.
241. Boulatov R, Collman JP, Shiryaeva IM, Sunderland CJ. J Am Chem Soc. 2002; 124:11923–11935. [PubMed: 12358536]
242. Chishiro T, Shimazaki Y, Tani F, Tachi Y, Naruta Y, Karasawa S, Hayami S, Maeda Y. Angew Chem Int Ed. 2003; 42:2788–2791.
243. Liu J-G, Naruta Y, Tani F. Angew Chem Int Ed. 2005; 44:1836–1840.
244. Ghiladi RA, Hatwell KR, Karlin KD, Huang HW, Moënne-Loccoz P, Krebs C, Huynh BH, Marzilli LA, Cotter RJ, Kaderli S, Zuberbühler AD. J Am Chem Soc. 2001; 123:6183–6184. [PubMed: 11414855]
245. Chatterjee S, Sengupta K, Hematian S, Karlin KD, Dey A. J Am Chem Soc. 2015; 137:12897–12905. [PubMed: 26419806]
246. Collman JP, Decréau RA. Chem Commun. 2008:5065–5076.

247. Halime Z, Kieber-Emmons MT, Qayyum MF, Mondal B, Gandhi T, Puiu SC, Chufan EE, Sarjeant AAN, Hodgson KO, Hedman B, Solomon EI, Karlin KD. Inorg Chem. 2010; 49:3629–3645. [PubMed: 20380465]
248. Garcia-Bosch I, Adam SM, Schaefer AW, Sharma SK, Peterson RL, Solomon EI, Karlin KD. J Am Chem Soc. 2015; 137:1032–1035. [PubMed: 25594533]
249. Sheng Y, Abreu IA, Cabelli DE, Maroney MJ, Miller AF, Teixeira M, Valentine JS. Chem Rev. 2014; 114:3854–3918. [PubMed: 24684599]
250. Hough MA, Hasnain SS. Structure. 2003; 11:937–946. [PubMed: 12906825]
251. Hough MA, Hasnain SS. J Mol Biol. 1999; 287:579–592. [PubMed: 10092461]
252. Valentine JS, Doucette PA, Zittin Potter S. Annu Rev Biochem. 2005; 74:563–593. [PubMed: 15952898]
253. Paulsen CE, Carroll KS. Chem Rev. 2013; 113:4633–4679. [PubMed: 23514336]
254. Nagy P, Kettle AJ, Winterbourn CC. J Biol Chem. 2009; 284:14723–14733. [PubMed: 19297319]
255. Das AB, Nagy P, Abbott HF, Winterbourn CC, Kettle AJ. Free Radic Biol Med. 2010; 48:1540–1547. [PubMed: 20211247]
256. Nagy P, Lechte TP, Das AB, Winterbourn CC. J Biol Chem. 2012; 287:26068–26076. [PubMed: 22648418]
257. Das AB, Nauser T, Koppenol WH, Kettle AJ, Winterbourn CC, Nagy P. Free Radic Biol Med. 2014; 70:86–95. [PubMed: 24561577]
258. Hart PJ, Balbirnie MM, Ogihara NL, Nersissian AM, Weiss MS, Valentine JS, Eisenberg D. Biochemistry. 1999; 38:2167–2178. [PubMed: 10026301]
259. Smirnov VV, Roth JP. J Am Chem Soc. 2006; 128:16424–16425. [PubMed: 17177351]
260. Maji RC, Das PP, Mishra S, Bhandari A, Maji M, Patra AK. Dalton Trans. 2016; 45:11898–11910. [PubMed: 27383660]
261. Kolks G, Frihart CR, Rabinowitz HN, Lippard SJ. J Am Chem Soc. 1976; 98:5720–5721. [PubMed: 956576]
262. O'Young C-L, Dewan JC, Lilienthal HR, Lippard SJ. J Am Chem Soc. 1978; 100:7291–7300.
263. Strothkamp KG, Lippard SJ. Acc Chem Res. 1982; 15:318–326.
264. Sato M, Nagae S, Uehara M, Nakaya J. J Chem Soc Chem Comm. 1984:1661–1663.
265. Pierre J-L, Chautemps P, Refaif S, Beguin C, Marzouki AE, Serratrice G, Saint-Aman E, Rey P. J Am Chem Soc. 1995; 117:1965–1973.
266. Mao Z-W, Chen M-Q, Tan X-S, Liu J, Tang W-X. Inorg Chem. 1995; 34:2889–2893.
267. Ohtsu H, Shimazaki Y, Odani A, Yamauchi O, Mori W, Itoh S, Fukuzumi S. J Am Chem Soc. 2000; 122:5733–5741.
268. Ohtsu H, Fukuzumi S, Itoh S, Nagatomo S, Kitagawa T, Ogo S, Watanabe Y. Chem Commun. 2000:1051–1052.
269. Halcrow MA. Angew Chem Int Ed. 2001; 40:346–349.
270. Hemp J, Robinson DE, Ganesan KB, Martinez TJ, Kelleher NL, Gennis RB. Biochemistry. 2006; 45:15405–15410. [PubMed: 17176062]
271. Davidson VL. Biochemistry. 2007; 46:5283–5292. [PubMed: 17439161]
272. Yukl ET, Wilmot CM. Curr Opin Chem Biol. 2012; 16:54–59. [PubMed: 22387133]
273. Klinman JP, Bonnot F. Chem Rev. 2014; 114:4343–4365. [PubMed: 24350630]
274. DuBois JL, Klinman JP. Arch Biochem Biophys. 2005; 433:255–265. [PubMed: 15581581]
275. Moore RH, Spies MA, Culpepper MB, Murakawa T, Hirota S, Okajima T, Tanizawa K, Mure M. J Am Chem Soc. 2007; 129:11524–11534. [PubMed: 17715921]
276. Dove JE, Schwartz B, Williams NK, Klinman JP. Biochemistry. 2000; 39:3690–3698. [PubMed: 10736168]
277. Ghosh S, Cirera J, Vance MA, Ono T, Fujisawa K, Solomon EI. J Am Chem Soc. 2008; 130:16262–16273. [PubMed: 18998639]
278. Chen ZW, Datta S, Dubois JL, Klinman JP, Mathews FS. Biochemistry. 2010; 49:7393–7402. [PubMed: 20684524]

279. Finney J, Moon HJ, Ronnebaum T, Lantz M, Mure M. Arch Biochem Biophys. 2014; 546:19–32. [PubMed: 24407025]

280. Firbank SJ, Rogers MS, Wilmot CM, Dooley DM, Halcrow MA, Knowles PF, McPherson MJ, Phillips SE. Proc Natl Acad Sci USA. 2001; 98:12932–12937. [PubMed: 11698678]

281. Rogers MS, Hurtado-Guerrero R, Firbank SJ, Halcrow MA, Dooley DM, Phillips SEV, Knowles PF, McPherson MJ. Biochemistry. 2008; 47:10428–10439. [PubMed: 18771294]

282. Cowley RE, Cirera J, Qayyum MF, Rokhsana D, Hedman B, Hodgson KO, Dooley DM, Solomon EI. J Am Chem Soc. 2016; 138:13219–13229. [PubMed: 27626829]

283. Fujieda N, Ikeda T, Murata M, Yanagisawa S, Aono S, Ohkubo K, Nagao S, Ogura T, Hirota S, Fukuzumi S, Nakamura Y, Hata Y, Itoh S. J Am Chem Soc. 2011; 133:1180–1183. [PubMed: 21218798]

284. Fujieda N, Yabuta S, Ikeda T, Oyama T, Muraki N, Kurisu G, Itoh S. J Biol Chem. 2013; 288:22128–22140. [PubMed: 23749993]

285. Fujieda N, Itoh S. Bull Chem Soc Jpn. 2016; 89:733–742.

286. Sprakel VSI, Feiters MC, Meyer-Klaucke W, Klopstra M, Brinksma J, Feringa BL, Karlin KD, Nolte RJM. Dalton Trans. 2005:3522–3534. [PubMed: 16234934]

287. Walli A, Dechert S, Bauer M, Demeshko S, Meyer F. Eur J Inorg Chem. 2014; 2014:4660–4676.

288. Ravikiran B, Mahalakshmi R. RSC Adv. 2014; 4:33958–33974.

289. Uchida T, Mogi T, Nakamura H, Kitagawa T. J Biol Chem. 2004; 279:53613–53620. [PubMed: 15465820]

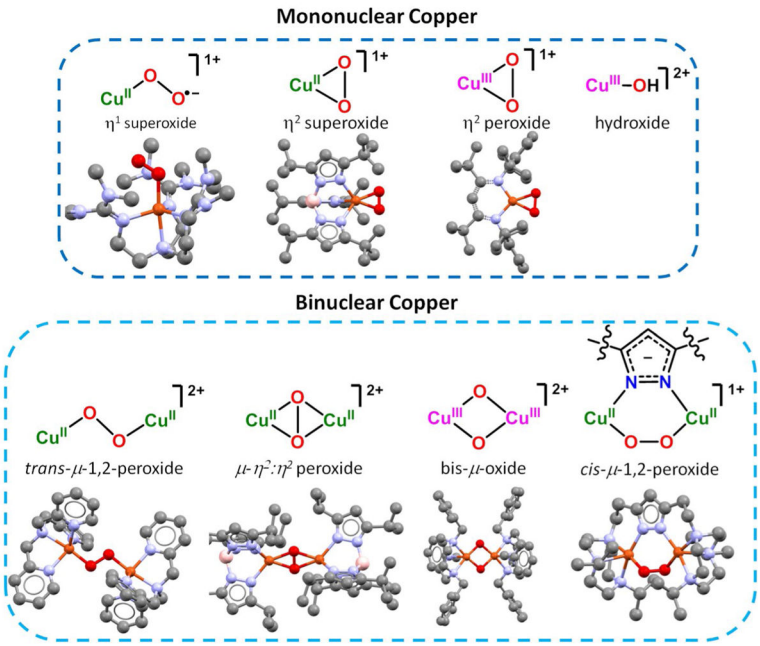

Fig. 1.

Synthetically derived mono- and binuclear copper-(di) oxygen complexes. Representative crystal structures are shown for the intermediates that have been structurally characterized [18–20, 28, 32–34]. Only the η^1 superoxide and μ-η^2:η^2 peroxide moieties have been observed crystallographically in biological systems [38–41]

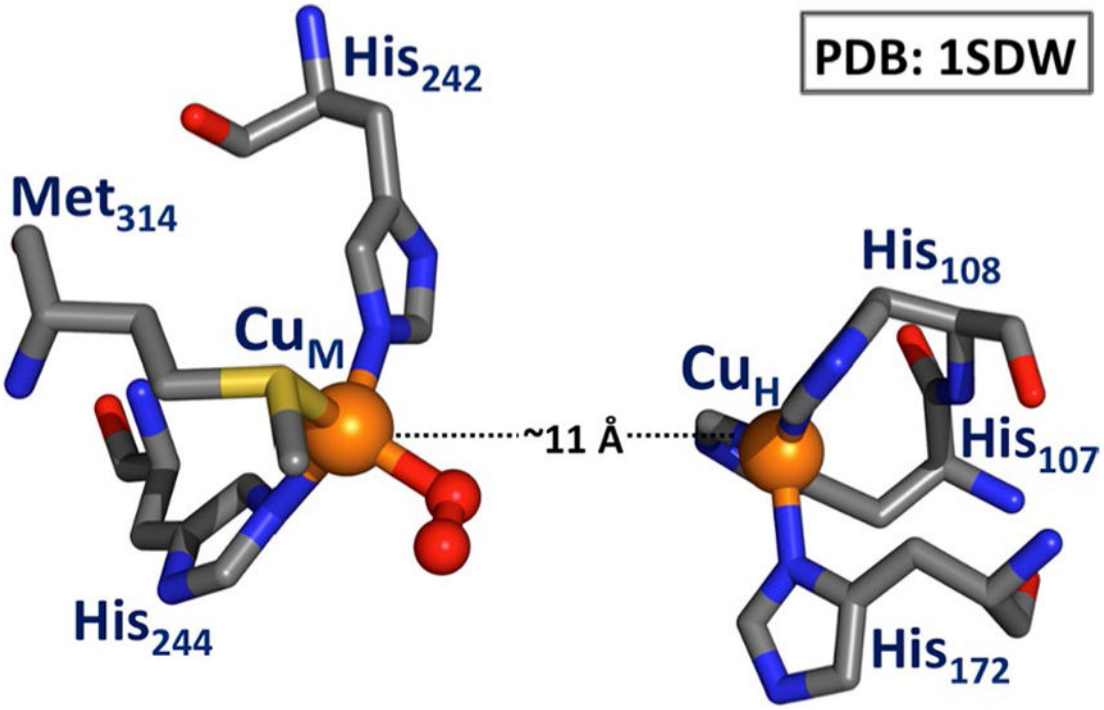

Fig. 2.
X-ray crystal structure of the active site of PHM in its oxy-form [38]

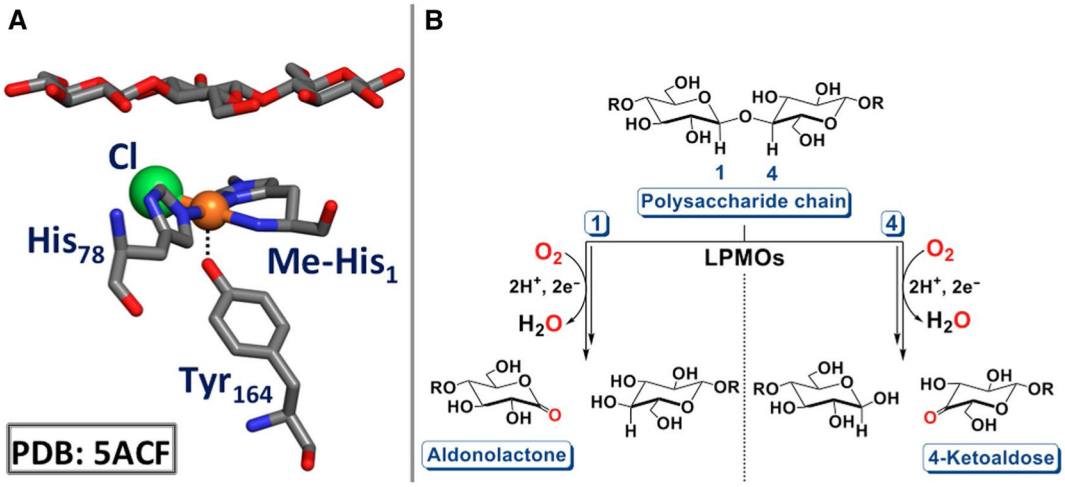

Fig. 3.

a X-ray crystal structure of LPMO with substrate bound [78]. **b** Catalytic reactions performed by LPMOs with products shown, derived from either H-atom abstraction at C1 or C4 [77, 80]

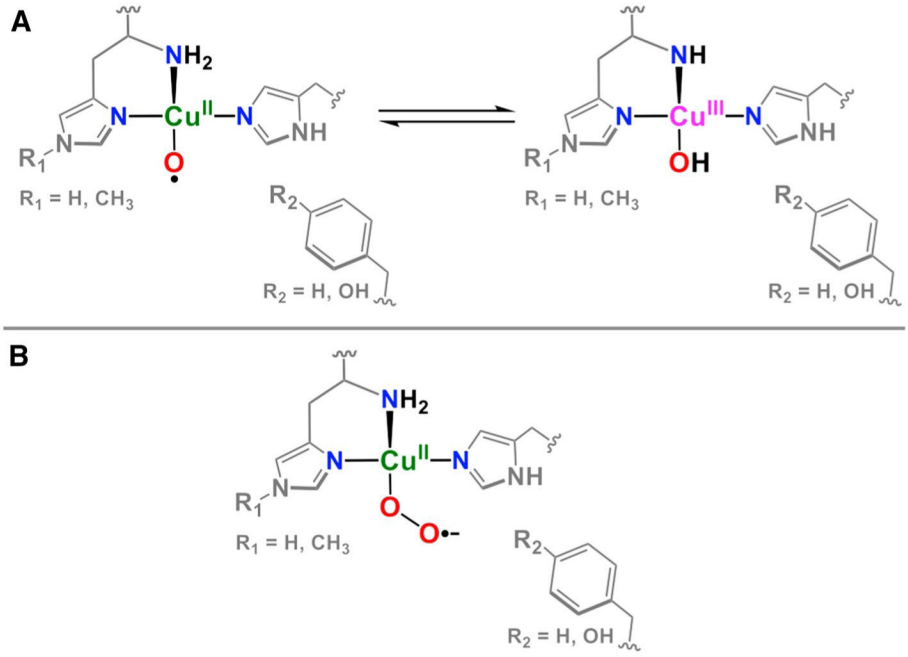

Fig. 4.

Possible reactive copper-(di)oxygen species in the catalytic cycle of LPMOs. **a** Tautomerization between a copper(II)-oxyl species (Cu^{II}-O˙) and a copper(III) hydroxide species (Cu^{III}-OH) [83]. **b** A cupric superoxide species ($Cu^{II}-O_2^{\cdot-}$) [84]

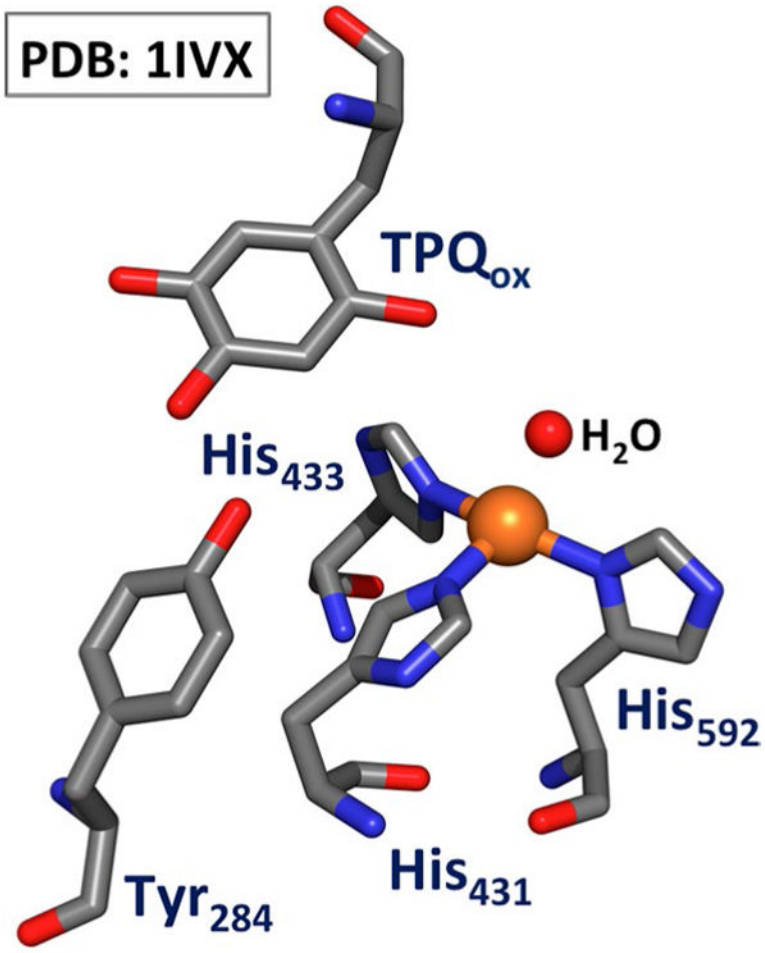

Fig. 5.

X-ray crystal structure of mature (processed) copper amine oxidase from *A. globiformis* in the fully oxidized form [90]

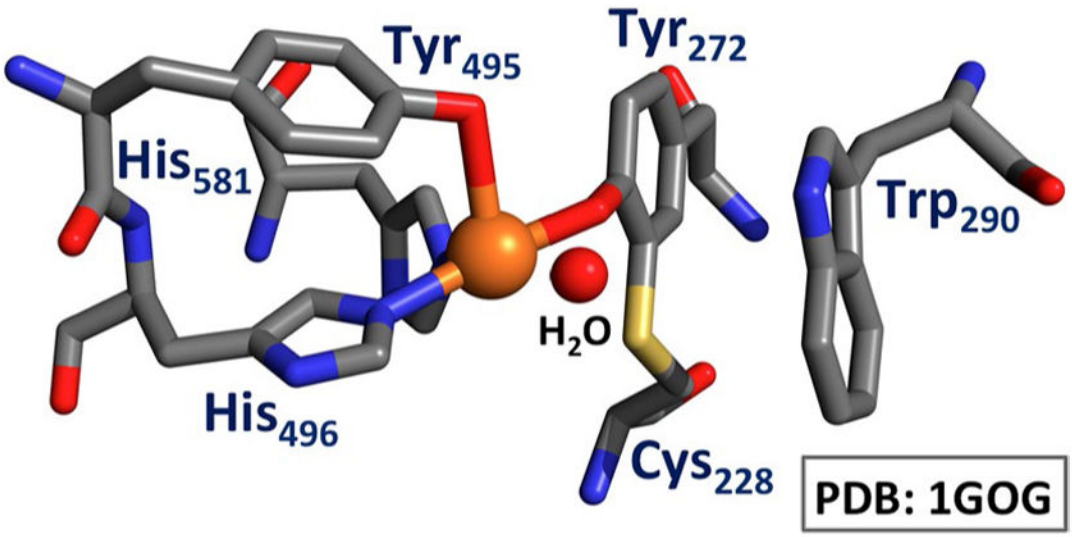

Fig. 6.

X-ray crystal structure of the active site of mature (processed) galactose oxidase from *D. dendroides* in the oxidized form [101]

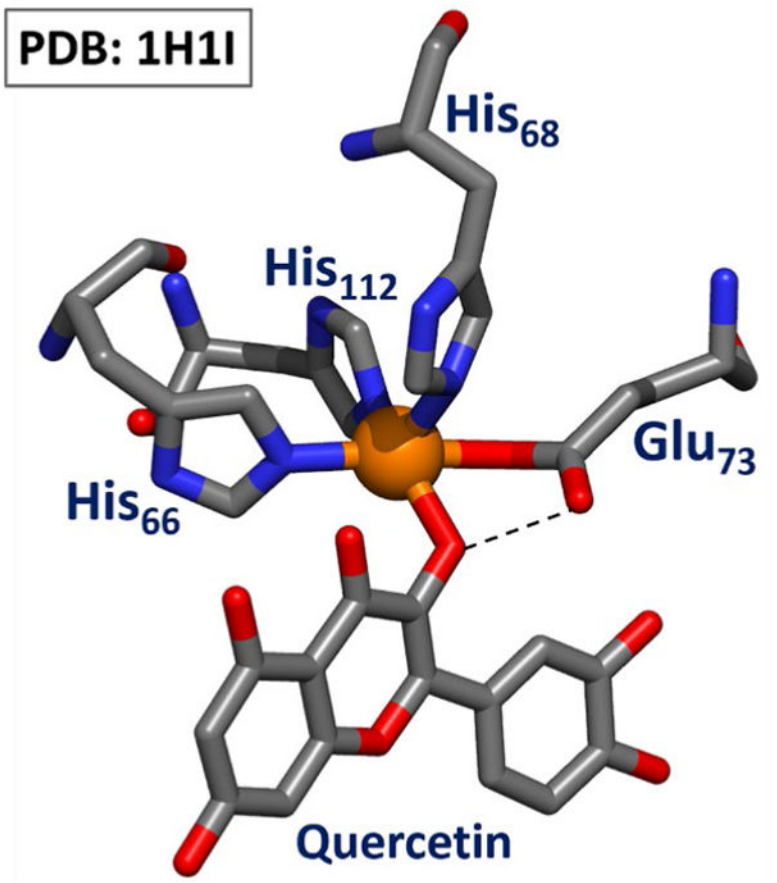

Fig. 7.

X-ray crystal structure of the enzyme-substrate complex of quercetin 2,4-dioxygenase (2,4-QD) [116]. Important hydrogen bonding between Glu_{73} and bound quercetin is shown as a *dashed line*

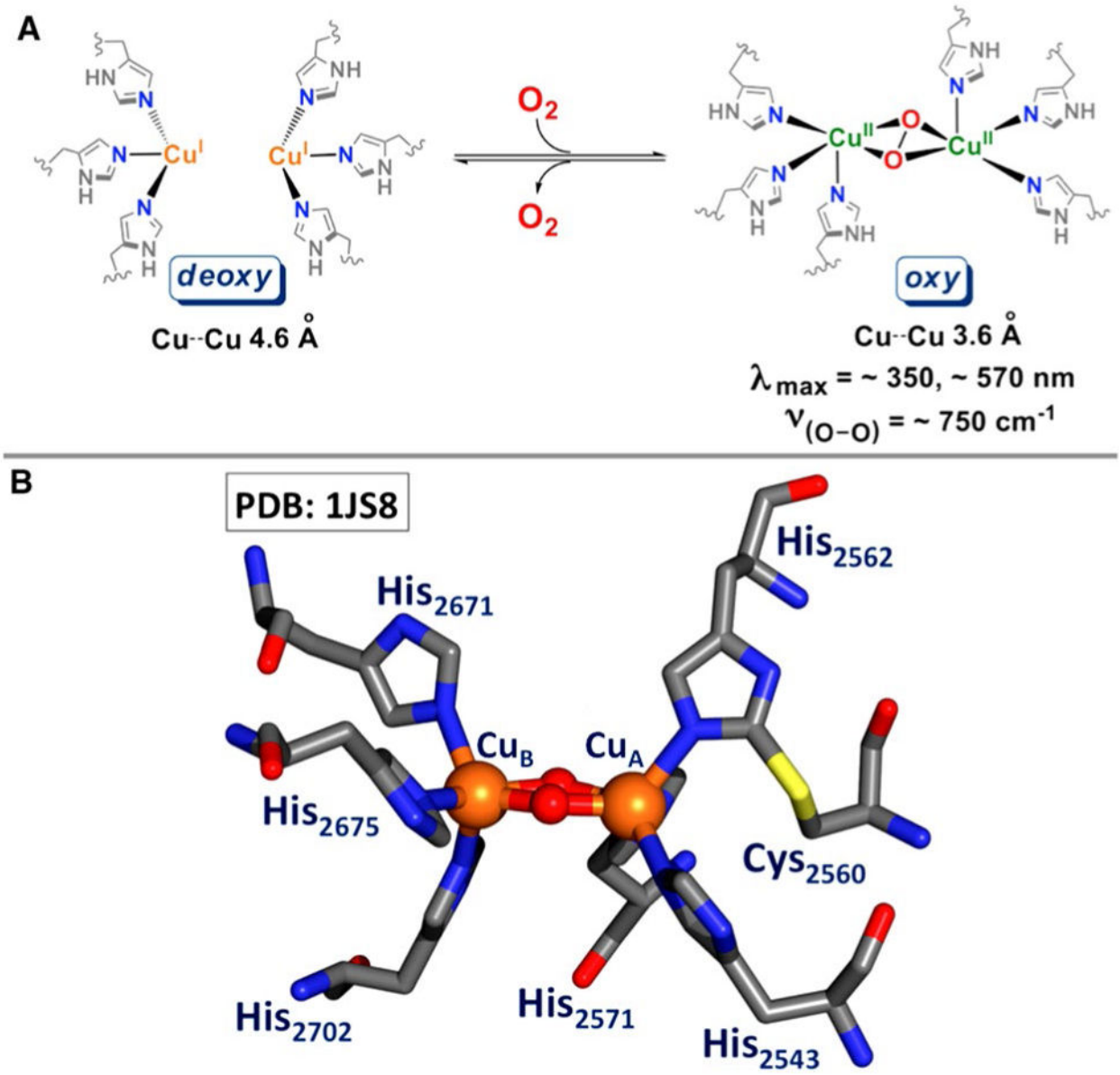

Fig. 8.

a General reaction of deoxy-Hc with O_2 [131]. **b** X-ray crystal structure of the oxy-form of Hc from *O. dofleini* [130]

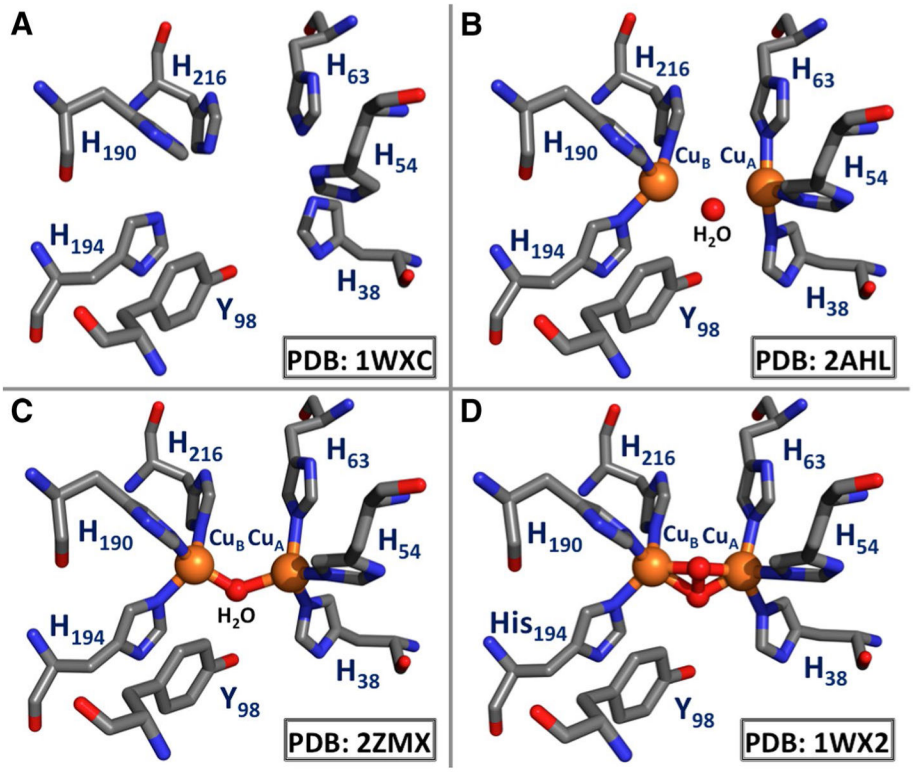

Fig. 9.

X-ray crystal structure of the **a** Apo-form (copper free), **b** Deoxy-form, **c** Met1-form (one water molecule), and **d** Oxy-form all from *S. castaneoglobisporus* tyrosinase [154]. This organism's active site does not possess the His-Cys crosslink

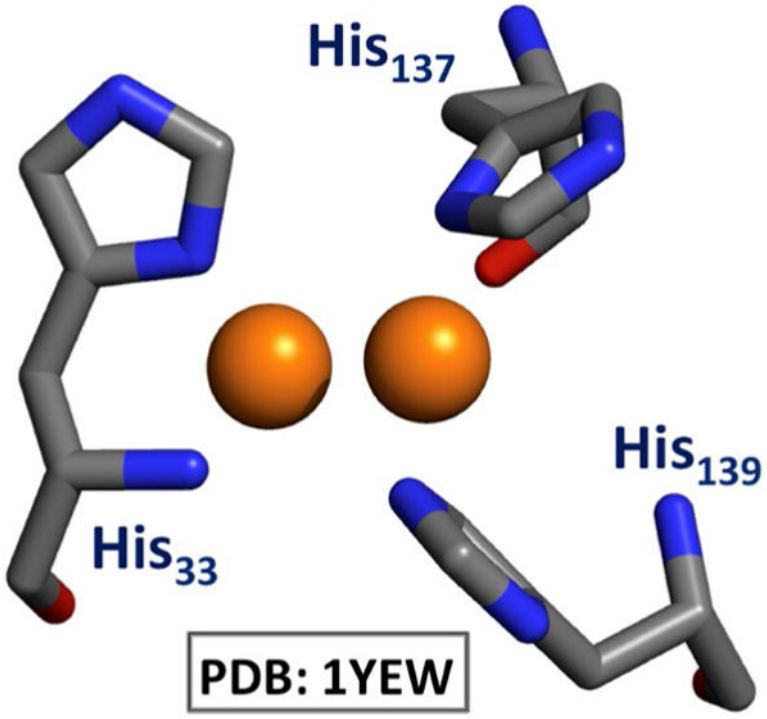

Fig. 10.
X-ray crystal structure of the binuclear copper site in pMMO [186]

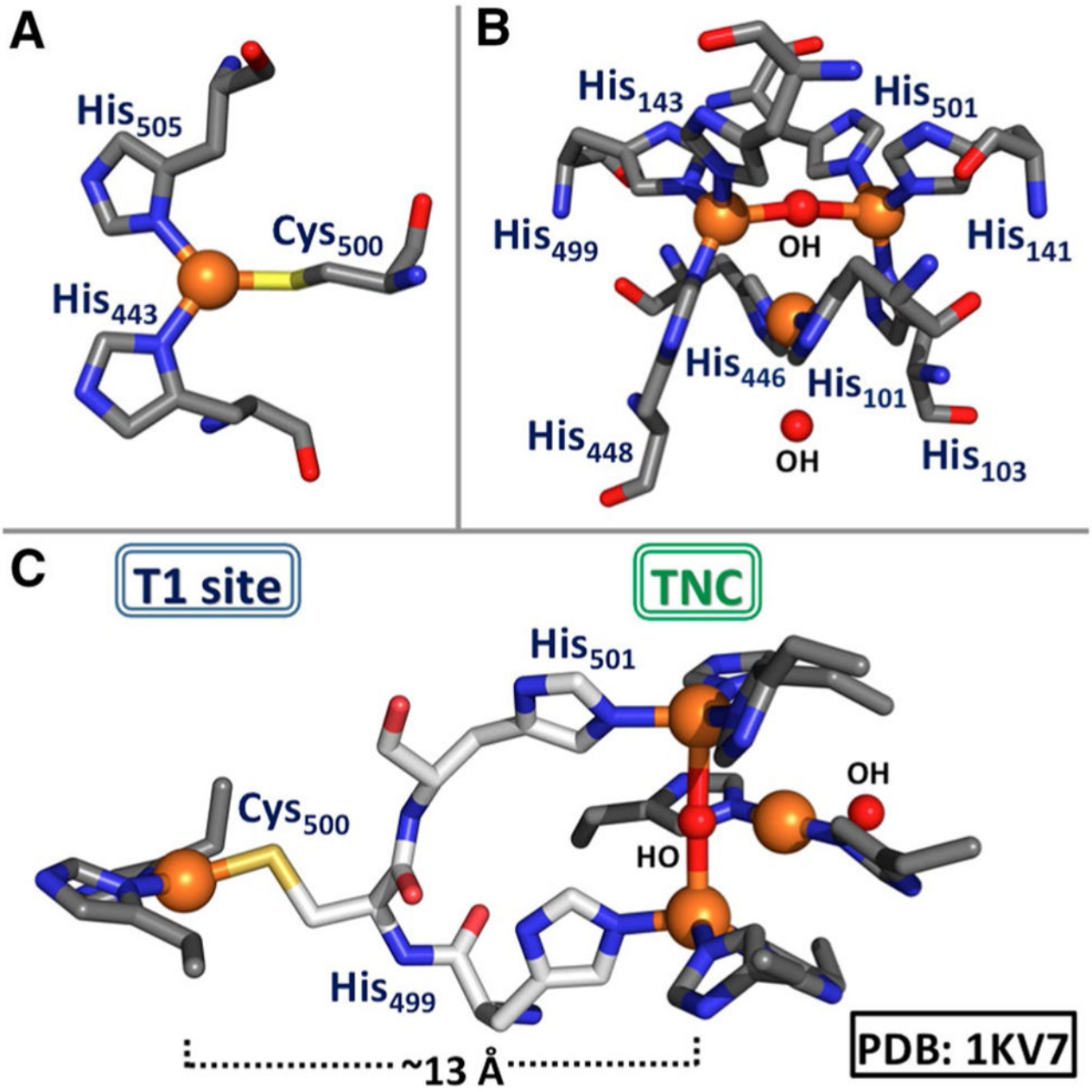

Fig. 11.

X-ray crystal structure of the resting oxidized state of the MCO, Cu-efflux oxidase (CueO) [193]. **a** The T1 site of MCOs. **b** The TNC of MCOs. **c** The amino acid backbone connectivity between the T1 and TNC sites

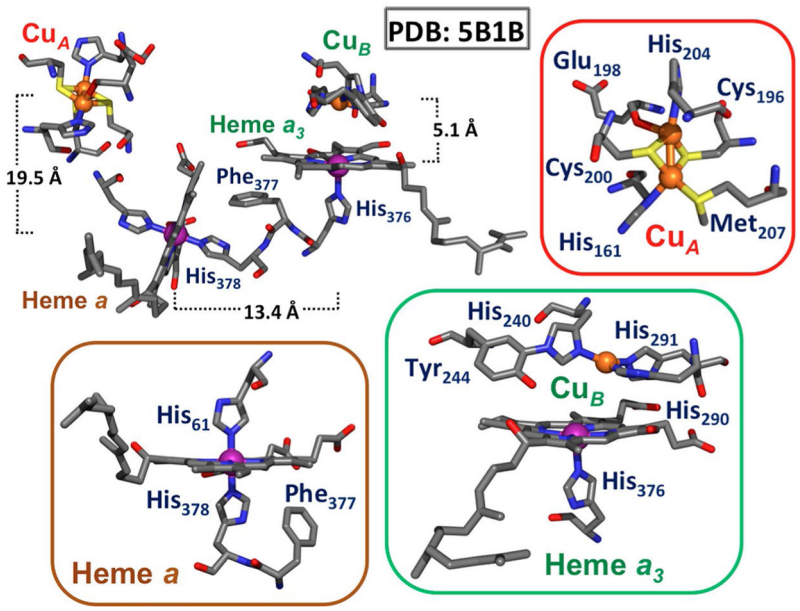

Fig. 12.

The four redox active metal sites of bovine heart C*c*O (*top left*) [219]. Heme *a* active site (*bottom left*). Dioxygen reduction site composed of heme a_3 and Cu_B (*bottom right*). Active site of the binuclear T1 copper site referred to as Cu_A (*top right*). Bovine heart C*c*O numbering is used throughout the text

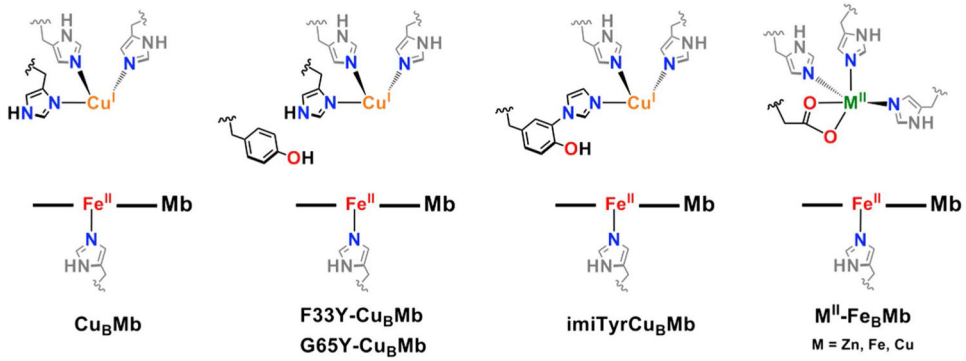

Fig. 13.

Active sites of myoglobin engineered to contain a copper binding site. *Left* Cu_BMb contains two additional histidines in the distal binding pocket [232]. *Middle-Left* F33Y-Cu_BMb and G65Y-Cu_BMb contain two additional histidines and a tyrosine in the distal binding pocket [235]. *Middle-Right* imiTyrCu_BMb contains an additional histidine, and an unnatural histidine crosslinked to tyrosine in the distal binding pocket [237]. *Right* M^{II}-Fe_BMb contains two additional histidines and a glutamate in the distal binding pocket [238]

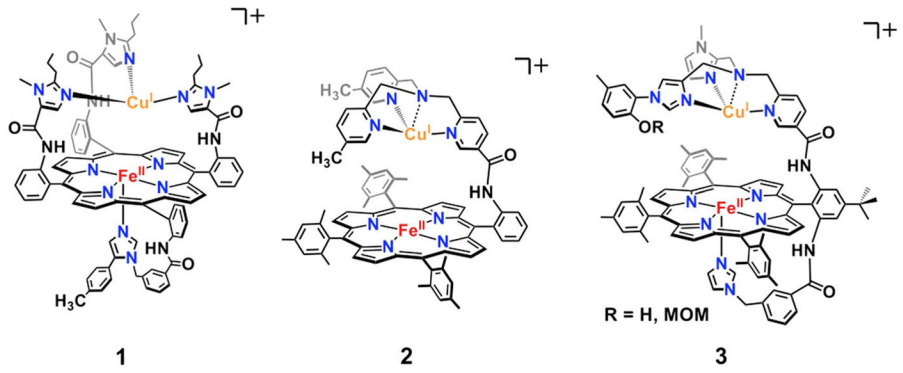

Fig. 14.

Synthetic heme-copper models designed by Collman (*left*) [239] and Naruta (*middle, right*) [242, 243]

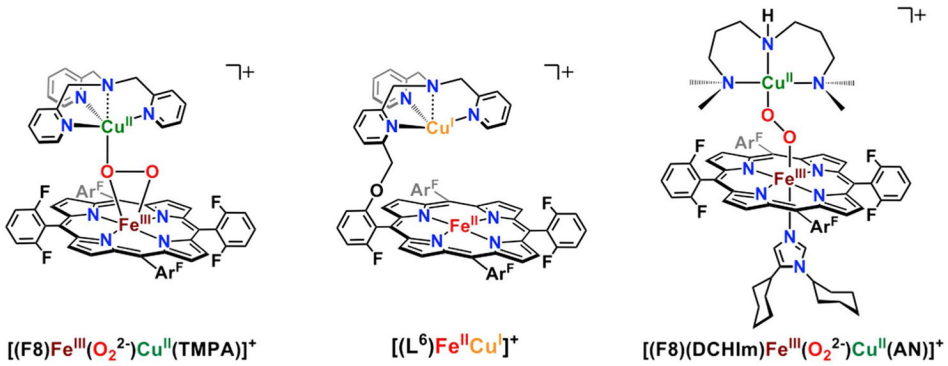

Fig. 15.

Synthetic heme-copper models designed by Karlin and coworkers [244, 245, 247]

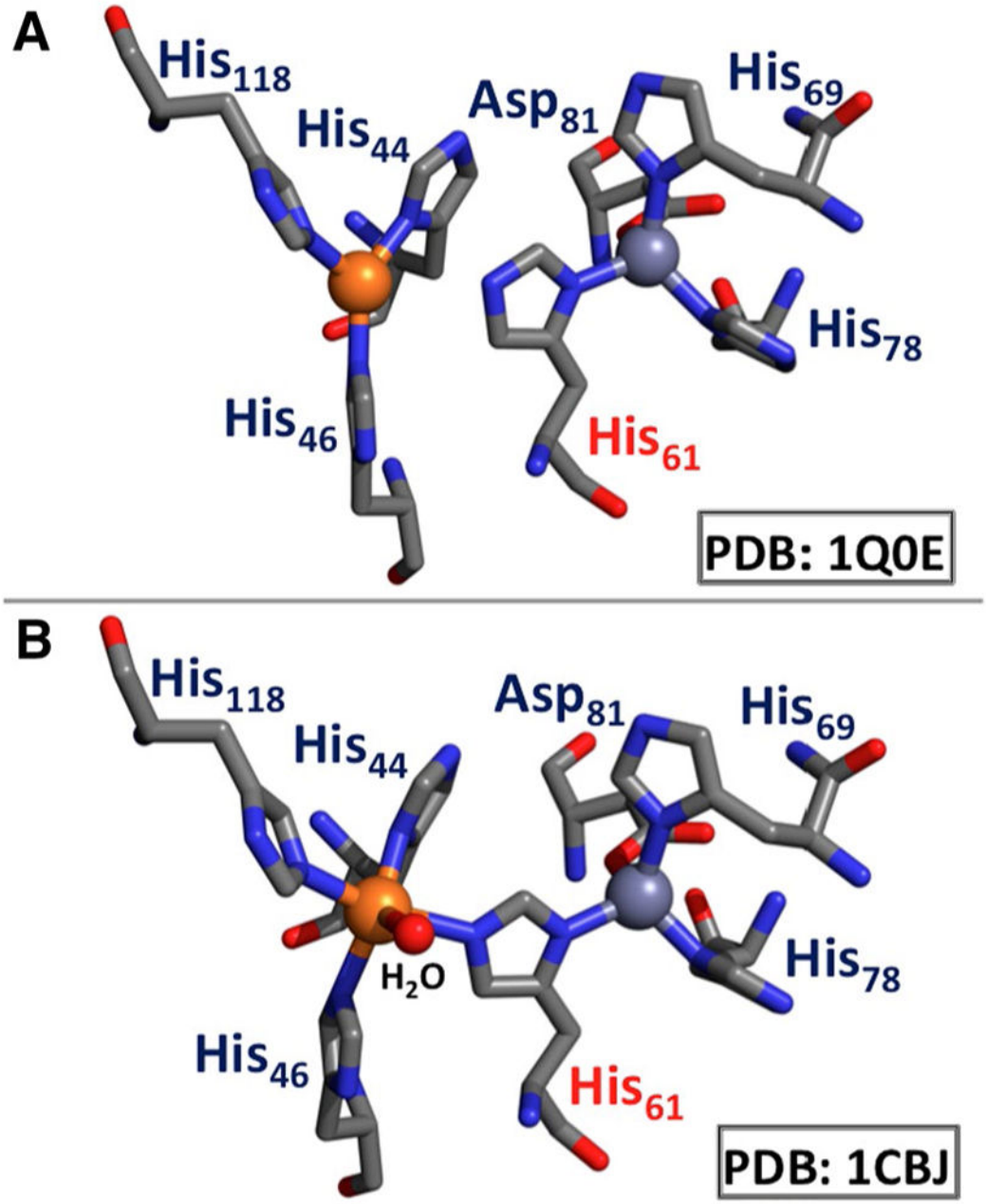

Fig. 16.
X-ray crystal structures of **a** reduced [250] and **b** oxidized CuZnSOD [251]

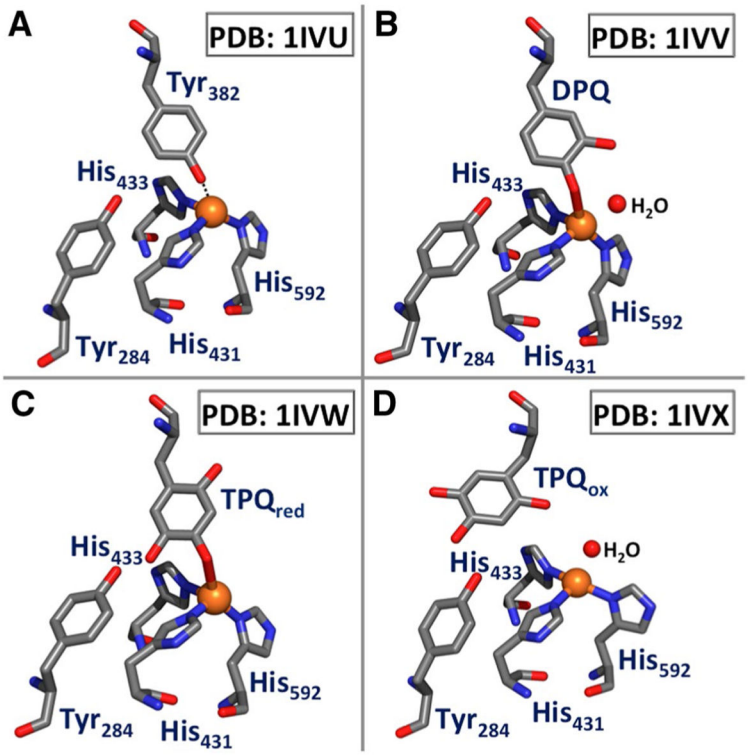

Fig. 17.

X-ray crystal structures from *A. globiformis* copper amine oxidase following the biogenesis of TPQ [90]. **a** Preprocessed active site prior to O_2 exposure. **b** Active site following initial tyrosine oxygenation yielding a DPQ intermediate. **c** Formation of TPQ_{red} following copper assisted hydrolysis of DPQ. **d** Processed active site following biogenesis shown in the active form

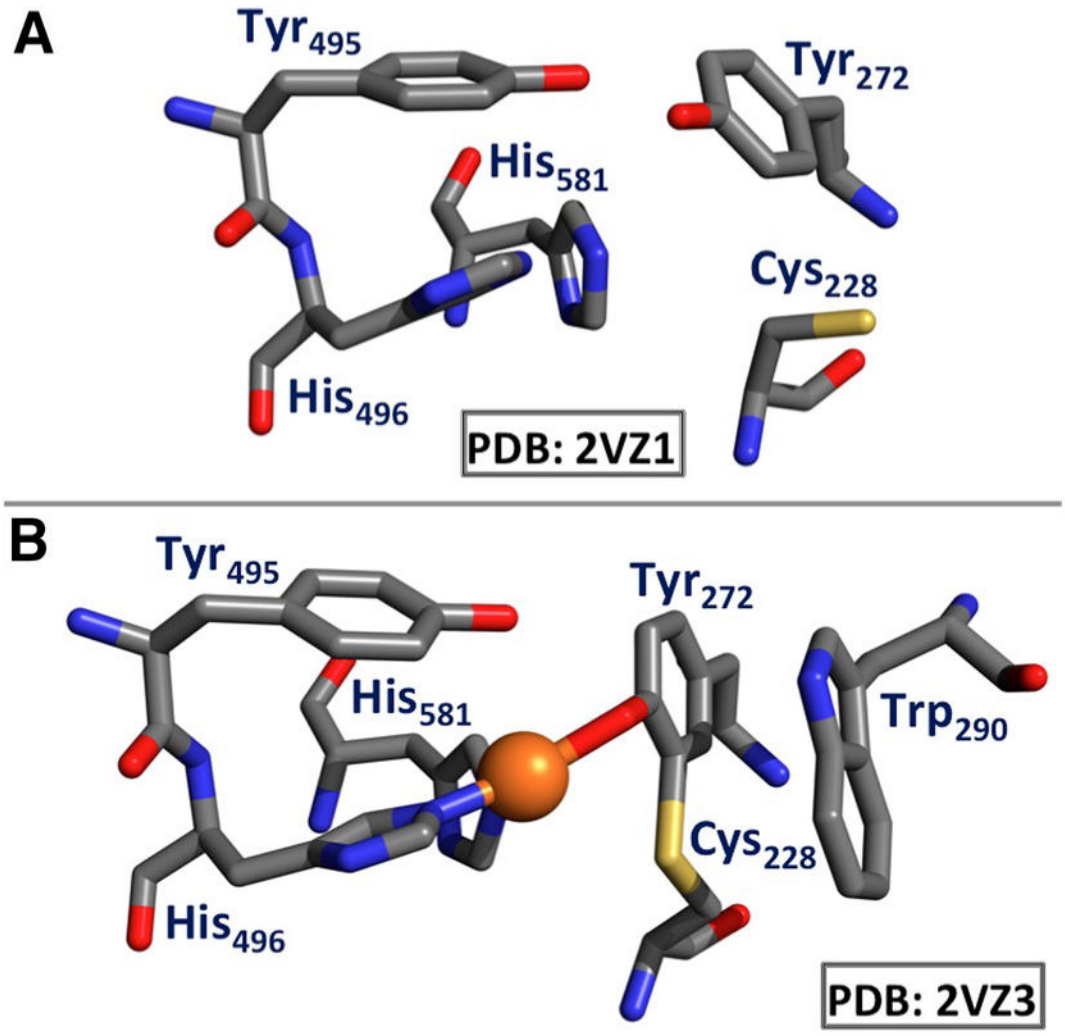

Fig. 18.

X-ray crystal structure of *apo*-GO (**a**) and oxidized mature GO (**b**) from *F. graminearum* [281]

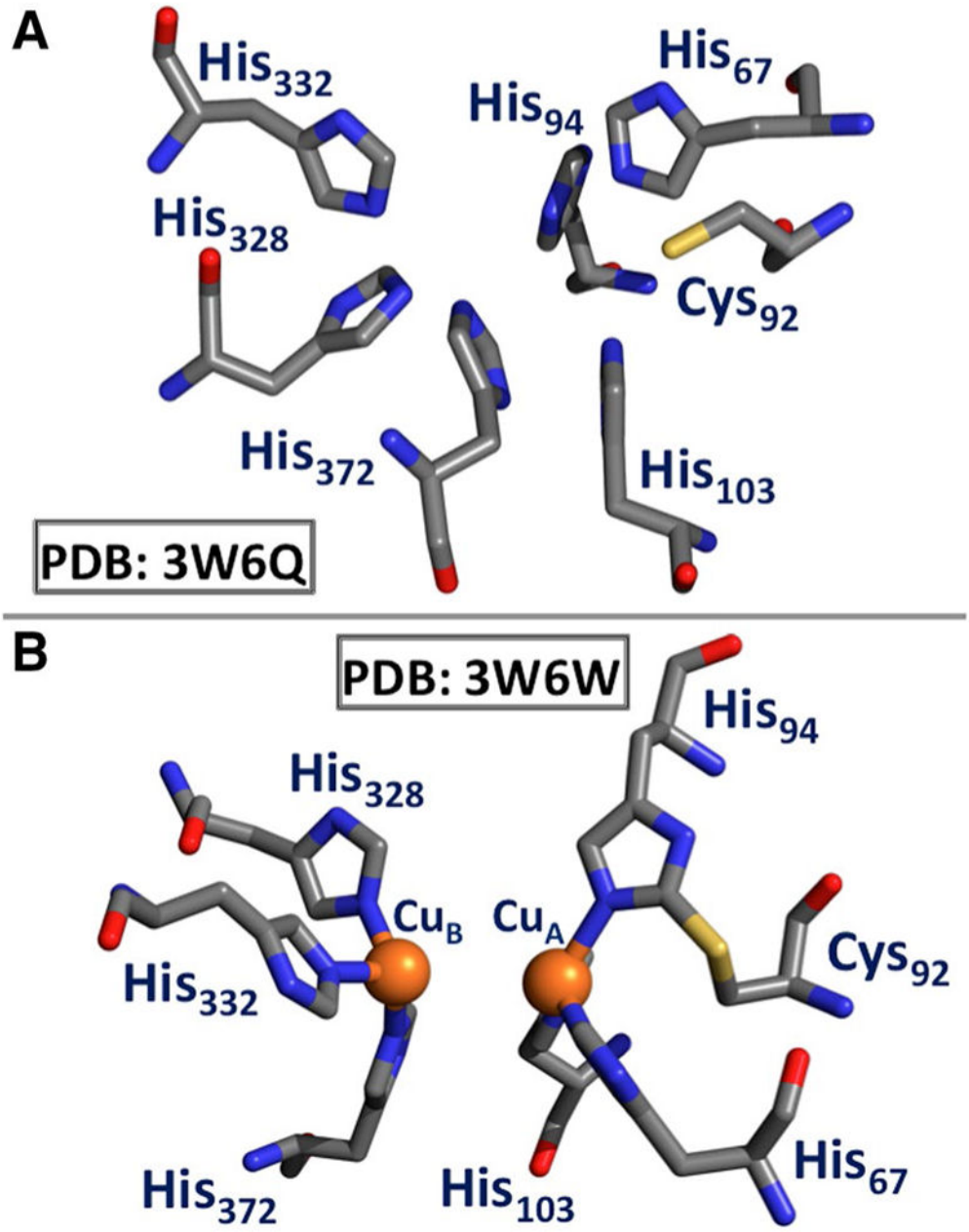

Fig. 19.

X-ray crystal structures of **a** apo-Ty and **b** met-Ty showing the absence and formed His-Cys crosslink, respectively [284]

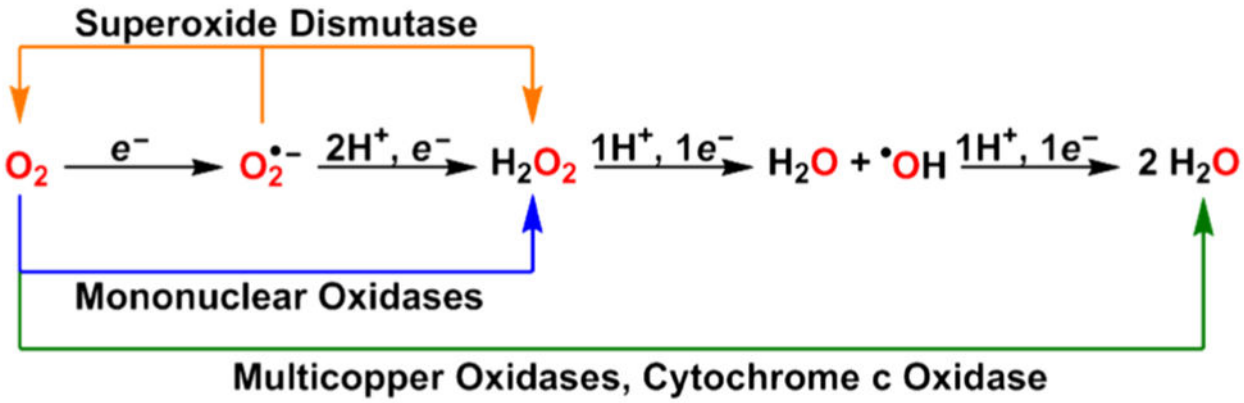

Scheme 1.

Aqueous reduction of O_2 and pertinent intermediates. Reduction potentials can be found in Ref. [7]. Copper-containing enzymes that perform parts of this reduction are shown

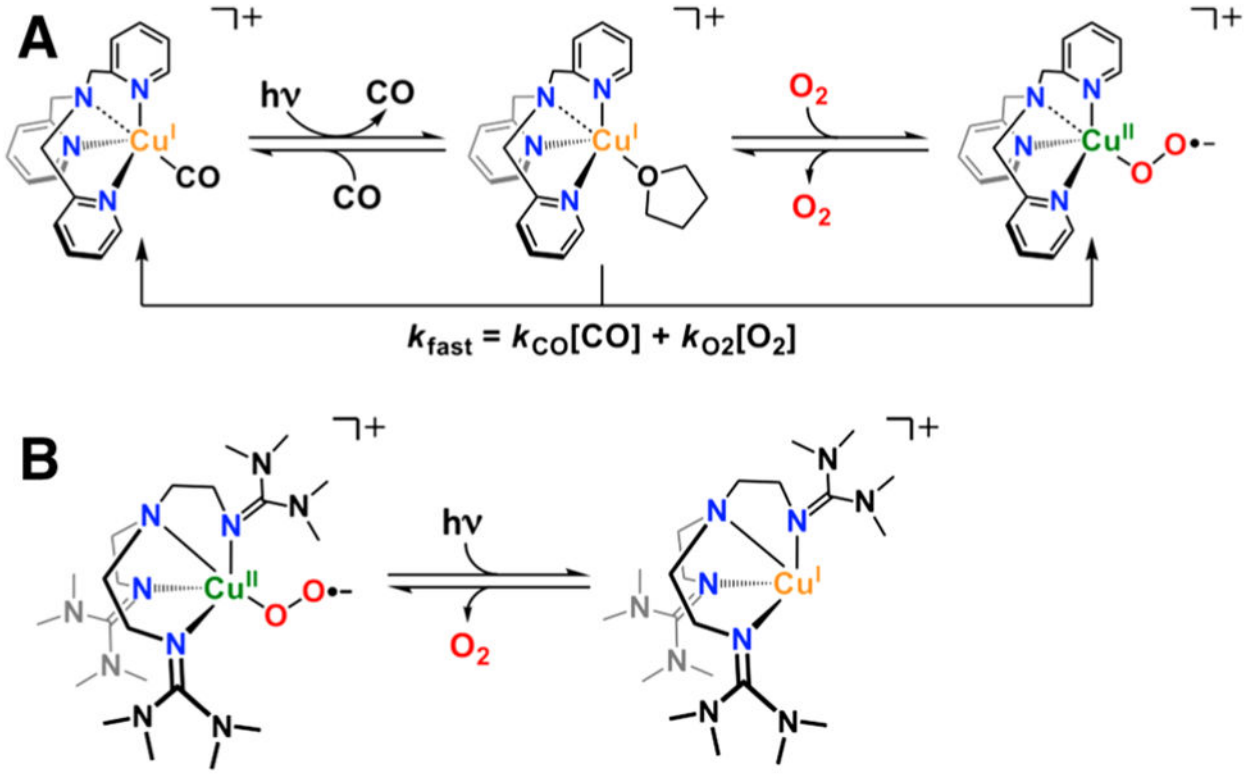

Scheme 2.

a "Flash-and-trap" technique used to photorelease CO from a Cu^{I}-CO complex in order to measure the O_2 binding vs. CO rebinding kinetics in THF [48]. **b** Photolysis of a cupric superoxide complex, with rebinding of O_2 [49]

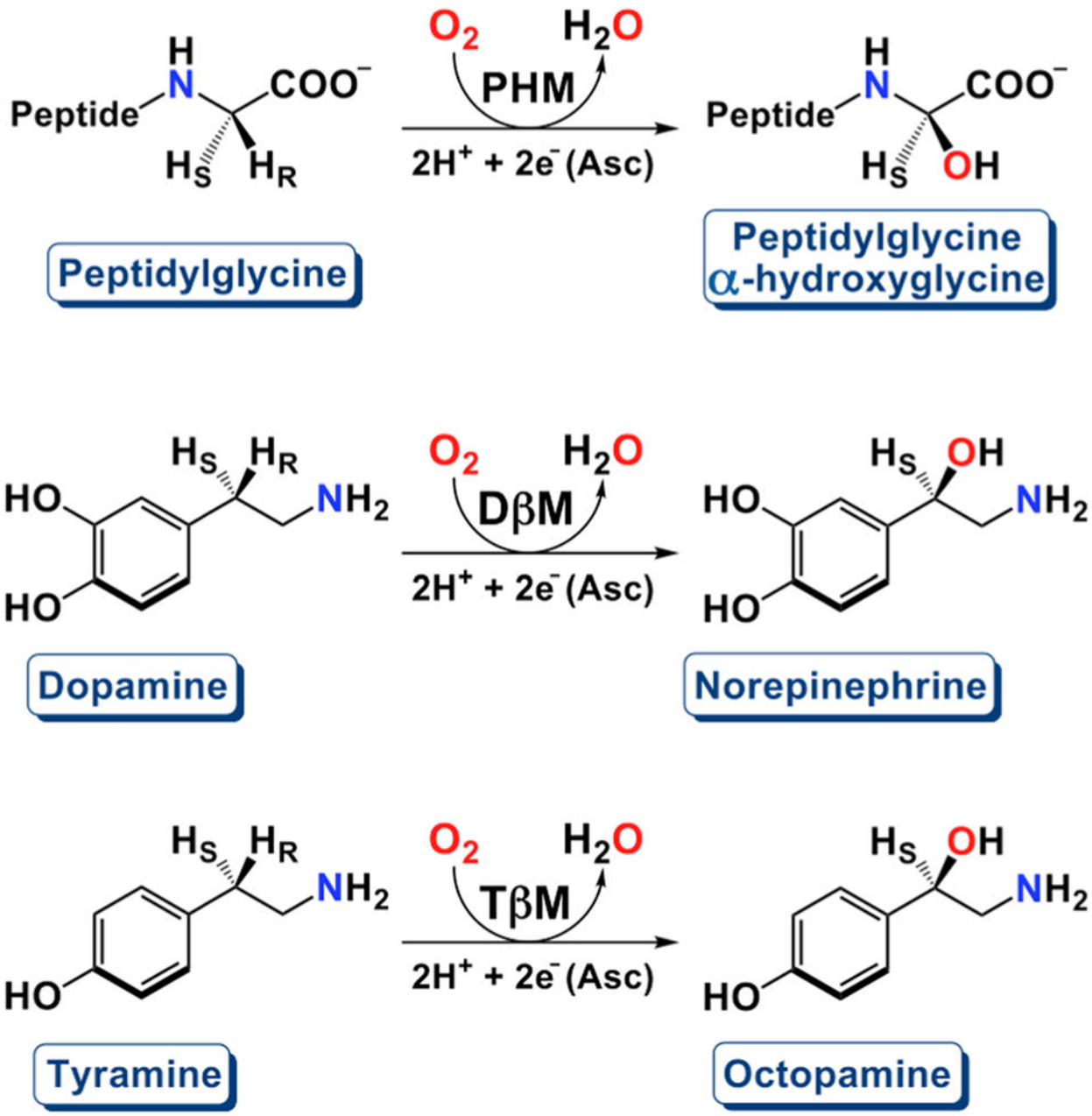

Scheme 3.
Catalytic reactions of the enzymes PHM, DβM, and TβM [57]

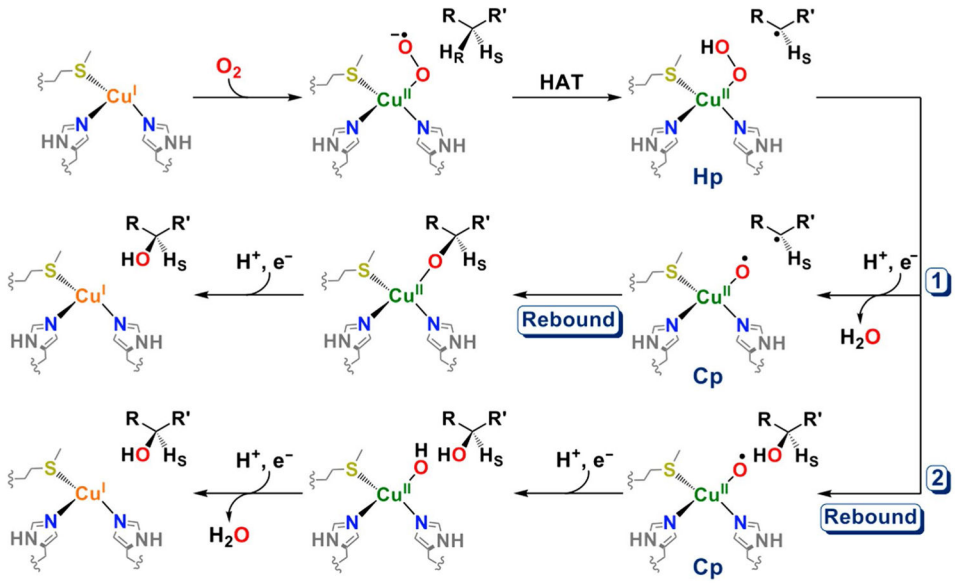

Scheme 4.

The proposed enzymatic mechanism of PHM, DβM, and TβM [17, 60, 61]

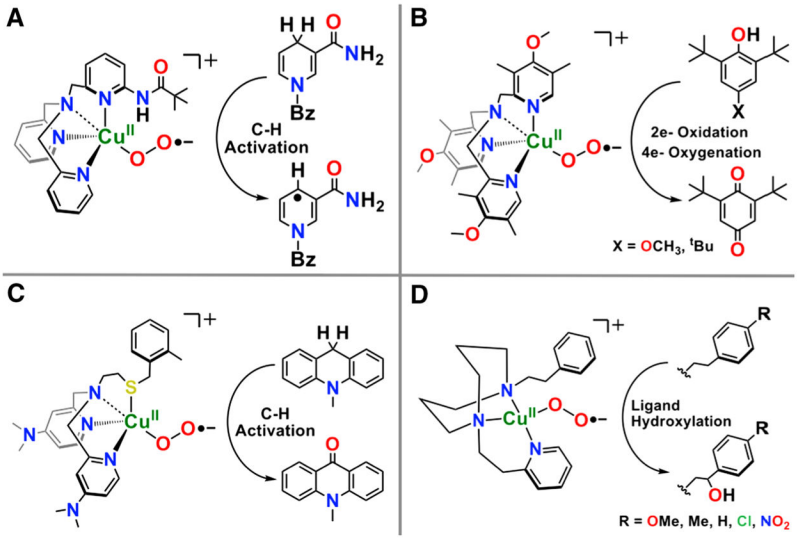

Scheme 5.

a $[\mathrm{Cu^{II}}(^{\mathrm{PV}}\mathrm{TMPA})(\mathrm{O_2^{\cdot -}})]^{+}$ and its C–H activation reactivity [63]. **b** $[\mathrm{Cu^{II}}(^{\mathrm{DMM}}\mathrm{TMPA})(\mathrm{O_2^{\cdot -}})]^{+}$ and its reactivity with phenolic substrates [64]. **c** $[\mathrm{Cu^{II}}(^{\mathrm{DMA}}\mathrm{N_3S})(\mathrm{O_2^{\cdot -}})]^{+}$ and its reactivity with *N*-methyl-9,10-dihydroacridine [67]. **d** $[\mathrm{Cu^{II}}(\mathrm{PEDACO\text{-}\ EtPh\text{-}\ R})(\mathrm{O_2^{\cdot -}})]^{+}$ and its intramolecular ligand hydroxylation reactivity [52]

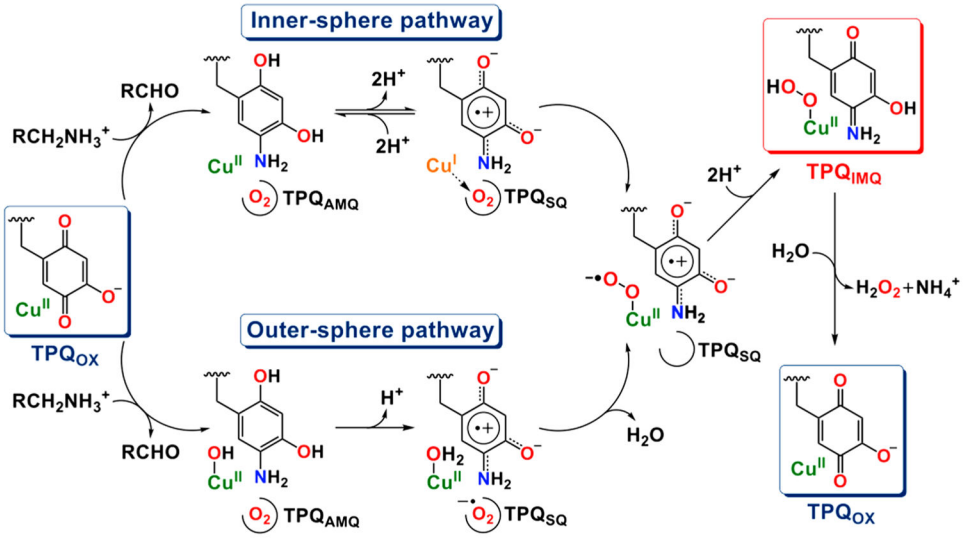

Scheme 6.

The catalytic mechanism of amine oxidase [91]. *Top* proposed pathway for inner-sphere reduction of O_2 by Cu^I yielding TPQ_{SQ} and cupric superoxide [94]. *Bottom* proposed outer-sphere reduction of O_2 by TPQ_{AMQ} yielding TPQ_{SQ} and cupric superoxide [93]

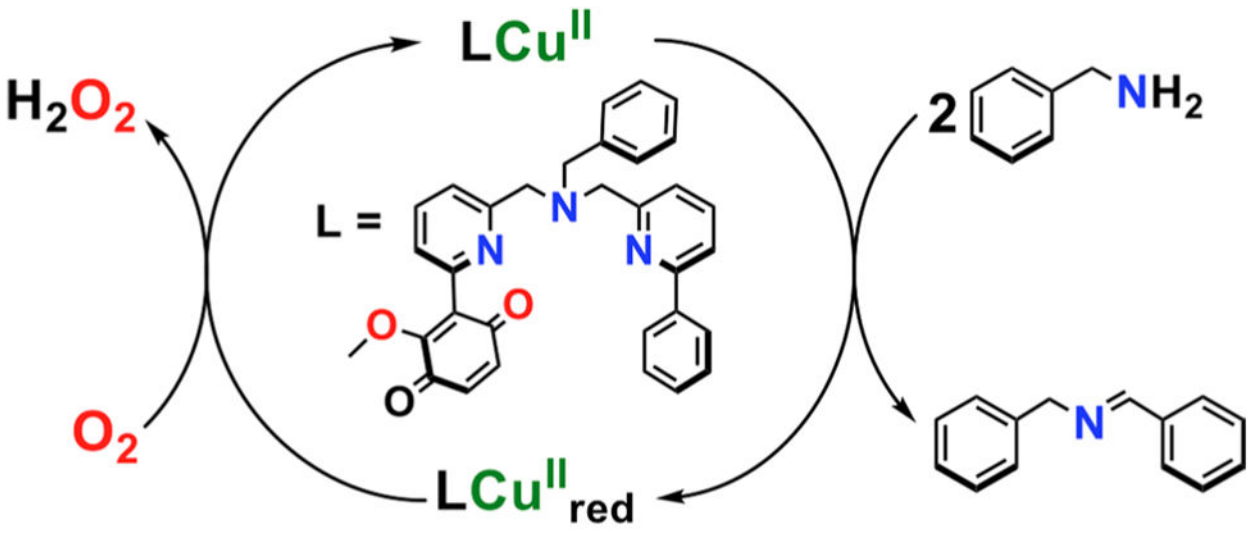

Scheme 7.
Transamination of benzylamine facilitated by a Cu^{II}-TPQ model complex [96]

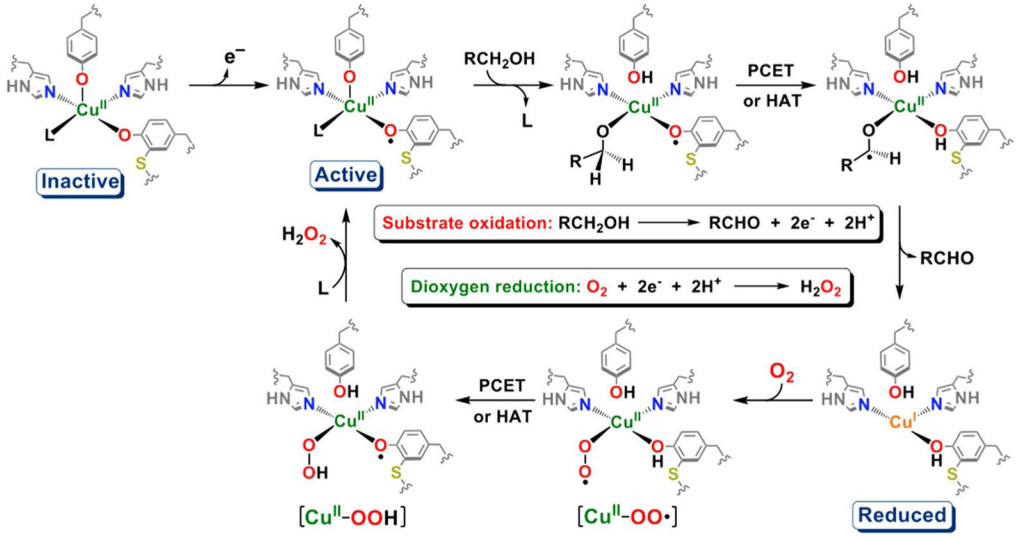

Scheme 8.

The proposed catalytic mechanism of galactose oxidase [98, 104]

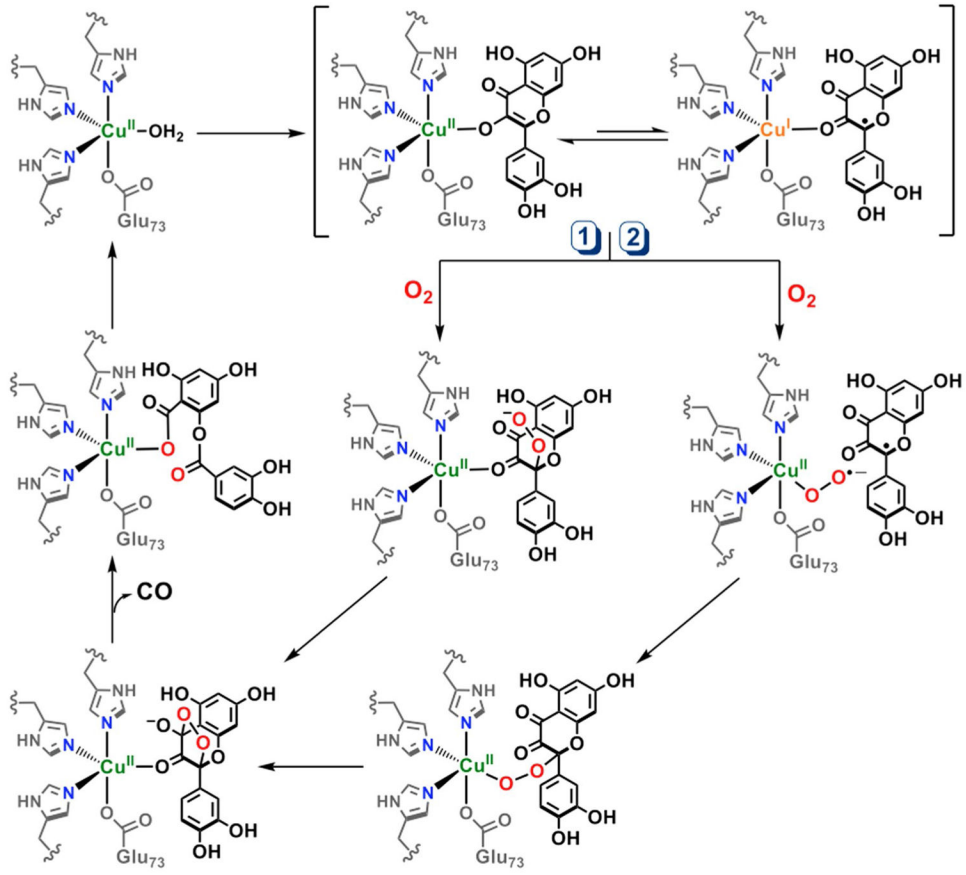

Scheme 9.
The proposed enzymatic mechanism of 2,4-QD [116]

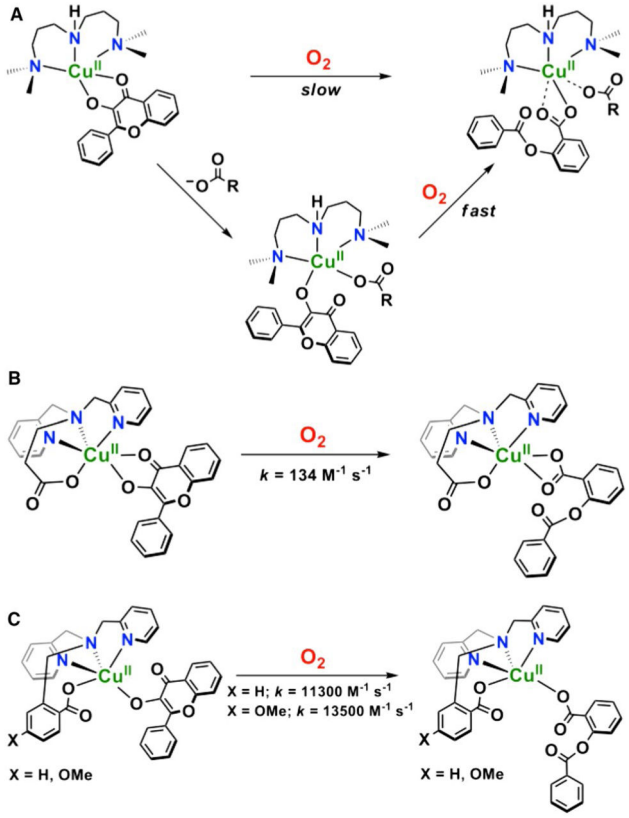

Scheme 10.

a Selected example of rate enhancement from addition of exogenous acetates [123]. **b** Reactivity with an intramolecular acetate ligand moiety [122]. **c** Rate enhancement from changing electronics of the intramolecular acetate ligand moiety [124, 125]

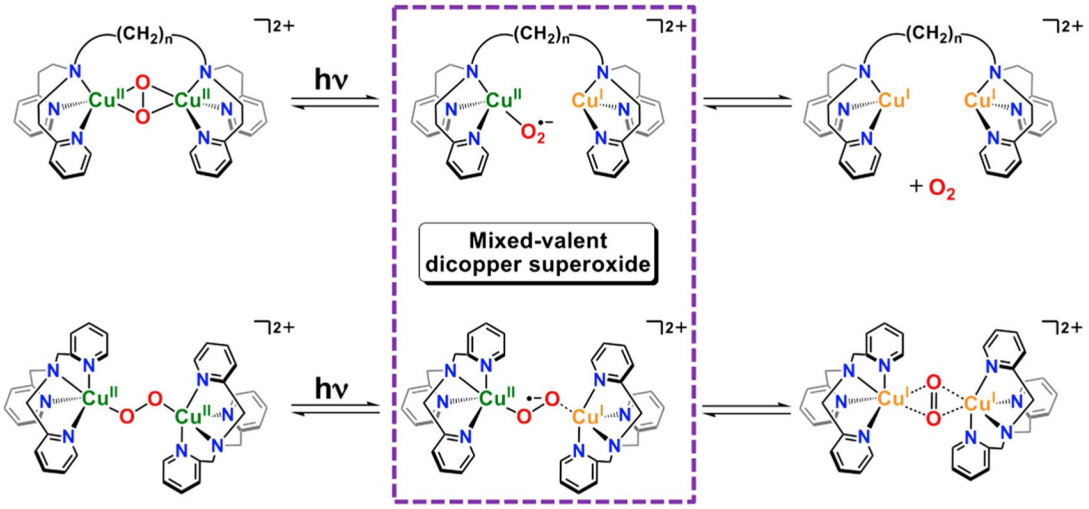

Scheme 11.

Photoexcitation of a μ-η^2:η^2-peroxide (*top*, n = 3 or 5) and a μ-1,2-peroxide (*bottom*) leads to the observation of novel mixed-valent dicopper superoxide complexes, which is then converted to the dicopper(I) complexes [151]. Only the starting μ-η^2:η^2-peroxide fully releases O_2, while the μ-1,2-peroxide keeps O_2 caged until rebinding occurs

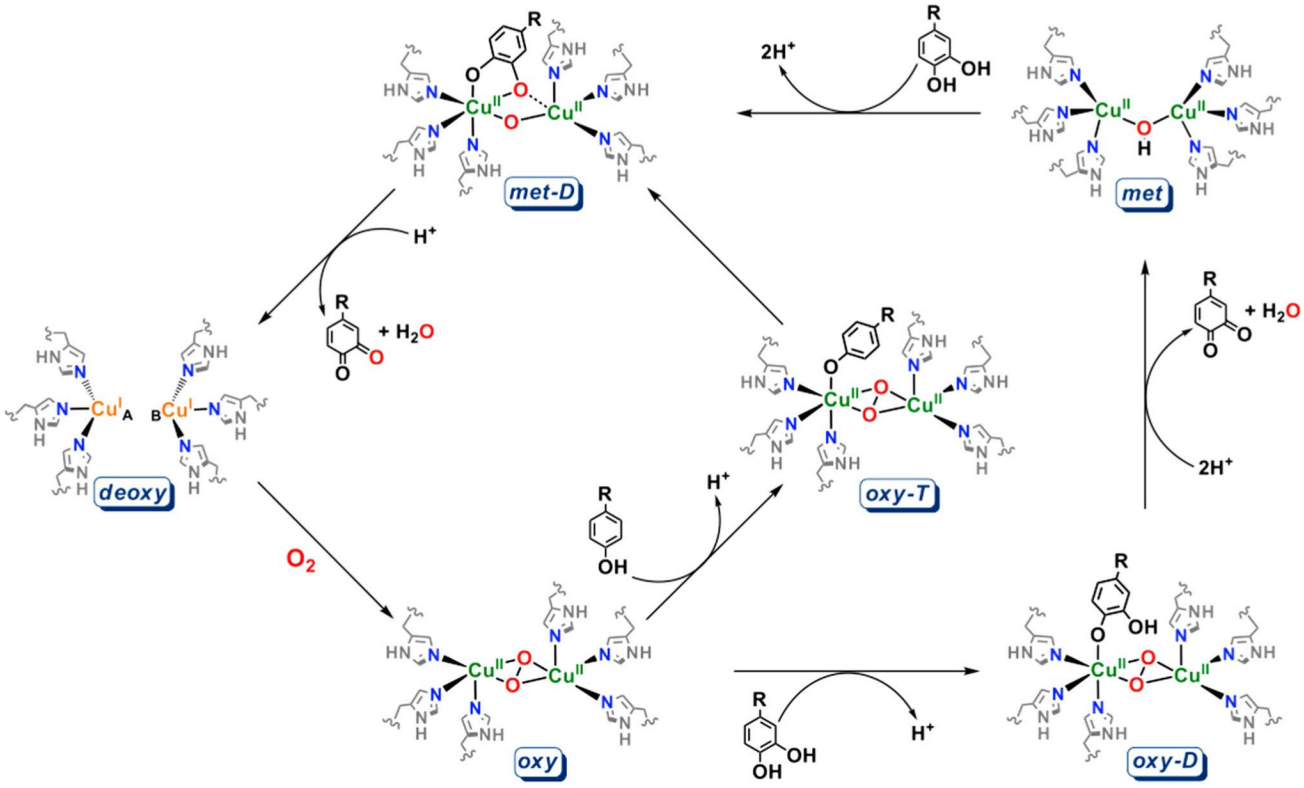

Scheme 12.

The proposed catalytic mechanism for the oxidation of *o*-catechol to *o*-quinone by catechol oxidase and tyrosinase (*outer cycle*), and proposed mechanism for the oxidation of phenol to *o*-quinone by tyrosinase (*inner cycle*) [12]

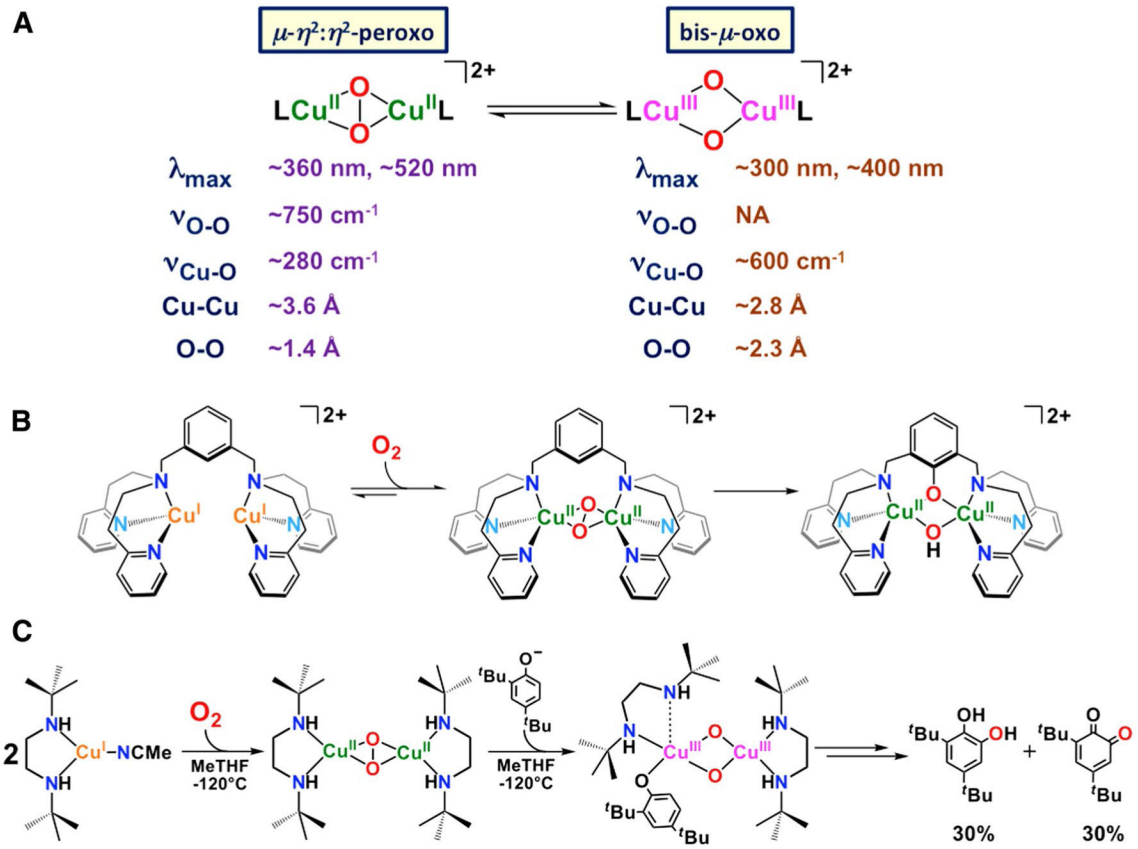

Scheme 13.

a Equilibrium between the μ-η^2:η^2-peroxodicopper(II) and bis(μ-oxo)dicopper(III) cores and their spectroscopic parameters [13]. **b** Intramolecular hydroxylation by a μ-η^2:η^2-peroxodicopper(II) complex [172]. **c** Internal hydroxylation of phenolate by a phenolate-bound bis(μ-oxo)dicopper(III) complex [171]

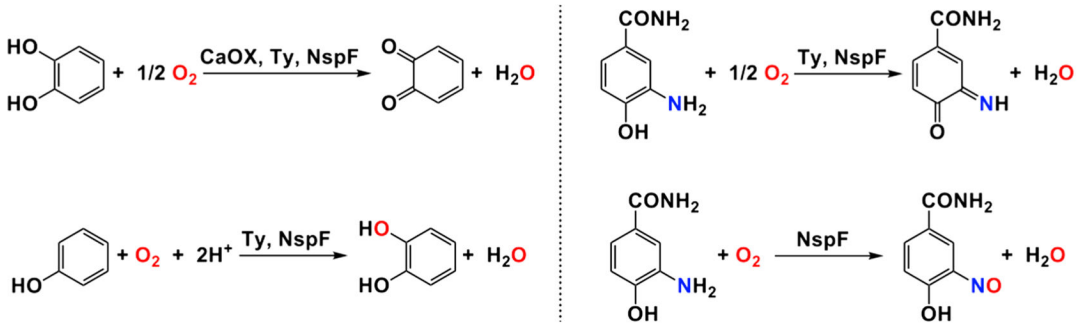

Scheme 14.

Different functions of the subclasses of coupled binuclear copper enzymes family [12]

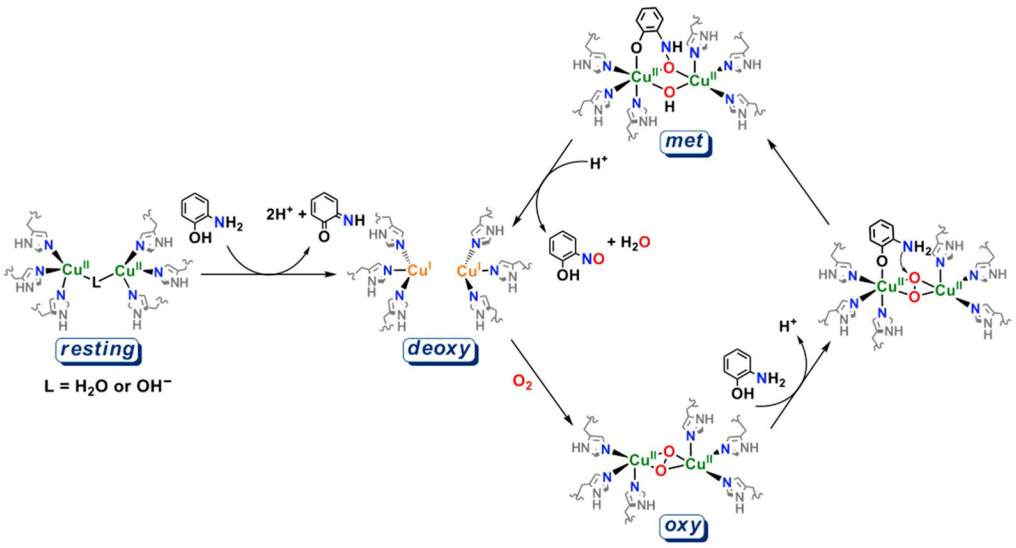

Scheme 15.

The proposed electrophilic mechanism for the oxidation of *o*-aminophenols by NspF (hydroxyanilinase activity) [179]

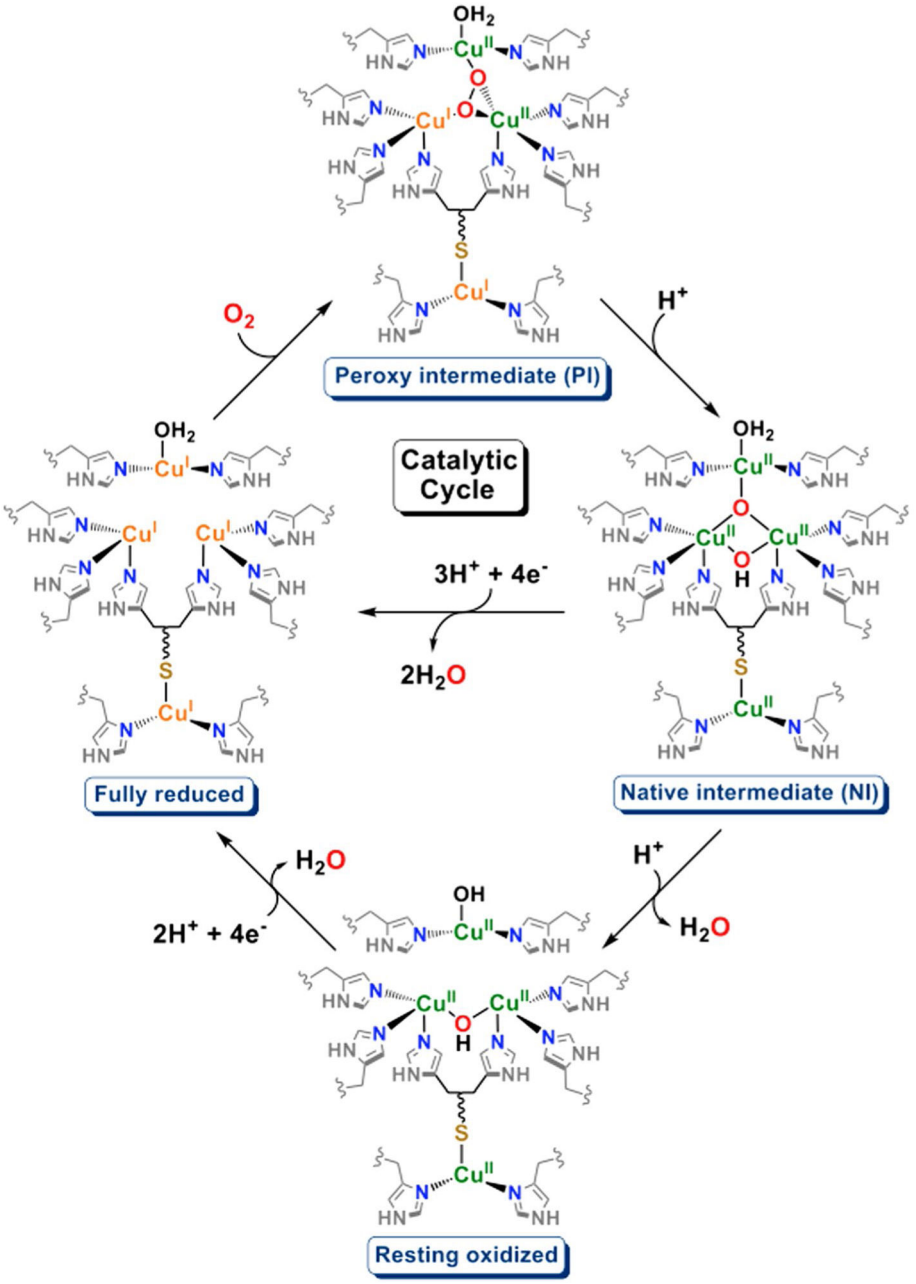

Scheme 16.

Reduction of O_2 at the TNC. O_2 is first reduced by two electrons, resulting in **PI** which is then further reduced with cleavage of the O-O bond, resulting in **NI** [209]

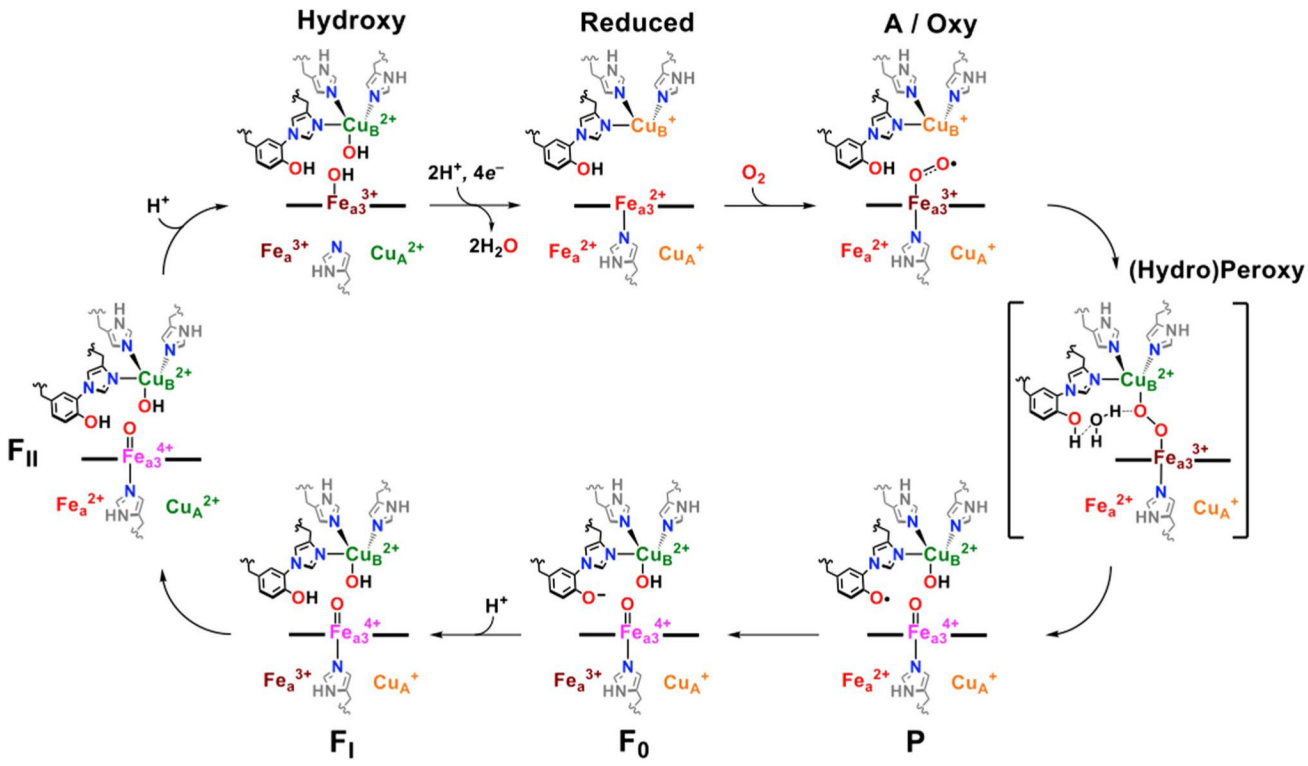

Scheme 17.

Proposed catalytic mechanism of C*c*O [228]. See text for further explanation

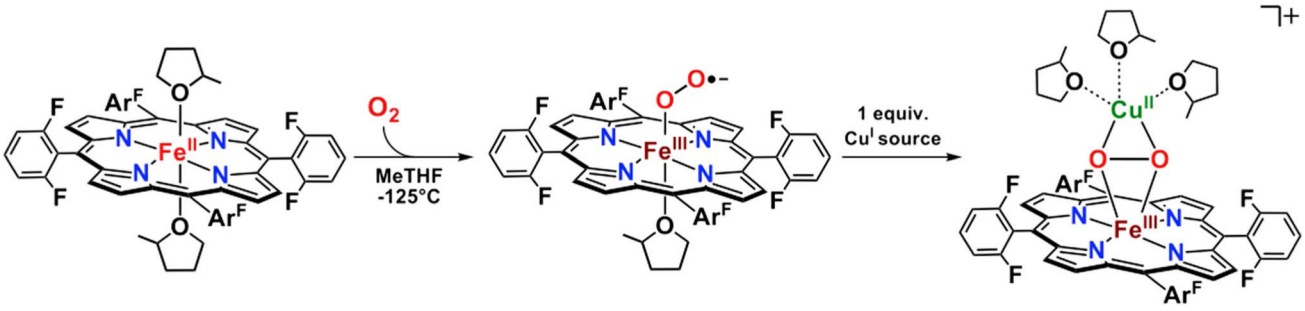

Scheme 18.

Generation of the naked synthon through the addition of 1 equiv. of a Cu^{I} source to a ferric superoxide [248]

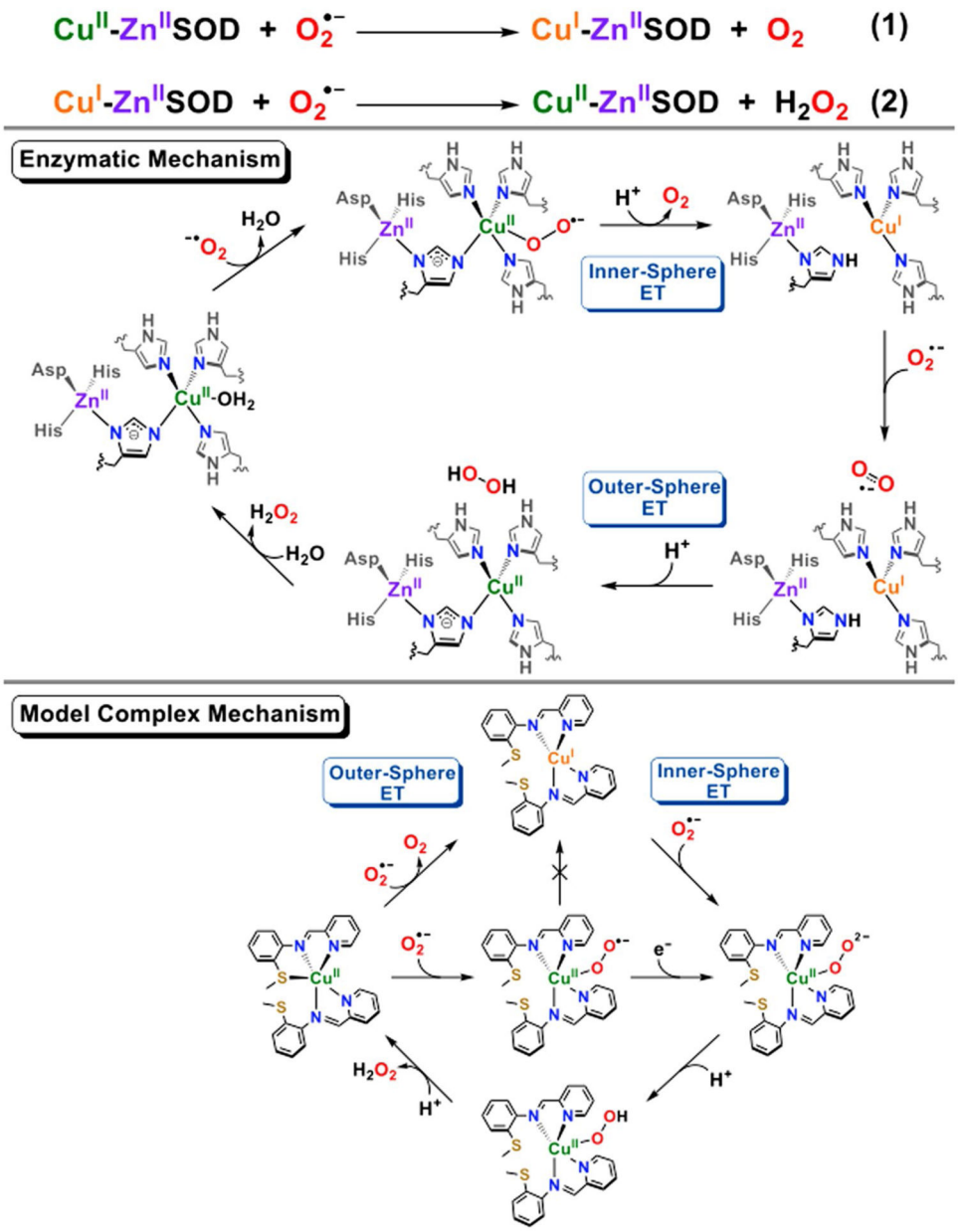

Scheme 19.

Top the two steps of superoxide dismutation by CuZnSOD. *Middle* the proposed enzymatic mechanism of CuZnSOD [258, 259]. *Bottom* the proposed mechanism for a model complex of CuZnSOD [260]

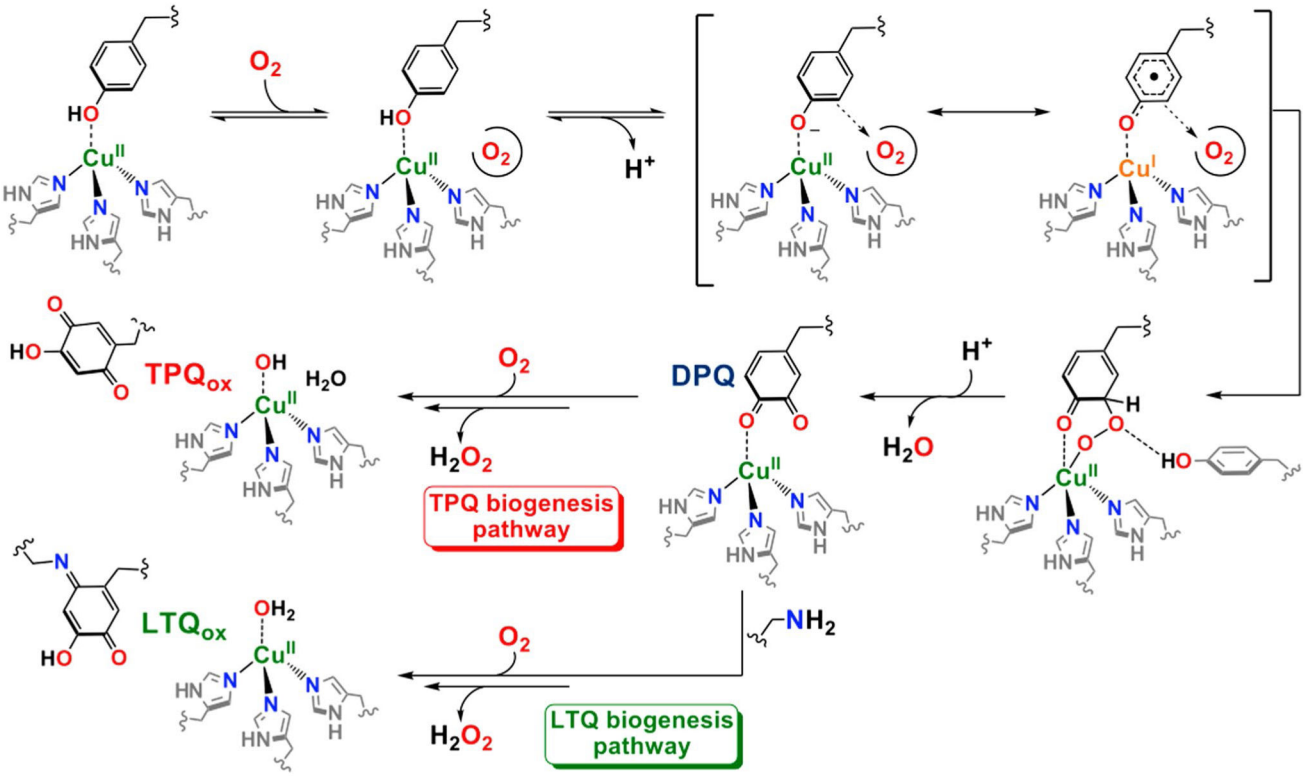

Scheme 20.

The proposed mechanism of TPQ or LTQ biogenesis by copper amine oxidase [87]

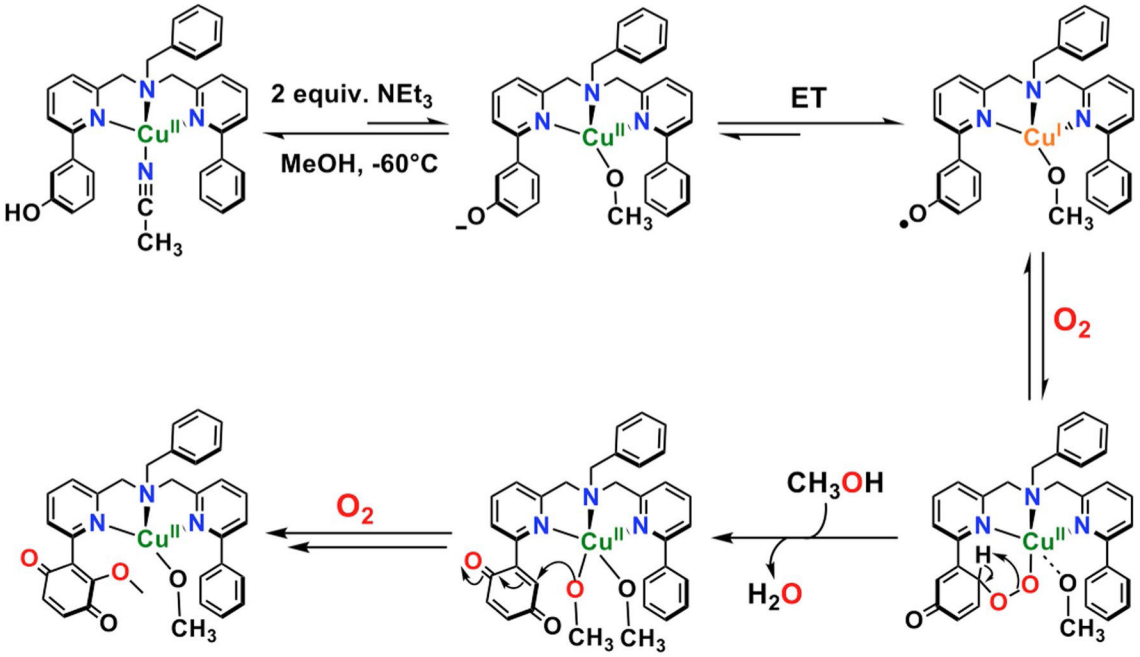

Scheme 21.

The proposed mechanism of post-synthetic modification of a CAO model compound to generate a TPQ-like moiety [96]

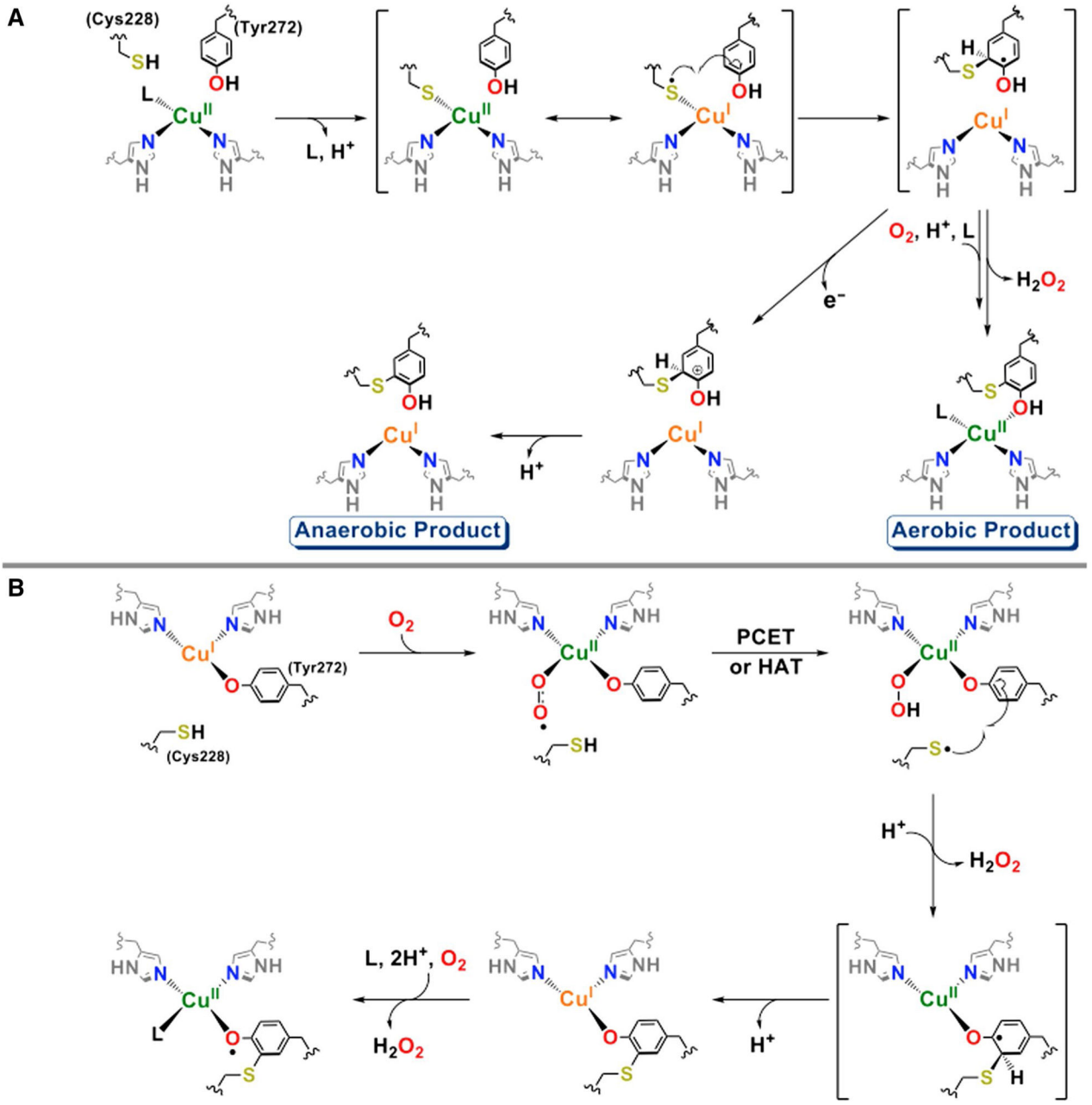

Scheme 22.

a The proposed mechanism of tyrosine-cysteine crosslink formation, starting from an initial cupric center. Both aerobic and anaerobic pathways are depicted [281]. **b** The proposed mechanism of tyrosine-cysteine crosslink formation, starting from an initial cuprous center [99]

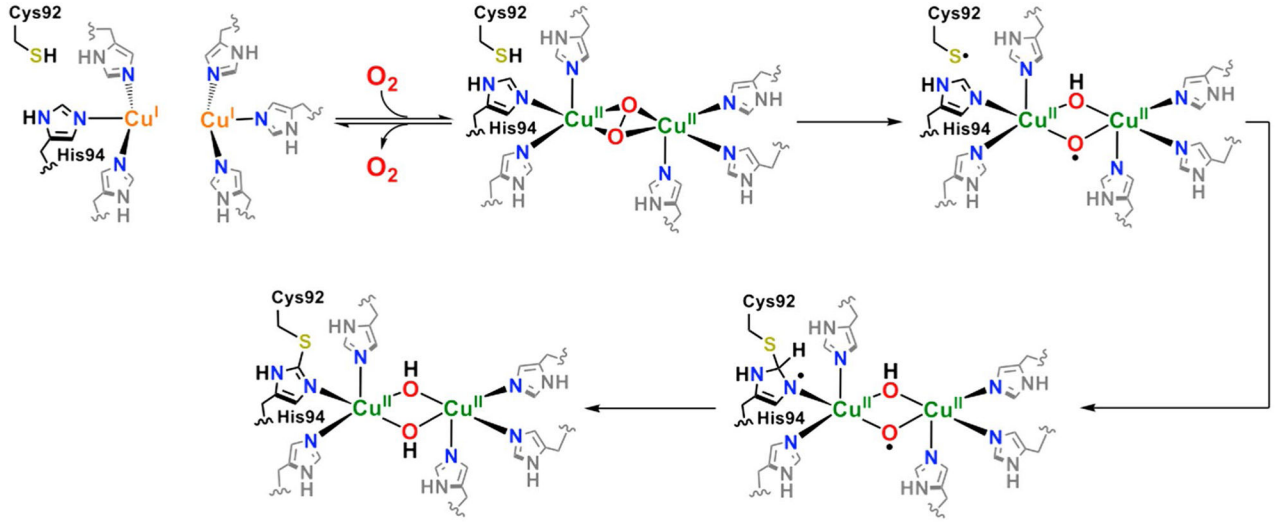

Scheme 23.

The proposed mechanism of His-Cys formation in coupled binuclear copper enzymes [285]

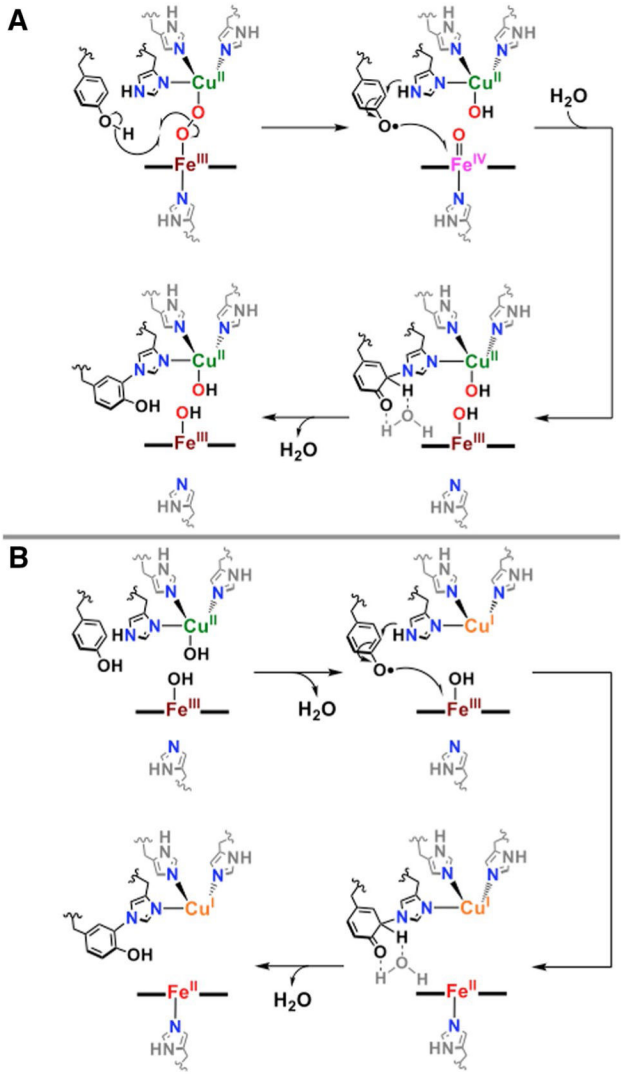

Scheme 24.

Proposed (possible) mechanisms for an (**a**) O_2-dependent and an (**b**) O_2-independent formation of the Tyr-His crosslink in C*c*O

Table 1

Kinetic and thermodynamic parameters for O_2 reactions with selected Cu^I and heme complexes at 25 °C

Compound	k_{O2} (M^{-1} s^{-1})	k_{-O2} (s^{-1})	K_{O2} (M^{-1})	References
[Cu(TMPA)(THF)]$^+$ *a,b*	1.3×10^9	1.5×10^8	15.4	[48]
[Cu(TMPA)(EtCN)]$^+$ *b,c*	5.8×10^7	1.5×10^8	3.8×10^{-1}	[51]
[Cu(TMG_3Tren)]$^+$ *b,d*	2.7×10^7	1.5×10^7	~1	[49]
[Cu(PEDACO-^{i}Pr]$^+$	5.9×10^2	1.5×10^6	6.3×10^1	[52]
[Cu(PEDACO-^{i}Pr]$^+$ *b,e,f*	3.2×10^1	4.6×10^2	6.7×10^{-2}	[52]
Hc monomer a *g*	4.6×10^7	4.1×10^2	1.1×10^5	[53]
Hc hexamer a *g*	3.1×10^7	1.9×10^2	1.6×10^5	[53]
Tyrosinase *g*	2.3×10^7	1.1×10^3	2.2×10^4	[54]
Myoglobin	$1.4–25 \times 10^7$	12–23,000	$0.74–117 \times 10^4$	[50]
Hemoglobin	$2.9–22 \times 10^7$	21–620	$2.87–47.6 \times 10^5$	[50]

TMPA tris-[(2-pyridyl)methyl]amine, *TMG3Tren* [tris-(tetramethylguanidino)]tris-(2-aminoethyl)amine, *PED-ACO-^{i}Pr* 1-isopropyl-5-[2-(2-pyridyl)ethyl]-1,5-diazacyclooctane

a In THF

b These compounds form η^1 cupric superoxide species

c In EtCN

d In MeTHF

e In acetone

f Extrapolated to 25 °C from data given in Ref. [52]

g These compounds form μ-η^2:η^2-peroxodicopper(II) products